MODELLING LONG TERM MORPHOLOGICAL CHANGE USING XBEACH

A THESIS SUBMITTED TO
THE GRADUATE SCHOOL OF NATURAL AND APPLIED SCIENCES
OF
MIDDLE EAST TECHNICAL UNIVERSITY

BY

ERDİNÇ SÖĞÜT

IN PARTIAL FULFILLMENT OF THE REQUIREMENTS
FOR
THE DEGREE OF MASTER OF SCIENCE
IN
CIVIL ENGINEERING

DECEMBER 2014

Approval of the thesis:

MODELLING LONG TERM MORPHOLOGICAL CHANGE USING XBEACH

submitted by **ERDİNÇ SÖĞÜT** in partial fulfilment of the requirements for the degree of **Master of Science in Civil Engineering Department, Middle East Technical University** by,

Prof. Dr. Gülbin Dural Ünver _____
Dean, Graduate School of **Natural and Applied Sciences**

Prof. Dr. Ahmet Cevdet Yalçıner _____
Head of Department, **Civil Engineering**

Prof. Dr. Ahmet Cevdet Yalçıner _____
Supervisor, **Civil Engineering Department, METU**

Dr. Işıkhan Güler _____
Co-Supervisor, **Civil Engineering Department, METU**

Examining Committee Members:

Prof. Dr. Ayşen Ergin _____
Civil Eng. Dept., METU

Prof. Dr. Ahmet Cevdet Yalçıner _____
Civil Eng. Dept., METU

Dr. Işıkhan Güler _____
Civil Eng. Dept., METU

Asst. Prof. Dr. Gülizar Özyurt Tarakcıoğlu _____
Civil Eng. Dept., METU

Dr. Cüneyt Baykal _____
COCONET Project, EU Project

Date: 05.12.2014

I hereby declare that all information in this document has been obtained and presented in accordance with academic rules and ethical conduct. I also declare that, as required by these rules and conduct, I have fully cited and referenced all material and results that are not original to this work.

Name, Last Name : Erdinç Söğüt

Signature :

ABSTRACT

MODELLING LONG TERM MORPHOLOGICAL CHANGE USING XBEACH

Söğüt, Erdinç
M.S., Department of Civil Engineering
Supervisor: Prof. Dr. Ahmet Cevdet Yalçıner
Co-Supervisor: Dr. Işıkhan Güler
December 2014, 117 pages

In this study, the XBeach Model, a two-dimensional depth averaged coupled hydrodynamic and morphologic numerical model, is used to determine the long-term behaviour of sediment transport process and morphological changes in Yumurtalık region in Adana, Turkey. Firstly, general information about the types of sediment transport processes and available coastal numerical models is given. Secondly, the structure of XBeach model, the boundary conditions and the model parameters that need to be defined are briefly discussed. Thirdly, the wave climate of the study area is studied and the representative waves that are used as the offshore wave boundary conditions in the numerical model are presented. Using the wave conditions obtained for the study area, a calibration study for the numerical model is first performed to determine the model parameters. In the calibration study, the field data composed of cross-shore profile measurements for the years 2006 and 2009 are used as initial and final bathymetries. Then, using the model parameters obtained from the calibration study, the numerical model is applied to the field measurements taken in 2009 and 2011, as a verification study. The model results are compared with the field measurements and they are found to be generally in agreement both qualitatively and quantitatively. According to the results of field measurements, it is observed that there exists a cross-shore dominated sediment transport in Yumurtalık region. A

similar behaviour is also observed from the model results. From this study, it is found that XBeach might be considered as a numerical tool that can be applied in such medium to long term morphological modelling problems.

Keywords: Longshore sediment transport, Cross-shore sediment transport, Long term, XBeach, Calibration, Verification

ÖZ

UZUN DÖNEMLİ MORFOLOJİK DEĞİŞİMLERİN XBEACH KULLANILARAK MODELLENMESİ

Söğüt, Erdinç
Yüksek Lisans., İnşaat Mühendisliği Bölümü
Tez Yöneticisi: Prof. Dr. Ahmet Cevdet Yalçıner
Ortak Tez Yöneticisi: Dr. Işıkhan Güler
Aralık 2014, 117 sayfa

Bu çalışmada, Xbeach modeli, iki boyutlu derinlik ortalamalı hidrodinamik ve morfolojik numerik model, Yumurtalık, Adana, Türkiye bölgesinin uzun dönemli sediman taşınım karakteristiği ve morfolojik değişimlerin belirlenmesinde kullanılmıştır. İlk olarak, sediman taşınım tipleri ve bu taşınım tiplerini modellemede kullanılan mevcut modeller kısaca anlatılmıştır. İkinci olarak, XBeach modelinin genel yapısı, belirlenmesi gereken sınır koşullar ve model parametreleri hakkında genel bilgiler verilmiştir. Üçüncü olarak, çalışma bölgesinin dalga iklimi belirlenmiş ve numerik modelde derin deniz sınır koşulları olarak kullanılan temsili dalgalar sunulmuştur. Çalışma bölgesi için belirlenen dalga koşulları kullanılarak, model parametrelerini belirlemek amacıyla bir kalibrasyon çalışması yapılmıştır. Kalibrasyon çalışmasında, 2006 ve 2009 yıllarında kıyıya doğru profiller olarak alınan saha ölçümleri, ilk ve son batimetrik haritalar olarak kullanılmıştır. Daha sonra, kalibrasyon çalışması sonucunda belirlenen parametreler ile 2009 ve 2011 yıllarına ait saha ölçümleri kullanılarak modelin doğruluk çalışması yapılmıştır. Model sonuçları saha ölçümleri ile karşılaştırılmış, sonuçların hem niteliksel hem de nicel olarak uyumlu olduğu gözlemlenmiştir. Saha ölçümleri sonuçlarına göre, Yumurtalık bölgesinde kıyıya doğru sediman taşınımının baskın olduğu

gözlemlenmiştir. Benzer olarak, model sonuçlarında da baskın sediman taşınımının kıyıya doğru olduğu belirlenmiştir. Yapılan tüm bu çalışma sonucunda, Xbeach modelinin, uzun dönemli morfolojik değişimleri numerik olarak modellemede düşünülebileceği gözlemlenmiştir.

Anahtar Kelimeler: Kıyı boyu sediman taşınımı, Kıyıya doğru sediman taşınımı, Uzun dönem, XBeach, Kalibrasyon, Doğruluk

To My family…

ACKNOWLEDGEMENTS

I would like to express my deepest gratitude to Prof. Dr. Ahmet Cevdet Yalçıner, Dr. Işıkhan Güler and Dr. Cüneyt Baykal for their supervision, support and valuable suggestions during this thesis study. It has always been a privilege to work with them. They always supported me and never let me alone during my hard times. They always shared their knowledge and experiences with me without getting tired. I will always be appreciated to them for their continuous help and support.

I would like to extend my sincere thanks to Assist. Prof. Dr. Gülizar Özyurt Tarakcıoğlu. She always trusted in me and guided me for during my study.

I would like to thank to my work friends Dr. Hülya Karakuş Cihan and Dr. Mustafa Esen for their valuable discussions, support and continuous help during my thesis study. I will always be appreciated to them for their support.

I would like to extend thanks to the staff and technicians of Coastal and Harbor Engineering Laboratory for their kindness and cheerfulness at all times.

I would like to thank to DOKAY for sharing site measurements which are used in this study.

Finally, I would like to thank my father Dinçer Söğüt, my mother Semanur Söğüt, my brother Hüseyin Erkut Söğüt, for their continuous help and support during my thesis study. They are the most valuable wealth of my life and with them I can achieve everything that I want.

TABLE OF CONTENTS

LIST OF FIGURES

FIGURES

LIST OF TABLES

TABLES

ABBREVIATIONS

1D	One Dimensional
2D	Two Dimensional
2-DH	Two Dimensional Horizontal
2-DV	Two Dimensional Vertical
3D	Three Dimensional
CEM	Coastal Engineering Manual
DMİGM	General Directorate of State Meteorological Affairs
ECMWF	European Centre for Medium-Range Wave Forecasts
EBP	Equilibrium Beach Profile
GENESIS	Generalized Model for Simulating Shoreline Change
GLM	Generalize Langrangian Mean
NW	North West
METU	Middle East Technical University
ONELINE	One-Dimensional Shoreline Change Model
Q3-D	Quasi Three Dimensional
SBEACH	Storm-Induced Beach Change Model
S	South
SE	South East
SSE	South South East
SSW	South South West
SW	South West
SWAN	Simulating Waves Nearshore Model
UNIBEST-TC	Cross-shore Profile Development Model
W	West
W61	Deep Water Wave Hindcasting Mathematical Model
WNW	West North West
WSW	West South West

WWF	World Wildlife Fund
XBeach	Extreme Beach Behaviour Model

LIST OF SYMBOLS

A	Dimensionless Sediment Scale Parameter (Section 2.2)
	*Wave action (Section 3.3.1)
A^*	Dimensional Proportionality Factor
A_{sb}	Bed Load Factor
A_{ss}	Suspended Load Factor
B	Berm Height
c	Phase Velocity
C	Depth Averaged Sediment Concentration
C_{eq}	Equilibrium Sediment Concentration
C_d	Drag Coefficient
c_g	Group Velocity
C_g	Group Velocity
c_x	Wave Action Propagation Speed In x-direction
c_y	Wave Action Propagation Speed In y-direction
c_θ	Wave Action Propagation Speed In θ-space
D	Sediment Grain Size
D*	Equilibrium Wave Energy Dissipation
D_c	Depth of Closure
D_g	Sediment Diffusion Coefficient
D_h	Sediment Diffusion Coefficient
D_r	Roller Energy Dissipation
$\overline{D_r}$	Roller Energy Dissipation According to Reniers et al, 2004a
D_w	Total Wave Energy Dissipation
$\overline{D_w}$	Total Wave Energy Dissipation According to Roelvink, 1993a
dx	Alongshore Grid Spacing
dy	Cross-shore Grid Spacing

d_{50}	Median Grain Size
E	Wave Energy Density
E_w	Total Wave Energy
f	Coriolis Viscosity
F_{eff}	Effective Fetch Length
F_i	Individual Fetch Length
f_{mor}	Morphological Acceleration Factor
F_x	Total Wave Force in x-direction
F_y	Total Wave Force in y-direction
g	Gravitational Acceleration
h	Predicted Depth of Beach Profile (Section 2.2)
	*Total Water Depth (Chapter 3)
h_b	Wave Breaking Depth
H_i	Individual Wave Height With Occurrence Probability P_i
h_0	The asymptotic Depth at a Great Offshore Distance (Section 2.2)
	*Initial Water Depth (Section 3.5.1)
H_0	Representative Wave Height
H_{max}	Maximum Wave Height
H_{m0}	Spectral Significant Wave Height
H_{rms}	Root Mean Square Wave Height
H_s	Significant Wave Height
H_{sb}	Significant Breaking Wave Height
H_{s0}	Deep Water Significant Wave Height
H_{s0}/L_0	Deep Water Significant Wave Steepness
$H_{s,12}$	Significant Wave Height Exceeded 12 hours Per Year
k	Decay Constant (Section 2.2)
	*Assigned Range to Compute Occurrence Probability (Section 4.3.4)
	*Wave Number (Section 3.3.1)
K	An Empirical Coefficient in Longshore Sediment Transport
k_x	Wave Vector Component in x-direction

k_y	Wave Vector Component in y-direction
L_0	Deep Water Wave Length
m	Slope Near Shoreline
m_b	Beach Slope From the Breaker Line to Shoreline
m_{cr}	Critical Slope
p	Porosity
P_i	Occurrence Probability of Waves With H_i
Q	Longshore Sediment Transport Rate (Section 2.1)
	*Annual Exceedence Probability (Section 4.3.4)
q	Sources or Losses of Sediment Along Coast
Q_b	Fraction of Breaking Waves
q_x	Sediment Transport Rate in x-direction
q_y	Sediment Transport Rate in y-direction
S_r	Roller Energy in Each Directional Bin
S_w	Wave Energy Density in Each Directional Bin
$S_{xx,r}$	Radiation Stress Due to Roller Action in x-direction along x-axis
$S_{xy,r}$	Radiation Stress Due to Roller Action in y-direction along x-axis
$S_{yy,r}$	Radiation Stress Due to Roller Action in y-direction along y-axis
$S_{xx,w}$	Radiation Stress Due to Wave Action in x-direction along x-axis
$S_{xy,w}$	Radiation Stress Due to Wave Action in y-direction along x-axis
$S_{yy,w}$	Radiation Stress Due to Wave Action in y-direction along y-axis
T_{m0}	Spectral Mean Energy Wave Period
T_p	Peak Wave Period
T_s	Significant Wave Period
	* Adaption Time for the Entrainment of the Sediment (Section 3.3.4)
$T_{s,12}$	Significant Wave Period Exceeded 12 Hours Per Year
u	Cross-shore Depth Averaged Velocity
u_{cr}	Critical Velocity for Sediment Motion Initiation
u_i	Velocity of Incoming Particle in x-direction
U_{land}	Wind Speed on Land at 10m Above Mean Sea Level

u_{mb}	Maximum Oscillatory Velocity Magnitude at Breaking
u_r	Outgoing Velocity in x-direction
u_{rms}	Near Bed Short Wave Orbital Velocity
Usea	Wind Speed on Sea at 10m Above Mean Sea Level
$\bar{u}$	Mean Velocity Current in x-direction
U_{land}	Wind Speed at 10m Above Stationary Sea Level on Land
u^E	Cross-shore Depth Averaged Eulerian Velocity
u^L	Cross-shore Depth Averaged Langrangian Velocity
u^S	Stokes Drift in x-direction
U_{sea}	Wind Speed at 10m Above Stationary Sea Level on Sea
v	Alongshore Depth Averaged Velocity
v_i	Velocity of Incoming Particle in y-direction
v_r	Outgoing Velocity in y-direction
$\bar{v}$	Mean Velocity Current in y-direction
v^E	Alongshore Depth Averaged Eulerian Velocity
v^L	Alongshore Depth Averaged Langrangian Velocity
v^S	Stokes Drift in y-direction
t	Time
w_f	Fall Velocity
x	Alongshore Distance
x_m	x-axis in Model Coordinates
x_{ori}	x-coordinate of Origin in World Coordinates
x_w	x-axis in World Coordinates
y	Shoreline Position (Section 2.1)
	*Distance From Shoreline (Section 2.2)
y_{ori}	y-axis in Model Coordinates
y_m	y-coordinate of Origin in World Coordinates
y_w	y-axis in World Coordinates
z_b	Bed Level
z_s	Surface Elevation of Incoming Long Wave
z_{s0}	Mean Water Level

β^-	Reimann Variant
ω	Fall Velocity (Section 2.2)
	Absolute Radial Frequency (Section 3.3.1)
ω_s	Fall Velocity
κ	Constant Relates Wave Height to the Water Depth
η	Water Level
ρ	Density of Water
θ	The Angle of Incidence With Respect to Computational x-axis
θ_b	Wave Angle at Breaking
θ_i	Incoming Wave Angle
θ_r	Outgoing Wave Angle
σ	Intrinsic Wave Frequency
γ	Breaker Index
γ_b	Breaker Index
α_b	Calibration Factor
α_i	Angle of Direction of Individual Fetch Length
τ_{bx}	Bed Shear Stress in x-direction
τ_{by}	Bed Shear Stress in y-direction
τ_{sx}	Wind Stress in x-direction
τ_{sy}	Wind Stress in y-direction
υ_h	Viscosity
Δz_b	Bed Level Change
Δt	Time Step
Δx	Change in x-direction

CHAPTER 1

INTRODUCTION

In the history of human being, it is observed that sea and human have always been in interaction from different point of views. From the early stages of the history to today, human have seen the sea as the source of life and wealth. Most of the large and important cities are constructed near to sea side in order to benefit from the supplies obtained from sea such as fish, petroleum, etc. For this purpose, marine structures such as harbours have been constructed. However, as these marine structures are constructed, questions have arisen in the minds of coastal engineers. They started to think about the answers of variety of problems such as what the effect of constructing a breakwater on shoreline change will be. Experiments and field measurements are conducted to understand the general behaviour of the physical processes observed at nearshore and formulations are provided to guide coastal engineers. Although, there exists an important amount of knowledge on the sediment transport and resulting beach morphology and shoreline changes in coastal areas, still these processes could not be solved accurately or modelled numerically. The main reasons are that physical processes observed nearshore area are very complex, dynamic and they can occur in different time scales. In order to determine the general behaviour of coastal processes in an area, site specific features such as;

- Storm history
- Wave Climate
- Bathymetry of the area
- Sediment grain size and gradation
- Existing coastal structures or formations, if any
- Sources of accretion and erosion processes

should be determined. After determination of all features, their effects both in single and combined manner should be check in order to understand the correct behaviour of physical processes in nearshore.

At present, due to the increasing use of coastal areas, understanding the general behaviour of sediment transport processes has become more important in order to prevent fatal results such as loss of a beach which mainly depend on extensive and unconscious use of coastal regions. For this purpose, mathematical models have been developed in order to understand the general behaviour of coastal sediment transport processes by using the results of field measurements that have been collected to interpret these processes in short time. The mathematical models used today can be divided mainly in three categories. These models are;

1. Shoreline change models

These types of models are mainly used to simulate long term response of beaches to alongshore sediment transport process.

2. Beach profile models

These types of models are mainly used to simulate short term profile evolutions of beaches mainly caused by cross-shore sediment transport.

3. Multi -dimensional models

These type of models are mainly used to simulate combined effect of both cross-shore and longshore sediment transport processes.

There is an important point that coastal engineers should be careful about. As the number of processes and parameters used in the modelling of nearshore area increase, more time and effort are needed for correct calibration and application of the model. That is why in the selection of the model to be used, the problem for which the answer is needed should be clearly defined.

The main purpose of this study is to understand the general behaviour of the sediment transport process observed in Yumurtalık region, Adana, Turkey. For this purpose, the numerical model called XBeach developed jointly by Unesco-IHE

Institute for Water Education, Deltares and Delft University of Technology is used. Although, XBeach, mainly developed to understand short time response of beaches under storm conditions, due to its ability to model both longshore and cross-shore sediment transport processes, it is preferred in this study.

In Chapter 2, general information about longshore and cross-shore sediment transport processes and the available numerical models used to simulate these processes are given.

In Chapter 3, general information about the coordinate system, grid definition, model formulations and boundary conditions used in XBeach model are given.

In Chapter 4, application of XBeach model in Yumurtalık region is presented.

In Chapter 5, according to the result of study, discussions, conclusion and recommendations about future studies are presented.

CHAPTER 2

LITERATURE SURVEY

One of the most important common heritages for human being is the coastal regions. The misunderstanding of the behaviour of natural processes in these areas often causes fatal results such as beach erosion due to improper construction of a marine structure. The coastal processes are very sophisticated dynamic events that change from microscale to macroscale phenomena such as the movement of a particular sand grain to the effect of global sea level rise on beach (Hanson, 1987). In order to have a quantitative understanding of characteristics of nearshore coastal processes, various studies have been conducted. In this chapter, general information about sediment transport processes that are the basis of the numerical models and on overview of sediment transport models are presented.

2.1. Longshore Sediment Transport

When waves approach the shoreline with an oblique angle, they will cause sediment movement along the shore in the direction of propagation (Kamphius, 2010). The longshore sediment transport often manifests itself in the erosion and accretion processes around coastal structures (Fredsoe and Deigaard, 1992).

CERC-formula, or SPM-method after the Shore Protection Manual is one of the oldest and still successful method used to determine longshore sediment transport rate (Fredsoe and Deigaard, 1992). CERC-formula based on the assumption that the total longshore sediment transport rate is proportional to the longshore energy flux. in Eq. 2.1 CERC-formula is given.

$$Q = \frac{K}{16\sqrt{\gamma_b}} \rho g^{\frac{3}{2}} H_{sb}^{\frac{5}{2}} \sin(2\theta_b) \quad [2.1]$$

Here,

Q: Longshore sediment transport rate

K: An empirical coefficient

γ_b: Breaker index

ρ: Density of water

g: Gravitational acceleration

H_{sb}: Significant breaking wave height

θ_b: Wave angle at breaking

As the value of the K coefficient, 0.39 is recommended by the Shore Protection Manual. However, the CERC-formulation is best used if the K coefficient is calibrated with data of particular site. By this way, this formulation can be used to estimate longshore sediment transport rate with reasonable confidence. Sometimes however, it is not possible to have adequate data to calibrate the K coefficient. The use of the CERC-formula in such situations provides only order of magnitude accuracy (Fowler et. al., 1995; Wang et. al., 1998). The CERC-formula sometimes over- and/or under- estimates the longshore sediment transport rate during the storms. It indicates that the value of the K coefficient value, which is suggested as 0.39 by the Shore Protection Manual, can also be higher in such conditions (Miller, 1998).

In order to predict the value of the K coefficient, Bailard (1981, 1984) developed an energy based relationship which uses the root mean square breaking wave height. The equation suggested by Bailard (1981, 1984) is presented in Eq.2.2.

$$K = 0.05 + 2.6\sin^2(2\theta_b) + 0.007\frac{u_{mb}}{w_f} \quad [2.2$$

Here,

u_{mb}: Maximum oscillatory velocity magnitude at breaking obtained from shallow water wave theory (Eq. 2.3)

w_f: Fall velocity

θ_b: Wave angle at breaking

$$u_{mb} = \frac{\gamma_b}{2}\sqrt{gh_b} \qquad [2.3]$$

Here,

γ_b: Breaker index

g: Gravitational acceleration

h_b: Wave breaking depth

In addition, del Valle et. al. (1993) provides a relationship between sediment median grain size and the K coefficient that decreases with increasing sediment size. In Eq. 2.4, this relation is presented.

$$K = 1.4e^{(-2.5d_{50})} \qquad [2.4]$$

Here,

d_{50}: Median grain size

Field measurements in the dynamic surf zone are non-controllable and nonrepeateable, which may lead to large uncertainties (Schoones and Theron, 1993; Wang et. al., 1998; Wang and Kraus, 1999). Also, only a limited number of parameters can be measured in the field. Therefore; the laboratory studies on longshore sediment transport becomes more advantageous than field measurements since are controllable and repeatable. Thus, the measurements obtained in laboratory are more accurate than field data. Until Kamphuis (2002), the laboratory data have not been used in the longshore sediment transport rate calculations due to the small scales of the laboratory models (Ernest et. al., 2004). Kapmhuis (2002) found that the scale effects and uncertainties of a small scale model were less than the field measurements. It is difficult to enhance the estimates longshore sediment transport

models by only using of the field measurements. This is because; large uncertainties exist in the measurement of the basic variables. Therefore, controlled or controllable model tests should be used to improve the estimates of longshore sediment transport models despite the shortcoming of these physical models (Kamphuis, 2002). In Eq. 2.5, formulation suggested by Kamphuis (2002) to determine longshore sediment transport rate is given.

$$Q = 2.27 H_{sb}^{2} T_{p}^{1.5} m_{b}^{0.75} d_{50}^{-0.25} \sin^{0.6}(2\theta_{b}) \qquad [2.5]$$

Here,

Q: Longshore sediment transport rate

H_{sb}: Significant breaking wave height

T_p: Peak wave period

m_b: Beach slope from the breaker line to the shoreline

d_{50}: Median grain size

θ_b: Wave angle at breaking

2.2. Cross-shore Sediment Transport

The concept of equilibrium beach profile (EBP) is one of the major interests of the coastal engineers for about half a century (Dong, 2008). With EBP concept it is stated that a beach will reach the equilibrium shape, in which there is no net sediment transport, when it is exposed to a given wave data for a period of time (Özkan-Haller and Brundidge, 2007). The verification of this definition for equilibrium beach profiles should be done with many laboratory tests conducted on the change of beach profiles. However, in natural beaches, forces that play an important role in sediment transport are never constant and the change of beach profile occurs almost every time on the contrary to the laboratory conditions (Larson et. al., 1998). Despite the difference, it is found that laboratory conditions and natural beaches tend to show similar behaviours such as bar formation. From these previous studies, four main features of equilibrium beach profiles are well-known. These features are;

- Equilibrium beach profiles tend to be concave upwards

- Smaller sand grains results with milder slopes on the contrary larger sand diameters results in steeper slopes.
- The face of the beach is nearly planar
- Waves with higher steepness results with milder slopes and tendency of bar formation (Dean, 1991).

In one of the first study on equilibrium beach profile concept, Bruun (1954) offered a power law in order to describe the depth of beach profile as a function of distance from shoreline for coasts of Denmark and California. In this study, he assumed that the bottom shear stress and the wave energy dissipations were constant at equilibrium. By using this assumption, he found that the power of 2/3 gives the best fit for equilibrium beach profile (Eq. 2.6). The equation suggested by Bruun (1954) for equilibrium beach profile is

$$h = A * y^{2/3} \qquad [2.6]$$

Here,

h: Predicted depth of beach profile at distance y (m)

A: Dimensional scale parameter ($m^{1/3}$)

y: Distance from shoreline (m)

Swart (1974) conducted various large scale wave tank experiments and developed empirical expressions which relate beach profile geometry to the wave conditions and sediment grain size. According to Swart's theory, the beach profile is divided into four different regions and for each region related empirical expression developed has to be used. The procedure suggested by Swart (1974) is not preferred in engineering applications since it is complex and involves application of numerous numbers of equations to make it simple and straightforward.

Vellinga (1983) developed a dune erosion profile model (Eq. 2.7) which includes the effects of deep water significant wave height (H_{s0}) and fall velocity (ω) by a numerous wave tank tests.

$$\left(\frac{7.6}{H_{s0}}\right)h = 0.47\left[\left(\frac{7.6}{H_{s0}}\right)^{1.28}\left(\frac{\varpi}{0.0268}\right)^{0.56} y + 18\right] - 2.0 \qquad [2.7]$$

Here,

h: Predicted depth of beach profile at distance y (m)

H_{s0}: Deep water significant wave height (m)

y: Distance from shoreline (m)

ω: Fall velocity (m/s)

Dean (1977) studied 504 beach profiles collected by Hayden et.al. (1975) along the Atlantic and Gulf coasts of the United States. His study was based on the uniform dissipation of wave energy flux in the surfzone and the assumption of spilling wave breaking (Wang and Kraus, 2005). Using this assumptions, least squares method was applied in order to fit an equation in the form

$$h = A * y^{m} \qquad [2.8]$$

Here,

h: Predicted depth of beach profile at distance y (m)

A: Sediment scale parameter

y: Distance from shoreline (m)

Dean (1977) found that for the uniform dissipation of wave energy flux in the surfzone, the exponent m (Eq. 2.8) 2/3 gives the best fit. As a result, following equation is suggested for describing equilibrium beach profiles by Dean (1977).

$$h = A * y^{2/3} \qquad [2.9]$$

The sediment scale parameter (A) and the equilibrium wave energy dissipation per unit volume (D_*) are related by

$$A = \left[\frac{24}{5} * \frac{D_*}{\rho g \sqrt{g} \kappa^2} \right]^{2/3} \text{ and } D_* = \frac{1}{h} \frac{\partial}{\partial y} (EC_g) \qquad [2.10]$$

Here

E: Wave energy density

Cg: Group velocity

ρ: Density of water

g: Gravitational acceleration

κ: Constant relates the wave height to the water depth within surfzone

D_*: The equilibrium wave energy dissipation per unit volume

Based on the least square fit (Eq. 2.9) suggested by Dean (1977) for equilibrium beach profiles, empirical correlations were suggested between sediment scale parameter (A) as a function of sediment grain size (D) and fall velocity (ω), by Moore (1982) and Dean (1987b). This relation is given in Fig. 2.1.

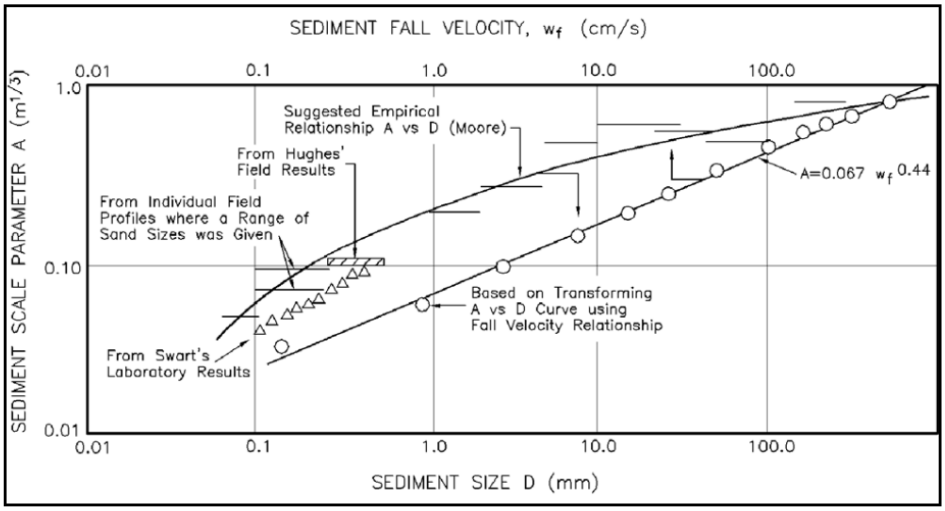

Figure 2.1: Change of sediment scale parameter (A) with sediment grain size (D) and fall velocity (ω) (Dean, 1987b)

The relation between sediment scale parameter (A) and sediment grain size (D) given in Fig. 2.1 are tabulated for grain sizes D=0.10mm to D=1.09mm in Table 2.1.

Table 2.1: Recommended sediment scale parameter (A) values for different sediment grain sizes (D) (CEM, 2003)

D (mm)	0.00	0.01	0.02	0.03	0.04	0.05	0.06	0.07	0.08	0.09
0.1	0.063	0.0672	0.0714	0.0756	0.0798	0.084	0.0872	0.0904	0.0936	0.0968
0.2	0.100	0.103	0.106	0.109	0.112	0.115	0.117	0.119	0.121	0.123
0.3	0.125	0.127	0.129	0.131	0.133	0.135	0.137	0.139	0.141	0.143
0.4	0.145	0.1466	0.1482	0.1498	0.1514	0.153	0.1546	0.1562	0.1578	0.1594
0.5	0.161	0.1622	0.1634	0.1646	0.1658	0.167	0.1682	0.1694	0.1706	0.1718
0.6	0.173	0.1742	0.1754	0.1766	0.1778	0.179	0.1802	0.1814	0.1826	0.1838
0.7	0.185	0.1859	0.1868	0.1877	0.1886	0.1895	0.1904	0.1913	0.1922	0.1931
0.8	0.194	0.1948	0.1956	0.1964	0.1972	0.198	0.1988	0.1996	0.2004	0.2012
0.9	0.202	0.2028	0.2036	0.2044	0.2052	0.206	0.2068	0.2076	0.2084	0.2092
1.0	0.21	0.2108	0.2116	0.2124	0.2132	0.214	0.2148	0.2156	0.2164	0.2172

Kriebel et.al. (1991) suggested a relation between sediment scale parameter (A) and fall velocity (ω) shown in Fig.2.1 which is valid for sediment grain sizes changing from D=0.10mm to D=0.40mm. The relationship between two parameters is given in Eq. 2.11.

$$A = 2.25\left(\frac{\varpi^2}{g}\right)^{1/3} \qquad [2.11]$$

Here,

A: Sediment scale parameter

ω: Fall velocity (m/s)

g: Gravitational acceleration (m/s^2)

Eq. 2.9 suggested by Dean (1977) has been most widely used equation in engineering practice. The popularity of this equation is largely due to the fact that it is a well-established equation for the relationship between sediment scale parameter (A) and sediment grain size (D) (Özkan-Haller, Brundidge, 2007). Although, Eq. 2.9 has been widely used in engineering practices, it has two limitations. These limitations are;

- The beach profile slope at the water line is infinite

- Eq. 2.9 is not able to represent bar formation.

Larson (1988) and Larson and Kraus (1989) overcome the first limitation by taking the gravity as the triggering force of downslope sediment transport. The expression they suggested for equilibrium beach profile is

$$y = \frac{h}{m} + \left(\frac{h}{A_*}\right)^{3/2} \qquad [2.12]$$

Here,

m: Slope near the shoreline

A_*: Dimensional proportionality factor similar to sediment scale factor (A)

h: Predicted depth of beach profile at distance y (m)

y: Distance from shoreline (m)

The attractiveness of Eq. 2.12 is mainly depend on the fact that there is only one free parameter which is A_* is needed to be determined since foreshore slope (m) can easily be determined without need of extensive underwater survey (Özkan-Haller, Brundidge, 2007). There is an important point that should be noted, the parameter A_* is not need to be equal to the sediment scale parameter, A defined in Eq. 2.6. Use of equilibrium beach profile formulation in Eq. 2.12 is become more useful if the parameter A_* can be related to sediment grain size (Özkan-Haller, Brundidge, 2007).

Bodge (1992) suggested an exponential beach profile in the form of

$$h(y) = h_0(1 - e^{-ky}) \qquad [2.13]$$

Here,

h_0: The asymptotic depth at a great offshore distance

k: Decay constant

h: Predicted depth of beach profile at distance y (m)

y: Distance from shoreline (m)

After fitting the exponential beach profile to the averages of the ten data sets provided by Dean (1977), Bodge (1992) found that the exponential form fits better

than the beach profile (Eq. 2.9) suggested by Dean (1977). Since the exponential beach profile has two free parameters, it is expected to fit better than Eq. 2.9. However, due to the requirement of determination of two free parameters in exponential beach profile, it can be applied in a diagnostic manner but not prognostically (CEM, 2003).

2.3. Overview Sediment Transport Models

Prediction of sediment transport and beach profile evaluation in coastal regions, especially in longer terms, is a difficult task since complex physical processes occurs in these areas at many scales in time and space (De Vriend, 1991a; Larson and Kraus., 1995).

Primary concerns of coastal planners and managers are the time scale of years to decades, longshore length scales changing between 10's-100's kilometres and cross shore length scales changing between 1's-10's kilometres. Prediction of coastal evolution with numerical models has been proved to be a good technique which helps to understand the processes involved and selection of the most appropriate project design. The numerical models used for sediment transport provide a framework both for organizing the collection and analysis of data and for the evaluation of different coastal evolutions scenarios. Numerical models are used for developing solutions for problems and for efficient evaluation of alternative designs in engineering applications (Hanson et. al., 2003).

Selection of appropriate model for a long term prediction of coastal evaluation requires a complete analysis of the problem under consideration and clear definition of the objective of predictions (Hanson et. al., 2003). After determination of the scope of study and coastal processes, numerical models from simple one dimensional to 3D sophisticated models can be used. The use of numerical models for different scales is given in Fig. 2.2.

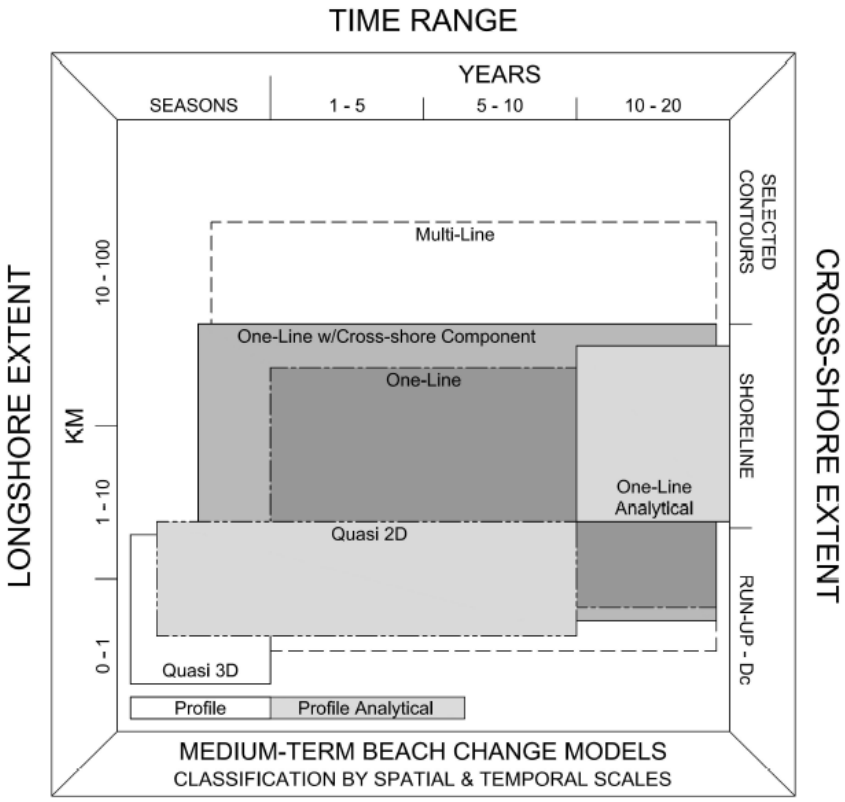

Figure 2.2: Classification of beach change models by spatial and temporal scale (Hanson et al., 2003)

Numerical models used in sediment transport processes can be classified under three main categories as

- Shoreline change models
- Beach profile models
- Multi-dimensional models

2.3.1. Shoreline Change Models

A common observation about beach profiles is that the beach profile maintains an average shape which is characteristic of the particular coast except the extreme changes due to storms. For example, in long term, steep beaches remain steep. Although seasonal changes in wave climate cause movement of shoreline to shoreward and seaward in a cyclic manner, the change in average slope, when

compared with total active profile, is relatively small. The point on which profile shape does not change is sufficient to specify the location of entire profile with respect to this point. That means, a contour line can be used in order to describe the profile change. Such models are called shoreline change or shoreline response models. Sometimes one-line model terminology is used to describe these types of models (Capobianco et al., 2002).

The general approach in shoreline change models is to divide coastline into a large number of cells and transport sediments from one cell to another by relating the longshore sediment transport parameters to wave parameters and longshore current velocities. The application of a continuity equation into a cell gives the shoreline change by comparing the volume of sand entering and exiting (Capobianco et. al., 2002). First shoreline change model based on the basic assumptions of the one-line theory is derived by Pelnard-Considere (1956). Although Pelnard-Considere (1956) developed his equation in the existence of a simple boundary, it is a favourable tool for the evaluation of shoreline change numerical models. The use of early shoreline change models was complex since they require many modifications and special works for the related study. However, this problem is overcome with the help of development in computer technology by developing more sophisticated models (Dabees, 2000).

Sand is transported alongshore between the two well-defined limiting elevations is another assumption made in longshore sediment transport process. The shoreward limit is located at the top of the active berm and the seaward limit is located where no significant depth changes occur, called as depth of closure (Capobianco et al., 2002).

From Eq. 2.14 which is presented by Hallermeier (1978), depth of closure can be calculated.

$$D_c = 2.28H_{s,12} - 68.5\left(\frac{H_{s,12}^2}{gT_{s,12}^2}\right) \qquad [2.14]$$

Here,

$H_{s,12}$: Significant wave height exceeded 12 hours per year

g: Gravitational acceleration

$Ts_{,12}$: Significant wave period exceeded 12 hours per year

The general approach used in these numerical models is to divide shoreline into a large number of individual cells and apply the equations that relate sediment transport rate to wave parameters and to velocities of alongshore currents in order to calculate transport of sand from one cell to another. From the application of continuity equation, shoreline changes are calculated by comparing volume of sand entering and exiting (Capobianco et al., 2002). Differential equation given in Eq. 2.15 can be used to calculate shoreline evolution.

$$\frac{\partial y}{\partial t} = -\frac{1}{(D_c + B)}\left(\frac{\partial Q}{\partial x} + q\right) \qquad [2.15]$$

Here,

y: Shoreline position

x: Alongshore coordinate

t: Time

Q: Longshore sand transport

q: Sources or losses along the coast

D_c: Depth of closure

B: Berm height

The model can be solved either using explicit or implicit scheme. Although, the explicit scheme is easier to program than an implicit scheme, it is inefficient to implement for general cases because of the critical stability condition. An implicit solution scheme based on a method given by Perlin and Dean (1978) is adapted and used in the development of GENESIS and ONELINE (Dabees, 2000).

2.3.2. Beach Profile Models

The main purpose of beach profile models is to simulate short term profile evolutions mainly caused by cross-shore sediment transport (Dabees, 2000). The working principles of these models are similar to the shoreline change models. Like shoreline change models, beach profile models also use the application of continuity equation to find the net sediment transport rate. Several models have been developed by Dally and Dean (1984), Kriebel and Dean (1984) and Larson and Kraus (1989) by taking the breaking waves as the main reason of beach profile evolution. By making wave transformation and calculating time averaged velocities across a profile, deterministic cross-shore sediment transport models are able to calculate the rate of sediment transport as a function of horizontal velocities and local bottom conditions using Bailard's (1981) energetics approach. UNIBEST-TC (Stive and Battjes, 1984; Roelvink et. al.,1995) can be given as an example for deterministic beach profile models (Dabees, 2000). These types of models have been extensively used to evaluate immediate profile response to storms and they have been quite successful in predicting these short-term events. However, because of the difficulties in the formulation of sediment transport that produce reliable profile evolution, application for medium or long term predictions have been limited (Hanson et. al., 2003).

2.3.3. Multi-Dimensional Models

The main purpose of these models is to make a description of bottom change which may vary in longshore and cross shore directions.

In a fully 3D model, all hydrodynamic equations are written in three dimensions. In Fig. 2.3 a finite difference model schematizing the domain over a 3D grid is shown.

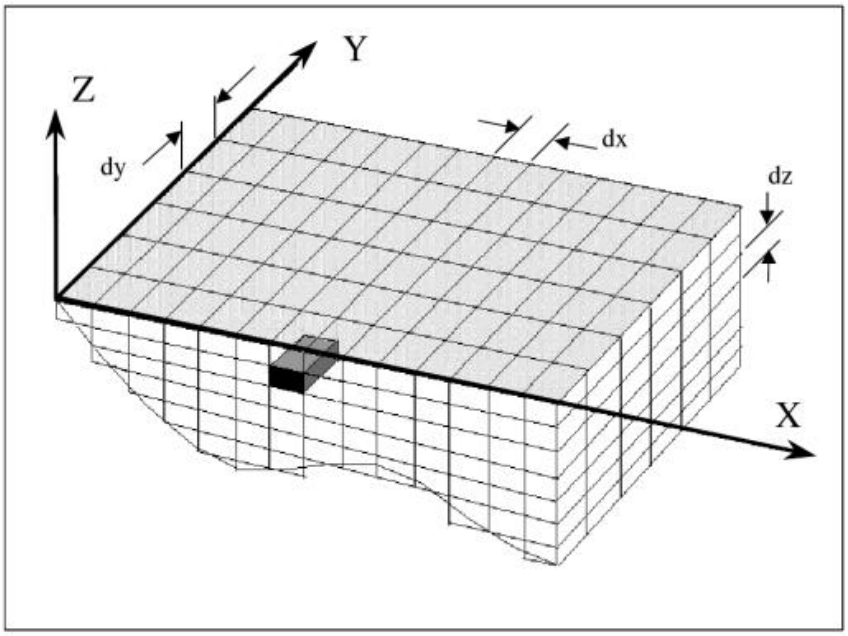

Figure 2.3: Three dimensional (3D) modelling (Kamphius, 2000)

Although, these models help coastal engineers to understand the nearshore processes occur in the vicinity of marine structures, they tend to be computationally intensive and their accuracy near the shoreline has not been demonstrated with related time scales (Miller and Dean, 2004).

Three dimensional (3D) models can be simplified into two dimensional (2D) models by using vertically integrated values for the fluid flow (Fig 2.4). This type of simplified models can be used to solve medium term sediment transport problems (Kamphius, 2000).

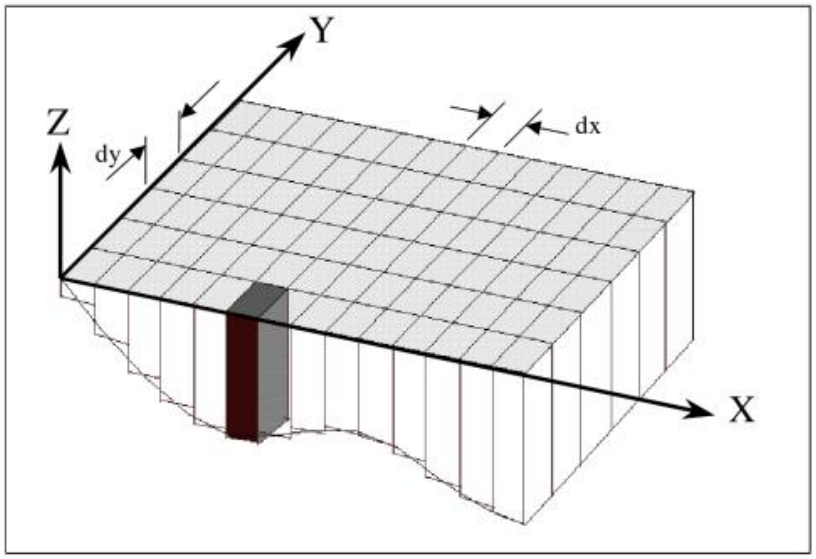

Figure 2.4: Two dimensional (2-DH) modelling (Kamphius, 2000)

These types of two dimensional (2-DH) models may have shortcoming due to using vertically integrating fluid velocities (Kamphius, 2000).

In addition, by ignoring all alongshore variations in water levels, three dimensional models (3D) can also be simplified into a cross shore model calculated over a two dimensional (2D) vertical grid (2-DV model), shown in Fig. 2.5.

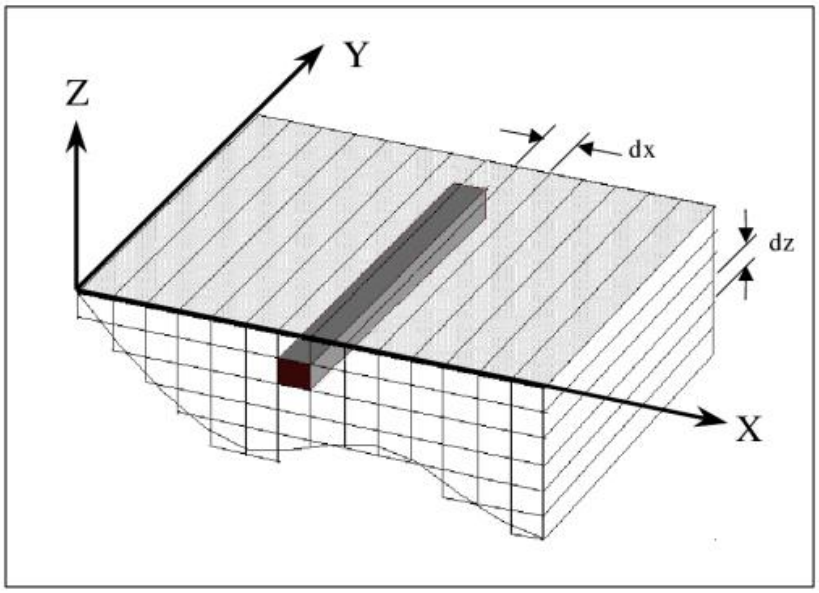

Figure 2.5: Two dimensional (2-DV) modelling (Kamphius, 2000)

In order to overcome the shortcomings of 2-DH models, by combining 2-DH and 2-DV models a quasi-three-dimensional model (Q3-D) has been developed. It is found that this type of model looks promising tool for medium-term problems since it can perform sophisticated computations in reasonable time (Kamphius, 2000).

The main difference between schematic 3D models and fully 3D models is that schematic 3D models simplifies the controlling equations of fully 3D models by, for example, calculating global transport rates instead of calculating point transport rates (CEM, 2003). An example schematized three dimensional (3D) model is presented by joint use of the shoreline change model GENESIS and the profile change model SBEACH (Larson and Kraus, 1989).

The working principles of the models given above are summarized below:

- Beach profile models describe the evolution of cross-shore profile. They are mainly used to simulate profile response to extreme events (short and medium term) and these models are one-dimensional (1D).

- Shoreline change models describe the evolution of shoreline. They are used to simulate long term change of shoreline and these models are one-dimensional (1D).

- 2-DH and 2-DV models are the combinations of beach profile and shoreline change models. They are mainly used to describe evolution of nearshore area.

- Quasi-three-dimensional models (Q3-D) are used to describe whole three-dimensional evolution of coastline. They are suitable for the analysis of initial response of the coastal systems (Capobianco et al., 2002).

CHAPTER 3

STRUCTURE OF XBEACH MODEL

XBeach, abbreviation of *eXtreme Beach* behaviour, is a numerical model developed in order to model nearshore responses under storm and hurricane conditions by Unesco-IHE Institute for Water Education, Deltares and Delft University of Technology (Roelvink, et al., 2010). This open source model is a 2D hydrodynamic-morphologic coupled model using a finite difference explicit scheme. It is able to solve time dependent short wave energy, flow and wave propagation, sediment transport and bed level morphological change (Roelvink, et al., 2010).

The model structure of XBeach is shown in Fig. 3.1.

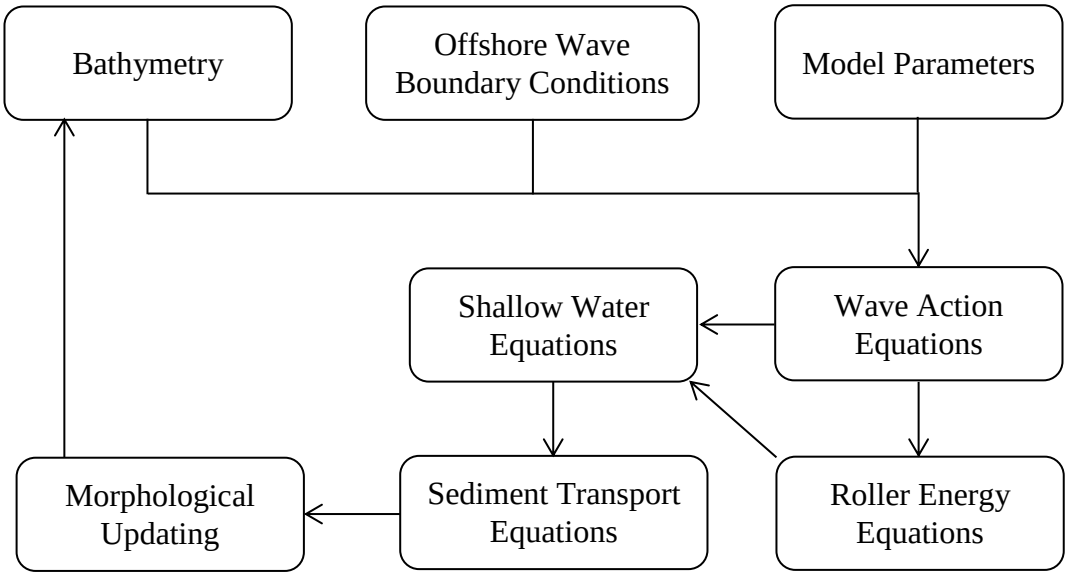

Figure 3.1: XBeach structure

As shown in Fig. 3.1, in XBeach, the first step is to define site and case related parameters which are bathymetry and offshore wave boundary conditions and the model parameters.

Second step is the computation of wave action equation defined in XBeach. In this step, the numerical model computes wave forcing in shallow water by solving time dependent wave action balance equation.

In the third step, roller energy equations are used to determine the surface stresses by taking the wave energy dissipation due to random wave breaking as a source term.

In the fourth step, using the momentum and mass conservation equations, mainly defined as shallow water equations are calculated.

In the fifth step, by using the sediment transport formulations equilibrium sediment concentration are calculated.

In the final step, morphological updating of the bathymetry is done and new bathymetry of the region is obtained.

The cycle defined above continues until the end of the simulation. In following parts of this chapter, the structure of XBeach shown in Fig. 3.1 will be presented in details.

3.1. Coordinate System

XBeach uses a coordinate system where x axis is always defined towards shoreline and y axis is defined alongshore. This coordinate system is defined relative to world coordinates by using origin of world coordinates and the orientation angle alpha defined counter clockwise with respect to x axis of world coordinates. XBeach coordinate system definition is shown in Fig.3.2.

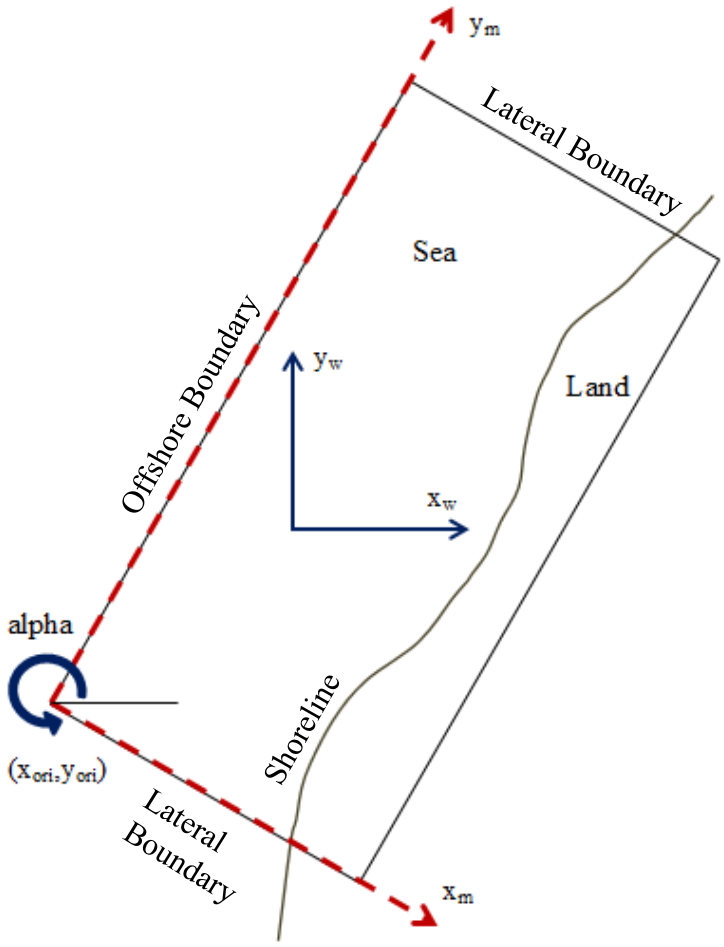

Figure 3.2: XBeach coordinate system definition

In Figure 3.2,

x_{ori}: x-coordinate of origin in world coordinates

y_{ori}: y-coordinate of origin in world coordinates

x_w: x-axis in world coordinates

y_w: y-axis in world coordinates

x_m: x-axis in model coordinates

y_m: y-axis in model coordinates

alpha: Grid orientation angle

3.2. Grid Definitions

Grids used in XBeach are staggered grids that mean bed levels, water levels, water depths and concentrations are defined in cell centers, on the other hand, velocities and sediment transports are defined in cell interfaces. In Fig. 3.3, grid system used in XBeach is shown.

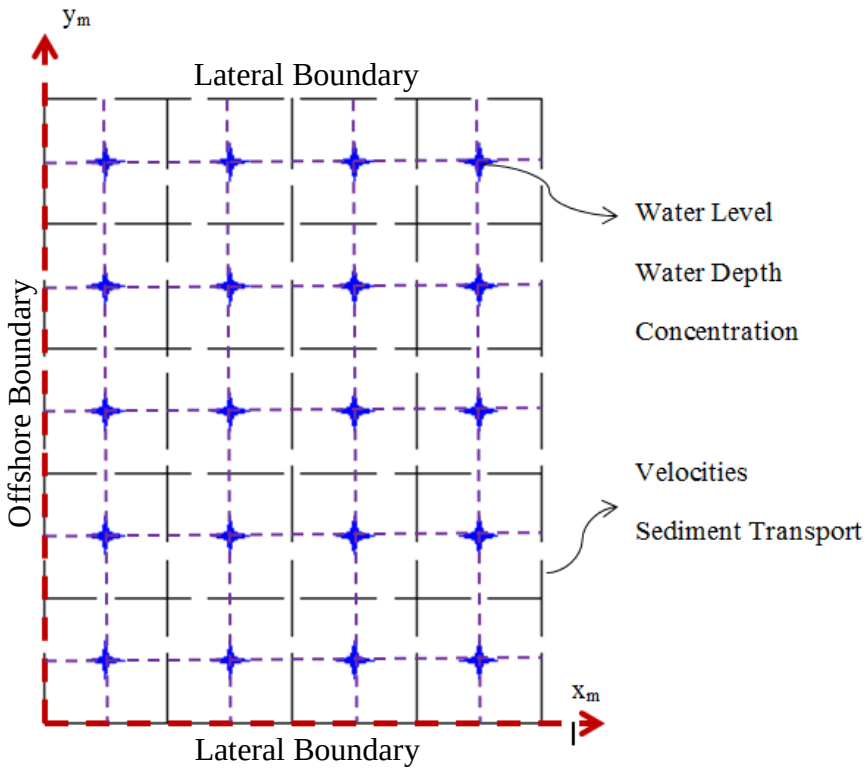

Figure 3.3: XBeach grid definition

3.3. Model Formulations

The governing model formulations used in XBeach are presented in the following order in this part of the study,

3.3.1. Wave action equation
3.3.2. Roller energy equation
3.3.3. Shallow water equations
3.3.4. Sediment transport equations
3.3.5. Morphological updating

3.3.1. Wave Action Equation

In XBeach, wave forcing in shallow water is obtained by solving time dependent wave action balance equation given in Eq.3.1.

$$\frac{\partial A}{\partial t}+\frac{\partial c_x A}{\partial x}+\frac{\partial c_y A}{\partial y}+\frac{\partial c_\theta A}{\partial \theta}=-\frac{D_w}{\sigma} \quad [3.1]$$

where wave action (A) is defined as;

$$A(x,y,t,\theta)=\frac{S_w(x,y,t,\theta)}{\sigma(x,y,t)} \quad [3.2]$$

Here,

D_w: The total wave energy dissipation

θ: The angle of incidence with respect to computational x-axis,

S_w: The wave energy density in directional bin

σ: Intrinsic wave frequency.

c_x: The wave action propagation speed for x direction

c_y: The wave action propagation speed for y direction

c_θ: The wave action propagation speed in space θ

The wave action propagation speeds for x and y directions, c_x and c_y in Eq. 3.1, are given in the following equations.

$$c_x(x,y,t,\theta)=c_g\cos\theta+u^L \quad [3.3]$$

$$c_y(x,y,t,\theta)=c_g\sin\theta+v^L \quad [3.4]$$

Here,

u^L: Cross-shore depth-averaged Langrangian velocity

v^L: Alongshore depth-averaged Langrangian velocity

c_g: Group velocity, obtained from linear theory.

Last terms of Eq. 3.3 and Eq. 3.4 are not taken into account if the wave current interaction is not used in model i.e. turned off in XBeach.

The propagation speed in space θ, c_θ given in Eq. 3.1, is obtained by using the following formula.

$$c_\theta(x,y,t,\theta) = \frac{\sigma}{\sinh 2kh}\left[\frac{\partial h}{\partial x}\sin\theta - \frac{\partial h}{\partial y}\sin\theta\right] + \cos\theta\left[\sin\theta\frac{\partial u}{\partial x} - \cos\theta\frac{\partial u}{\partial y}\right] + \sin\theta\left[\sin\theta\frac{\partial v}{\partial x} - \cos\theta\frac{\partial v}{\partial y}\right] \quad [3.5]$$

Here,

k: Wave number

h: Total water depth

u: Cross-shore depth averaged velocity

v: Alongshore depth averaged velocity

θ: The angle of incidence with respect to computational x-axis,

Taking into account bottom refraction (first term on the RHS) and current refraction (last two terms on the RHS) and h is the total water depth. The wave number k is obtained from the eikonal equations as follows.

$$\frac{\partial k_x}{\partial t} + \frac{\partial \omega}{\partial x} = 0 \quad [3.6]$$

$$\frac{\partial k_y}{\partial t} + \frac{\partial \omega}{\partial y} = 0 \quad [3.7]$$

Here,

k_x: Wave vector component in x-direction

k_y: Wave vector component in y-direction

ω: Absolute radial frequency

The wave number is then obtained from,

$$k = \sqrt{k_x^2 + k_y^2} \qquad [3.8]$$

Here,

k: Wave number

k_x: Wave vector component in x-direction

k_y: Wave vector component in y-direction

The absolute radial frequency is calculated from,

$$\omega = \sigma + k_x u^L + k_y v^L \qquad [3.9]$$

Here,

σ: Intrinsic wave frequency.

k_x: Wave vector component in x-direction

k_y: Wave vector component in y-direction

u^L: Cross-shore depth-averaged Langrangian velocity

v^L: Alongshore depth-averaged Langrangian velocity

ω: Absolute radial frequency

The total wave energy dissipation due to wave breaking is modelled according to Roelvink, 1993a is given in Eq. 3.10.

$$\overline{D_w} = \frac{\alpha}{\pi} Q_b \sigma E_w \qquad [3.10]$$

and

$$Q_b = 1 - \exp\left(-\left(\frac{H_{rms}}{H_{\max}} \right)^n \right) \quad with \quad H_{rms} = \sqrt{\frac{8E_w}{\rho g}}, H_{\max} = \frac{\gamma \tanh kd}{h} \qquad [3.11]$$

Here,

$\overline{D_w}$: Total wave energy dissipation due to wave breaking according to Roelvink, 1993a

E_w: Total wave energy

Q_b: Fraction of breaking waves

H_{rms}: Root mean square wave height

H_{max}: Maximum wave height

γ: Breaker index

ρ: Water density

g: Gravitational acceleration

k: Wave number

h: Total water depth

Total wave energy given in Eq. 3.10 and Eq. 3.11 are calculated by using the following formula.

$$E_w(x,y,t) = \int_0^{2\pi} S_w(x,y,t,\theta) d\theta \qquad [3.12]$$

Here,

S_w: Energy density in each directional bin

Total wave dissipation distributed proportionally over the wave directions is obtained by Eq. 3.13.

$$D_w(x,y,t,\theta) = \frac{S_w(x,y,t,\theta)}{E_w(x,y,t)} \overline{D_w}(x,y,t) \qquad [3.12]$$

Here,

S_w: Energy density in each directional bin

E_w: Total wave energy

$\overline{D_w}$: Total wave energy dissipation due to wave breaking according to Roelvink, 1993a

The components of radiation stresses are:

$$S_{xx,w}(x,y,t) = \int \left(\frac{c_g}{c}\left(1+\cos^2\theta\right) - \frac{1}{2} \right) S_w d\theta \quad [3.13]$$

$$S_{xy,w}(x,y,t) = \int \sin\theta\cos\theta \left(\frac{c_g}{c} S_w \right) d\theta \quad [3.14]$$

$$S_{yy,w}(x,y,t) = \int \left(\frac{c_g}{c}\left(1+\sin^2\theta\right) - \frac{1}{2} \right) S_w d\theta \quad [3.15]$$

Here,

S_{xx}, S_{yy}, S_{xy} : Radiation stresses due to wave action

According to Eq. 3.1 to Eq. 3.15 wave actions are solved in XBeach (Roelvink, et al., 2010).

3.3.2. Roller Energy Equation

The roller energy is coupled to the wave action equation or energy balance equation in which wave energy dissipation is used as a source for the roller energy equation (Roelvink, et al., 2010). The roller energy balance equation is presented in Eq. 3.16.

$$\frac{\partial S_r}{\partial t} + \frac{\partial c_x S_r}{\partial x} + \frac{\partial c_y S_r}{\partial y} + \frac{\partial c_\theta S_r}{\partial \theta} = -D_r + D_w \quad [3.16]$$

Here,

D_w: The total wave energy dissipation

D_r: Roller energy dissipation

S_r : Roller energy in each directional bin

c_x: The wave action propagation speed for x direction

c_y: The wave action propagation speed for y direction

c_θ: The wave action propagation speed in space θ

The roller energy propagation speeds in x and y directions given as c_x and c_y in Eq.3.6 can be calculated by using the following two equations.

$$c_x(x,y,t,\theta) = c\cos\theta + u^L \quad [3.17]$$

$$c_y(x,y,t,\theta) = c\sin\theta + v^L \quad [3.18]$$

Here,

c: The phase velocity found from linear theory

θ: The angle of incidence with respect to x-axis

u^L: Cross-shore depth-averaged Langrangian velocity

v^L: Alongshore depth-averaged Langrangian velocity

If the wave current interaction is not used, the last terms given in Eq.3.17 and Eq.3.18 are not taken into account.

The total roller energy dissipation is calculated according to Reniers et. al., 2004a is given in Eq. 3.19.

$$\overline{D_r} = \frac{2g\beta_r E_r}{c} \quad [3.19]$$

Here,

g: Gravitational acceleration

c: The phase velocity found from linear theory

E_r: Total roller energy

$\overline{D_r}$: Roller energy dissipation

Total roller energy distributed proportionally over the wave directions is obtained by Eq. 3.20.

$$D_r(x,y,t,\theta) = \frac{S_r(x,y,t,\theta)}{E_r(x,y,t)}\overline{D_r}(x,y,t) \quad [3.20]$$

Here,

S_r: Roller energy in each directional bin

Er: Total roller energy

$\overline{D_r}$: Roller energy dissipation according to Reniers et. al., 2004a

θ: The angle of incidence with respect to x-axis

The components of radiation stresses are:

$$S_{xx,r}(x,y,t) = \int \cos^2\theta \times S_r d\theta \quad [3.21]$$

$$S_{xy,r}(x,y,t) = \int \sin\theta\cos\theta \times S_r d\theta \quad [3.22]$$

$$S_{yy,r}(x,y,t) = \int \sin^2\theta \times S_r d\theta \quad [3.23]$$

Here,

S_{xx}, S_{yy}, S_{xy} : Radiation stresses due to roller action

The roller energy is calculated with the formulations given in Eq. 3.16 to Eq. 3.23 by XBeach.

The total wave forcing (Eq. 3.24) is obtained by the summation of wave and roller action induced radiations stresses.

$$F_x(x,y,t) = -\left(\frac{\partial S_{xx,w} + S_{xx,r}}{\partial x} + \frac{\partial S_{xy,w} + S_{xy,r}}{\partial y}\right)$$
$$F_y(x,y,t) = -\left(\frac{\partial S_{xy,w} + S_{xy,r}}{\partial x} + \frac{\partial S_{yy,w} + S_{yy,r}}{\partial y}\right) \quad [3.24]$$

Here,

F_x: Total wave forcing in x direction

F_y: Total wave forcing in y direction

$S_{xx,w}$, $S_{xy,w}$: Radiation stresses due to wave action

$S_{xx,r}$, $S_{xy,r}$: Radiation stresses due to roller action

3.3.3. Shallow Water Equations

Shallow water equations are used to compute low frequency and mean flow in XBeach. Depth averaged Generalized Langrangian Mean (GLM) formulation (Andrews and McIntyre, 1978) is used in order to include wave induced mass-flux and return flow. In such a framework, the momentum and continuity equations are formulated in terms of the Lagrangian velocity, u^L, which is defined as the distance a water particle travels in one wave period, divided by that period (Roelvink, et al.,2010). The relation between this velocity and Eulerian velocity, which is the depth averaged mean current velocity not induced by the waves, is given in Eq. 3.25 and Eq. 3.26.

$$u^L = u^E + u^S \quad [3.25]$$

$$v^L = v^E + v^S \quad [3.26]$$

Here,

u^L: Cross-shore depth-averaged Langrangian velocity

v^L: Alongshore depth-averaged Langrangian velocity

u^E: Cross-shore depth-averaged Eulerian velocity

v^E: Alongshore depth-averaged Eulerian velocity

u^S: Stokes drift in x direction

v^S: Stokes drift in y direction

The Eq. 3.27 given below is used to calculate Stokes drift values.

$$u^S = \frac{E_w \cos\theta}{\rho hc} \quad and \quad v^S = \frac{E_w \sin\theta}{\rho hc} \quad [3.27]$$

Here,

g: Gravitational acceleration

c: The phase velocity found from linear theory

h: Total water depth

E_W: Total wave energy

θ: The angle of incidence with respect to x-axis

The resulting GLM momentum equations are given by the Eq. 3.28, Eq. 3.29 and Eq. 3.30 given below.

$$\frac{\partial u^L}{\partial t} + u^L \frac{\partial u^L}{\partial x} + v^L \frac{\partial u^L}{\partial y} - fv^L - \nu_h \left(\frac{\partial^2 u^L}{\partial x^2} + \frac{\partial^2 u^L}{\partial y^2} \right) = \frac{\tau_{sx}}{\rho h} - \frac{\tau_{bx}^E}{\rho h} - g \frac{\partial \eta}{\partial x} + \frac{F_x}{\rho h} \quad [3.28]$$

$$\frac{\partial v^L}{\partial t} + u^L \frac{\partial v^L}{\partial x} + v^L \frac{\partial v^L}{\partial y} - fu^L - \nu_h \left(\frac{\partial^2 v^L}{\partial x^2} + \frac{\partial^2 v^L}{\partial y^2} \right) = \frac{\tau_{sy}}{\rho h} - \frac{\tau_{by}^E}{\rho h} - g \frac{\partial \eta}{\partial y} + \frac{F_y}{\rho h} \quad [3.29]$$

$$\frac{\partial \eta}{\partial t} + \frac{\partial h u^L}{\partial x} + \frac{\partial h v^L}{\partial y} = 0 \quad [3.30]$$

Here,

τ_{bx} and τ_{by}: Bed shear stresses

η: Represents water level

F_x and F_y: The wave induced forces

f : Coriolis viscosity

ν_h: Viscosity

u^L: Cross-shore depth-averaged Langrangian velocity

v^L: Alongshore depth-averaged Langrangian velocity

g: Gravitational acceleration

τ_{sx} and τ_{sy}: Wind stresses over the x and y directions, respectively

ρ: Water density

3.3.4. Sediment Transport Equations

Sediment transport in XBeach is modelled using depth averaged advection diffusion equation (Galappatti and Vreugdenhil, 1985) given below.

$$\frac{\partial hC}{\partial t}+\frac{\partial hCu^{E}}{\partial x}+\frac{\partial hCv^{E}}{\partial y}+\frac{\partial}{\partial x}\left[D_h h\frac{\partial C}{x}\right]+\frac{\partial}{\partial y}\left[D_h h\frac{\partial C}{y}\right]=\frac{hC_{eq}-hC}{T_s} \qquad [3.31]$$

Here,

C: Depth average sediment concentration varying on the wave group time scale,

C_{eq}: Equilibrium sediment concentration

D_h: Sediment diffusion coefficient

u^E: Cross-shore depth-averaged Eulerian velocity

v^E: Alongshore depth-averaged Eulerian velocity

h: Total water depth

T_s: Adaption time for the entrainment of the sediment.

The equation used to calculate T_s by using local water depth and sediment velocity is given in Eq. 3.32.

$$T_s=\max\left(0.05\frac{h}{w_s},0.2\right) \qquad [3.32]$$

Here,

h: Total water depth

ω_s: Sediment fall velocity

In XBeach, the equilibrium sediment concentration is calculated by using the sediment transport formulation of Soulsby-van Rijn (Soulsby, 1997).

$$C_{eq}=\frac{A_{sb}+A_{ss}}{h}\left(\left(\left|u^{\hat{E}}\right|^2+0.018\frac{u_{rms}}{C_d}\right)^{0.5}-u_{cr}\right)^{2.4}(1-\alpha_b m)=0 \qquad [3.33]$$

Here,

A_{sb}: Bed load coefficient

A_{ss}: Suspended load coefficient

h: Total water depth

u^E: Cross-shore depth-averaged Eulerian velocity

C_d: Drag coefficient

u_{rms}: Near bed short-wave orbital velocity

u_{cr}: Critical velocity for the sediment motion initiation

m: Bed slope

α_b: Calibration factor

Depending on the sediment transport, the bed level change is calculated by using Eq. 3.34.

$$\frac{\partial z_b}{\partial t} + \frac{f_{mor}}{(1-p)}\left(\frac{\partial q_x}{\partial x} + \frac{\partial q_y}{\partial y}\right) = 0 \qquad [3.34]$$

Here,

z_b: Bed level

p: Porosity

f_{mor}: Morphological acceleration factor

q_x: Sediment transport rate in x direction

q_y: Sediment transport rate in y direction

The sediment transport rates in x and y directions are calculated using Eq.3.35

$$q_x(x,y,t) = \left[\frac{\partial hCu^E}{\partial x}\right] + \left[\frac{\partial}{\partial x}\left[D_g h \frac{\partial C}{\partial x}\right]\right] \qquad [3.35]$$

$$q_y(x,y,t) = \left[\frac{\partial hCv^E}{\partial y}\right] + \left[\frac{\partial}{\partial y}\left[D_g h \frac{\partial C}{\partial y}\right]\right] \quad [3.36]$$

Here,

h: Total water depth

u^E: Cross-shore depth-averaged Eulerian velocity

v^E: Alongshore depth-averaged Eulerian velocity

C: Depth average sediment concentration varying on the wave group time scale

D_g: Sediment diffusion coefficient

3.3.5. Morphological Updating

For the updating bed-evolution, avalanching term is introduced in order to account for the slumping of sandy material during storm-induced dune erosion. This term is introduced when user defines the critical bed slope (Roelvink, et al.,2010).

$$\left|\frac{\partial z_b}{\partial x}\right| > m_{cr} \quad [3.37]$$

where the estimated bed slope is

$$\frac{\partial z_b}{\partial x} = \frac{z_{b,i+1,j} - z_{b,i,j}}{\Delta x} \quad [3.38]$$

Here,

z_b: Bed level

m_{cr}: Critital bed slope

The bed change within one step is given by

$$\Delta z_b = \min\left(\left(\left|\frac{\partial z_b}{\partial x}\right| > m_{cr}\right)\Delta x, 0.05\Delta t\right), \quad \frac{\partial z_b}{\partial x} > 0 \quad [3.39]$$

$$\Delta z_b = \max\left(-\left(\left| \frac{\partial z_b}{\partial x} \right| > m_{cr} \right) \Delta x, -0.05\Delta t \right), \quad \frac{\partial z_b}{\partial x} < 0 \qquad [3.40]$$

Here,

Δz_b: Bed level change in one step

m_{cr}: Critital bed slope

3.4. Wave Boundary Conditions

There is 12-number of ways to define offshore wave boundary conditions in XBeach. These boundary conditions are,

1. Stationary wave boundary conditions

Uniform, constant wave energy distribution is set based on user defined root mean square wave height (H_{m0}) and significant wave period (T_{m0})

2. Wave energy varying periodically in time

In this case, regular wave groups are used.

3. First order, long-crested irregular wave groups

Energy is read as a function of time. Time series is shifted along the y-axis to account for oblique incidence (Roelvink et. al., 2010).

4. Second order, long-crested irregular wave groups

Using Longuet-Higgins and Stewart's (1964) theory, a bound wave is added to the wave groups (Roelvink et. al., 2010).

5. Standard Jonswap spectrum

By using the user defined spectrum coefficients, time series of wave energy varying alongshore and bound long wave are generated based on the specified 2D Jonswap spectrum (Roelvink et. al., 2010).

6. Unmodified SWAN 2D spectrum output file

With this option unmodified SWAN 2D output file can be used.

7. Formatted variance-density spectrum file

When the user has a 2D spectrum even if it is not obtained from SWAN or it is not in the form of Jonswap spectrum, user is able to create formatted spectrum file that can be read by XBeach (Roelvink et. al., 2010).

8. Reuse boundary condition files from an earlier XBeach simulation

This boundary condition can be used if user does not want to recalculate the boundary conditions or wants to use the boundary conditions calculated in another XBeach simulation (Roelvink et. al., 2010).

9. Boundary conditions for non-hydrostatic model

With this option, user is able to create a non-hydrostatic model which means non-linear shallow water equations with dispersion terms are solved (Roelvink et. al., 2010).

10. No boundary condition

With this option, there is no need to enter boundary conditions in order to simulate the model.

11. Sequence of stationary sea states

With this option, user is able to define series of stationary sea states each with duration.

12. Sequence of sea states to make time-varying wave groups

With this option user is able to define a sea state for a certain duration, then can specify another sea state without having to stop the model (Roelvink et.al., 2010).

3.5. Flow Boundary Conditions

3.5.1. Offshore Boundary Conditions

In Xbeach, there are different options available to define offshore boundary by setting different values to a parameter called *front* in model.

If this parameter is set as 0, a simple one dimensional radiating boundary condition is activated.

$$u = \left(1 + \frac{\sqrt{gh}}{c_g}\right) u_i + \bar{u} - \sqrt{\frac{g}{h}}(z_s - z_{s0}) \qquad [3.41]$$

Here,

u_i: Velocity of incoming particle

z_s: Surface elevation of incoming long wave

z_{s0}: Mean water level

g: Gravitational acceleration

c_g: Group velocity

h: Total water depth

$\bar{u}$: Mean velocity of current

When the parameter *front* is set as 1, the formulation by Van Dongeren and Svendsen (1997) is activated which is actually based on Verboom et al. (1981) and Method of Characteristics. This boundary condition allows for oblique waves and reflected waves; therefore, it can be used both for 1D and 2D computations. By using this condition, the final boundary condition is found with the summation of u_i , the velocity of incoming particle, $\bar{u}$, the mean velocity of current and u_r , the outgoing velocity (Roelvink, et al., 2010).

$$u_r = \left(\frac{\cos\theta_r}{\cos\theta_r + 1}\right)\left[\beta^- - \bar{u} + 2\sqrt{gh_0} - u_i\left(\frac{c_g \cos\theta_i - \sqrt{gh_0}}{c_g \cos\theta_i}\right)\right] \qquad [3.42]$$

$$\theta_r = \arctan\left(\frac{u_r}{v_r}\right) = \arctan\left(\frac{u_r}{v - v_i - \bar{v}}\right) \quad [3.43]$$

$$u = u_i + u_r + \bar{u} \quad [3.44]$$

Here,

u_i and v_i: Velocities of incoming particle in x and y directions

u_r and v_r: Outgoing velocities in x and y directions

$\bar{u}$ and $\bar{v}$: Mean velocity of currents in x and y directions

g: Gravitational acceleration

h_0: Initial total water depth

c_g: Group velocity

β^- : Reimann variant

θ_i: Incoming wave angle

θ_i: Outgoing wave angle

When the parameter *front* is set as 2, a simple no flux boundary condition is activated. When the parameter *front* is set as 3, water level is set to defined value from a file.

3.5.2. Lateral Flow Boundary Conditions

The boundaries defined perpendicular to the coastline are called as lateral boundaries. These boundaries are generally artificial depending on the limitation of model domain. In Xbeach, there are two options available for defining lateral boundaries as Neumann boundaries and no-flux boundaries. Neumann boundaries are the ones in which there is locally no change in surface elevations and velocities. No-flux boundaries are preferred over Neumann boundaries in 1D models (Roelvink et. al., 2010).

Neumann boundary conditions are shown in Fig. 3.4.

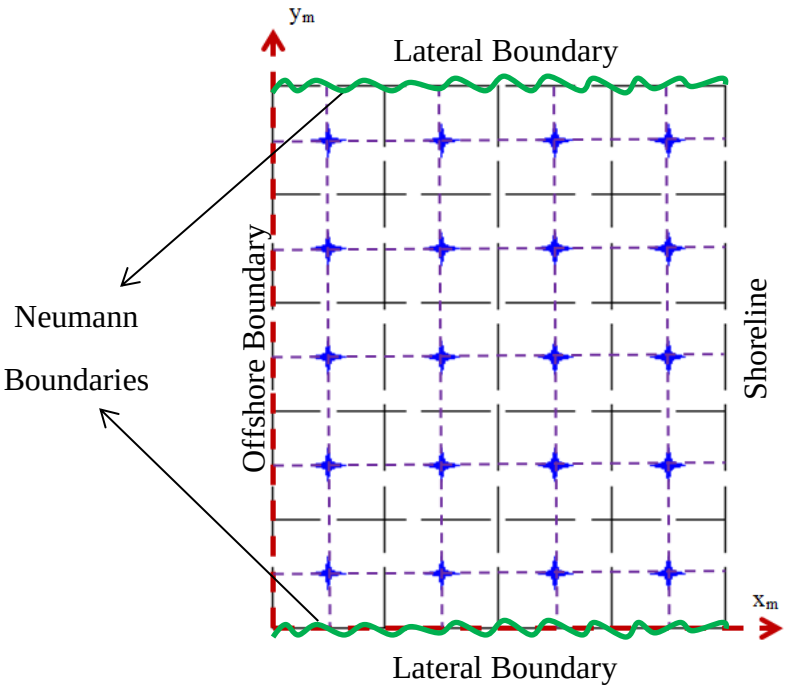

Figure 3.4: Neumann Boundary Conditions

CHAPTER 4

LONG TERM MODELLING OF YUMURTALIK REGION USING XBEACH

In this chapter, application of numerical model called XBeach (Roelvink et al.2010) and the comparison of the models results with field measurements are presented.

4.1. Introduction

Yumurtalık district in Adana, Turkey is located at a region where one of the most important crude oil pipelines, called Baku-Tbilisi-Ceyhan Crude Oil Pipeline (Fig. 4.1). This pipeline project is very important not only for Turkey but also for Caucasus since it is one of the most important trading incomes of the countries. The main purpose of this pipeline project is to make a link between Azerbaijani oil and world market.

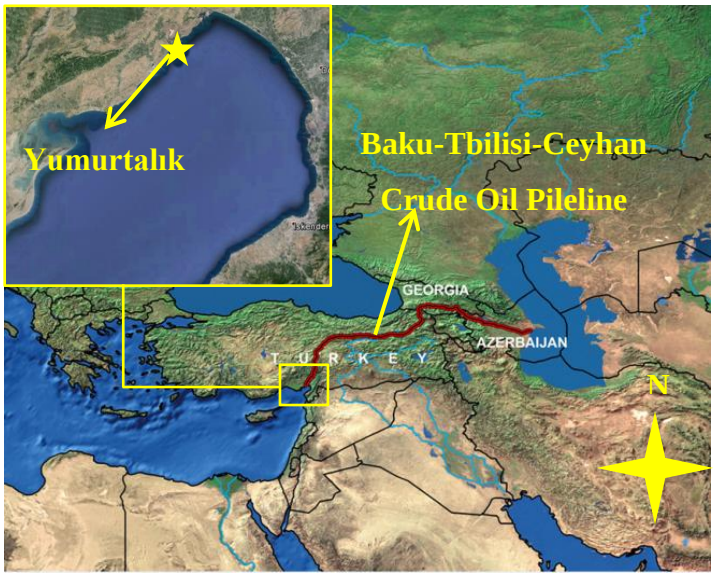

Figure 4.1: Location of Baku-Tbilisi-Ceyhan crude oil pipeline (http://www.botasint.com).

In order to transport Azerbaijani oil from Ceyhan, Turkey to world market, two piers, one causeway and two breakwaters (Fig. 4.2) were constructed in the area.

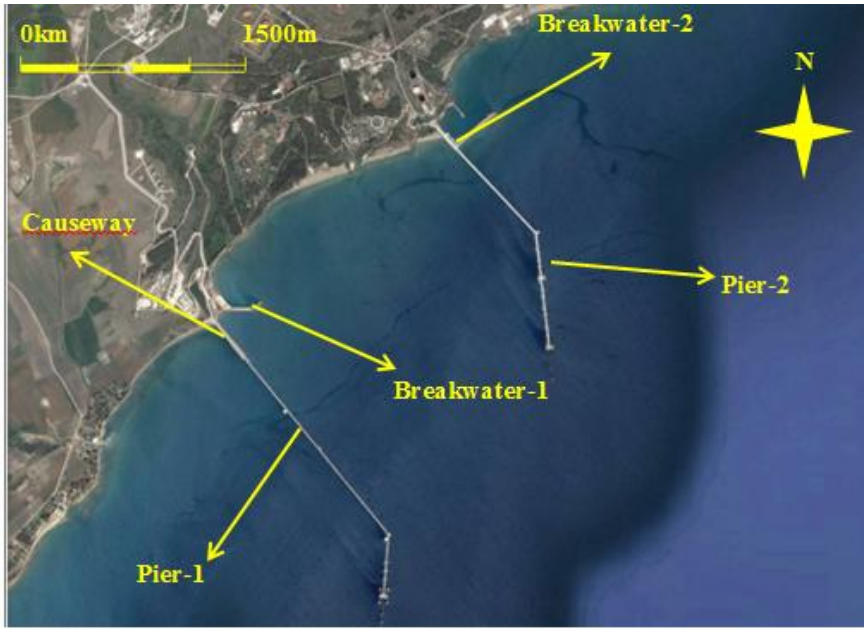

Figure 4.2: Plan view of marine structures in study area (Google Earth, 2014).

The evaluation of the effects of these breakwaters on sediment transport has become very important for two aspects. Firstly, the Gulf of Iskenderun, including the region of pipeline, is very important for the reproduction of endangered green sea turtles living in Mediterranean which are protected by World Wildlife Fund (WWF). Secondly, coastal erosion has become an increasing threat for the houses close to shoreline in the region. In order to understand the effects of the breakwaters to morphology, a monitoring process has been started on December, 2006 which is still ongoing. During this monitoring process until now, thirty shore-normal profiles which are approximately 200m long were selected and water depth measurements were taken on these profiles. During field measurements, no measurements were taken for shoreline change; therefore, no shoreline change comparison can be made.

In this study, the main purpose is to understand the general behaviour of sediment transport in the area in long term. For this purpose, although mainly developed for short term modelling, the open source numerical model called XBeach is preferred

since it is able to model both alongshore and cross shore sediment transport processes by making 2-DH (Fig. 2.4) simulations.

The terms long term and short term modelling given above can be simply defined as follows:

- Long term modelling refers to modelling sediment transport in seasonal and/or yearly time intervals to understand beach profile evolution or shoreline change during the defined time interval.
- Short term modelling refers to modelling sediment transport in hourly and/or daily time intervals to understand nearshore responses under extreme conditions.

The studies performed in order to understand general behaviour of sediment transport process in Yumurtalık region is presented in the following order.

In Section 4.2, detailed wind and wave climate analysis performed in order to determine wave characteristics in the Yumurtalık region are presented.

In Section 4.3, XBeach model prepared for Yumurtalık region with the assumptions made are given in this part of the study.

In Section 4.4, the evaluation of the results of the calibration study for XBeach model is presented.

In Section 4.5, according to the result of calibration study given in Part 4.4, the XBeach model verification and the evaluation of the results obtained from verification study are given.

In Section 4.6, depth of closure of the area is presented.

4.2. Wind and Wave Climate Analysis

4.2.1. Introduction

In wind and wave climate analysis, the following steps are followed.

- First wind data of Yumurtalık Meteorological Station (Fig.4.3) between the years 1973-2014 obtained from DMİGM (General Directorate of State Meteorological Affairs). Coordinates of the station are 36.7687N 35.7903E.

- Effective fetch lengths are calculated in order to obtain wave climate of the Yumurtalık region from wind data obtained.

- For wave hindcasting study "Deep Water Wave Hindcasting Mathematical Model, W61" (Ergin & Ozhan, 1986), mathematical model developed by METU, Department of Civil Engineering Ocean Engineering Research Centre, is used.

- By using the wave data obtained from the result of the mathematical model, W61, long term wave analysis is carried out.

4.2.2. Wind Data

In order to determine wave climate in the study area, data including the hourly average wind speeds and related directions measured on land at 10m above mean sea level at Yumurtalık Meteorological Station (Fig. 4.3) during the period of 1973-2014 are used. The selection of this station rather than other meteorological stations in the Gulf of Iskenderun and ECMWF depends on the following reasons:

- Yumurtalık Meteorological Station is determined as the best meteorological station since it is able to measure the wind speeds much correctly than the other stations near to study area. The main reason of this determination depends on the fact that the presence of buildings near to meteorological stations blocks the winds in the area. Although, all stations are surrounded by buildings Yumurtalık Meteorological Station is less affected from the blocking effect of buildings on winds; therefore, it is selected as best meteorological station for this study.

- The main reason of not using ECMWF wind data in this study is that since the Gulf of Iskenderun is a closed region, ECMWF stations in this area get affected from the land boundaries; therefore, they are not able to measure wind speeds as

correct as Yumurtalık Meteorological Station. Thus, ECMWF wind data is not used in this study.

Depending on the two reasons given above Yumurtalık Meteorological Station wind data is used as source term to determine deep water wave characteristics in this study.

Figure 4.3: Plan view of study area (Google Earth, 2014).

The wind data obtained from Yumurtalık Meteorological Station are measured on land. Since the boundary conditions of sea and land are different, wind speeds may vary; therefore, these wind data should be transformed to wind data measured on sea. In the transformation, Hsu (1980) formulation which gives the variation of wind speeds on land and sea presented in Eq. 4.1 is used.

$$U_{sea} = 3 \cdot (U_{land})^{2/3} \qquad [4.1]$$

According to this formula, wind speeds obtained from Yumurtalık Meteorological Station on land at 10m above stationary sea level are transformed into wind speeds on sea in order to use these data in wave hindcasting study.

4.2.3. Calculation of Effective Fetch Lengths

In order to transform wind data obtained from Yumurtalık Meteorological Station to wave data, effective fetch lenghts are calculated by assuming:

- Waves are generated over a range of 22.5˚ to either side of the wind direction and energy is transfer from wind to wave is proportional to cosine of the angle between waves wind and waves.
- Wave growth is proportional to fetch length.

For each direction, fetches are drawn with 7.50 degree intervals for each 22.50 degree interval on either side of the wind directions. By using the length of the fetches calculated, their weighted averages are taken for the determination of effective fetch lengths. For this calculation purpose, Eq. 4.2 given below is used.

$$F_{eff} = \frac{\sum F_i \cos^2 \alpha_i}{\sum \cos \alpha_i} \qquad [4.2]$$

where F_i is the fetch lengts and α_i is the direction.

A Google Earth image showing effective fetch directions is given in Fig. 4.4.

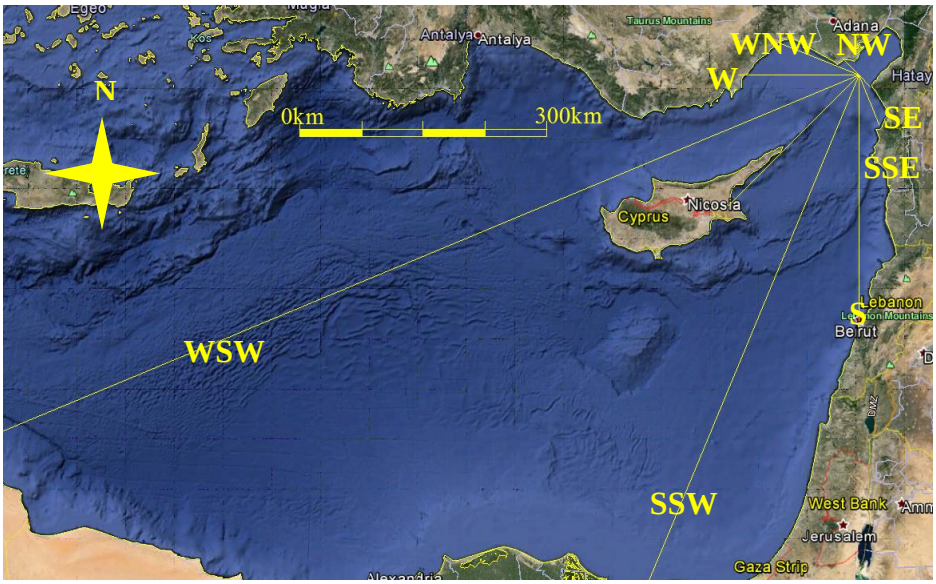

Figure 4.4: Effective fetch directions for study area (Google Earth, 2014).

For the directions NW to SE shown in Fig.4.4, effective fetch distances calculated are given in Table 4.1.

Table 4.1: Effective fetch lengths

Direction	Effective Fetch Lengths (km)
NW	22.82
WNW	73.23
W	501.91
WSW	575.12
SW	504.46
SSW	492.30
S	322.26
SSE	104.15
SE	28.52

4.2.4. Deep Water Significant Wave Steepness

Wave hindcasting studies are carried out in order to determine wave climate of the relevant region. For this study, wind data obtained from Yumurtalık Meteorological Station for the period of 1973-2014 and the effective fetch lengths calculated for each wind direction are used as the input parameters for the mathematical model, W61 which is used to determine hourly significant wave heights (H_{s0}, the average of 1/3 of the highest deep water wave heights) of the wind waves occurring during storms in the relevant years and their corresponding significant periods (T_s).

Using the deep water wave characteristics obtained from W61, deep water significant wave steepness (H_{s0}/L_0) is calculated as 0.039. The relationship between deep water significant wave height (H_{s0}) and deep water wave length (L_0) is shown in Fig 4.5.

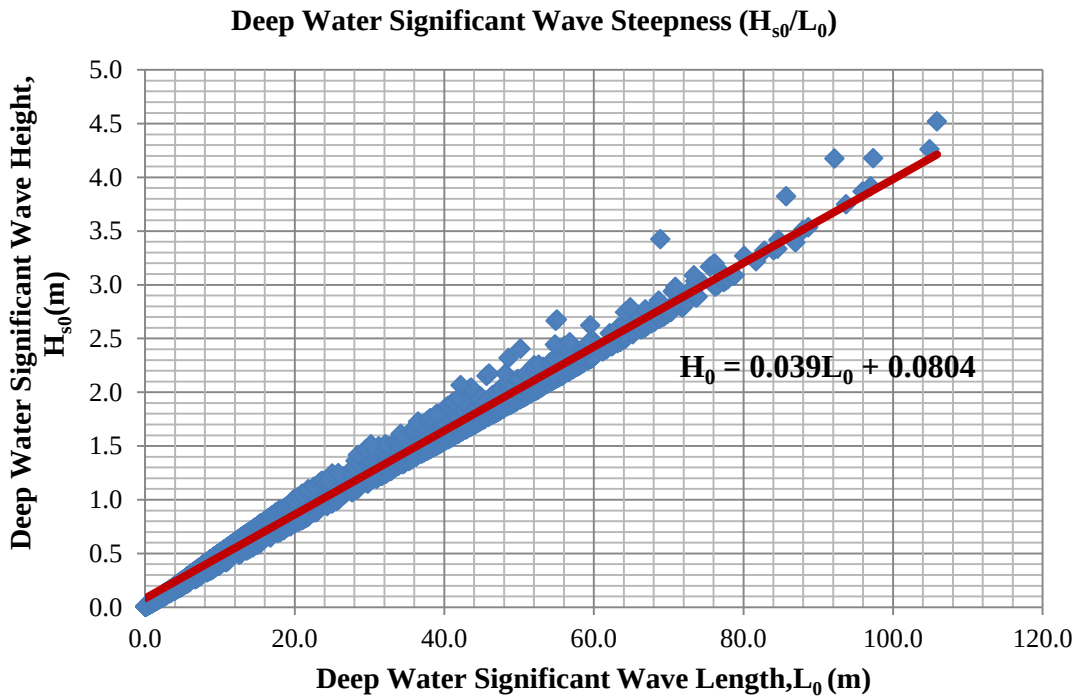

Figure 4.5: Deep Water Significant Wave Heights (H_{s0}) vs Deep Water Significant Wave Lengths (T_s)

4.2.5. Long Term Wave Statistics

Individual waves obtained as a result of wave hindcasting study are used to determine long term wave characteristics of the study area. Although, these wave characteristics are not used as input parameter for the XBeach model, in order to understand general behaviour of the wave climate in the region long term wave statistics is done. The annual exceedence probabilities of waves from different directions in a semi-log paper are given in Fig. 4.6.

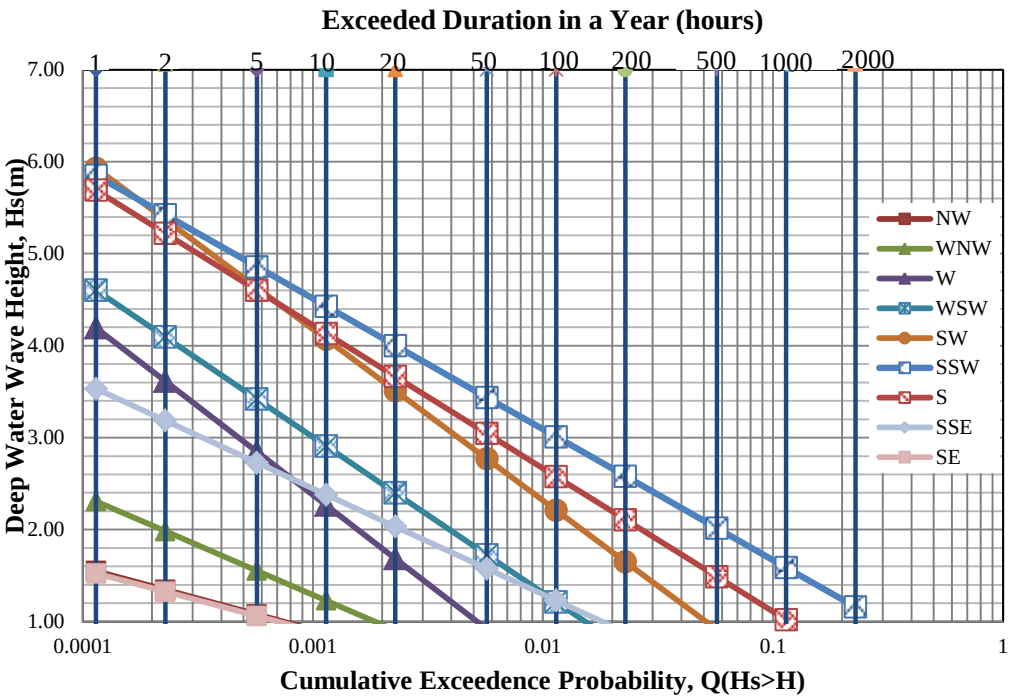

Figure 4.6: Long Term Wave Statistics Graph

For the given long term wave statistics graph, equations that gives the relationship between exceedance probabilities and deep water significant wave heights are presented in Table 4.2.

Table 4.2: Long Term Wave Statistics Probability Equations

Direction	Long Term Probability Equations
NW	H_s = -0.2931ln[Q(>Hs)]-1.1114
WNW	H_s = -0.4687ln[Q(>Hs)]-1.9467
W	H_s = -0.8378ln[Q(>Hs)]-3.41
WSW	H_s = -0.736ln[Q(>Hs)]-2.0777
SW	H_s = -0.8076ln[Q(>Hs)]-1.4013
SSW	H_s = -0.6173ln[Q(>Hs)]+0.2482
S	H_s = -0.6762ln[Q(>Hs)]-0.4472
SSE	H_s = -0.5ln[Q(>Hs)]-1.0069

Table 4.2 (Continue)

Direction	Long Term Probability Equations
SE	H_s = -0.2881ln[Q(>Hs)]-1.0913

4.2.6. Depth of Closure

Depth of closure of the study area is calculated by using the wave characteristics related with the dominant wave direction, which is determined as SSW, and the Eq. 2.14 suggested by Hallermeier (1978).

Significant wave height exceeded 12 hours per year ($H_{s,12}$) and significant wave period exceeded 12 hours per year ($T_{s,12}$) are determined as 4.31m and 8.42 sec, respectively. Using these values, depth of closure of the study area is determined as 8 m.

4.3. XBeach Model Set Up

4.3.1. Introduction

In this part of the thesis, assumptions, model set-up, model input parameters, calibration and verification studies of the model are presented.

4.3.2. Model Assumptions

In Chapter 3, it is described that XBeach is a numerical model used to understand extreme beach behaviour under storm and hurricane conditions. This brings a limitation to the program about the simulation time of the model (parameter named as tstop in XBeach) with maximum of 1 000 000 seconds which is approximately 12 days. Depending on this limitation, it is not possible to use XBeach in long-term simulations such as 3 or 4 years without making any assumptions. In order to overcome this limitation, consecutive runs by using the bathymetry of the previous run are carried out.

In Section 3.4, 12-way of defining offshore wave boundary conditions is described. In this study, boundary condition which used to define sequence of sea states to make time varying wave groups (12^{th} one) is selected to create randomness in the model.

Another important assumption made in this study is to assumption of the correctness of field measurements used in this study.

In addition to the assumptions given above since there is no information available for the sediment size from the field measurements, average sediment size (D_{50}) is assumed as 2 mm.

4.3.3. Model Domain

XBeach model is set up for the area between the two piers. A Google Earth image given in Fig. 4.7 shows the plan view of the study area for this model. The length between these two piers is about 2km long.

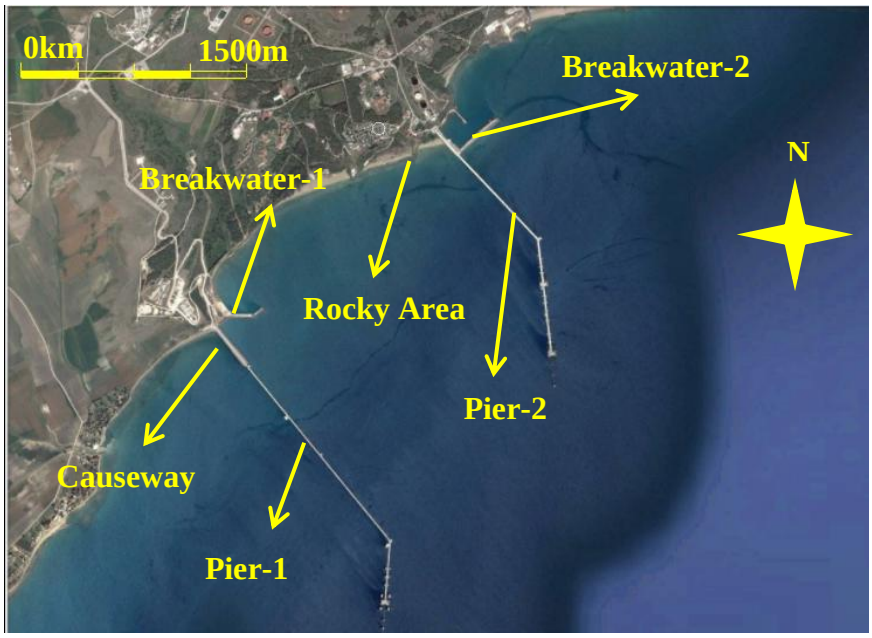

Figure 4.7: Plan view of the study area used in model (Google Earth, 2014).

In Fig. 4.7, from the marked regions, it can be seen that there exist five marine structures and a rocky region in the study area. For a correct model set up, the marine structures and the rocky area must be included in the model since they will play an

important role in sediment transport process for this region. In XBeach, however, there is no option available to define marine structures like breakwaters or groins as a structure. Instead of this, any structure or rocky area can be defined as non-erodible areas which work as the same manner with defining a marine structure. Therefore, in order to obtain a good model, the breakwaters, causeway and the rocky area shown in Fig. 4.7 are defined as non-erodible areas in the prepared XBeach model. However, the piers shown in Fig. 4.7 are not included in model since they are piled and their effect on sediment transport process is negligible.

In order to set up the model, the study area shown in Fig. 4.7 is digitized, and then by following the XBeach structure described in Chapter 3, the digitized area is transformed into model coordinates. The initial bathymetry of the area in December 2006, relationship between x-axes of world and model coordinates and December 2006 bathymetry in model coordinates are given in Fig. 4.8, Fig. 4.9 and Fig. 4.10, respectively.

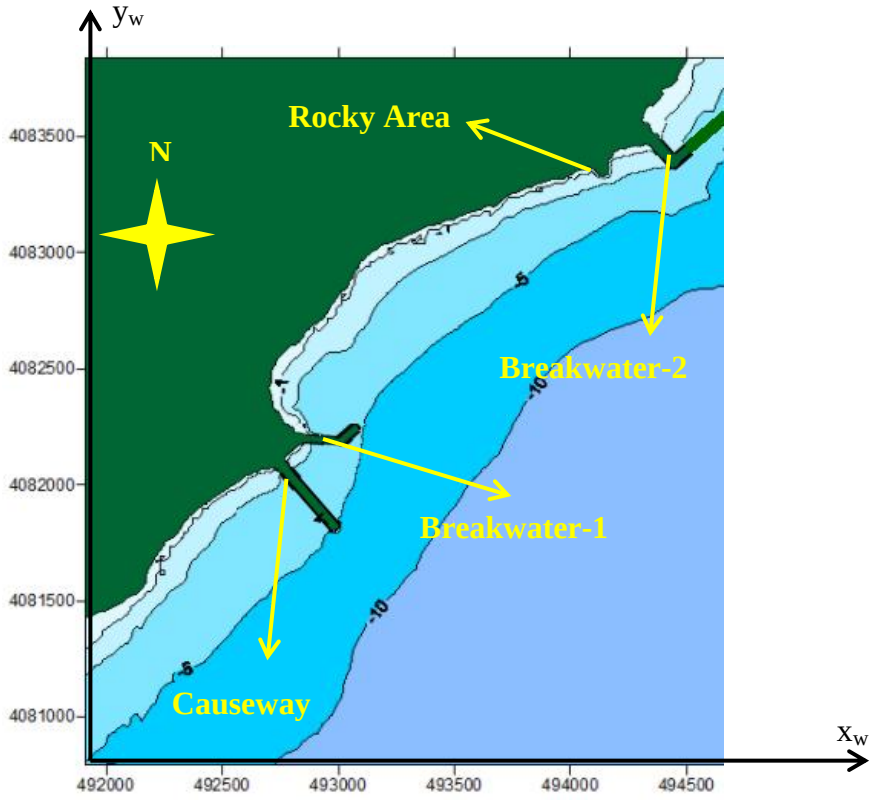

Figure 4.8: Digitized view of the study area in December 2006 in world coordinates

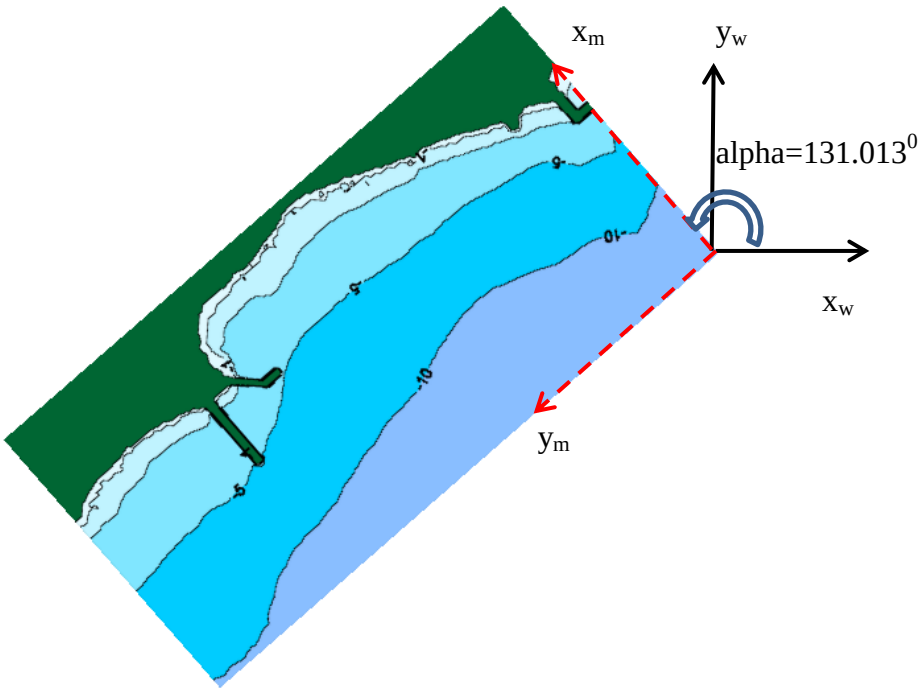

Figure 4.9: The Relationship between the x axes of world and model coordinates

In Chapter 3, it is said that the orientation of x-axis of model is towards shoreline and the angle measured counter clockwise between x-axes of world and model gives the orientation of grids used in model. From Fig. 4.9 the angle named as alpha is found as 131.013^0 measured counter clockwise.

The determination of angle alpha is important since it directly affects the direction of incoming waves provided in model. In addition, this angle can be used to transform model coordinated into world coordinates by defining origin location for the world coordinates.

December 2006 bathymetry in model coordinates used in XBeach is given in Fig. 4.10.

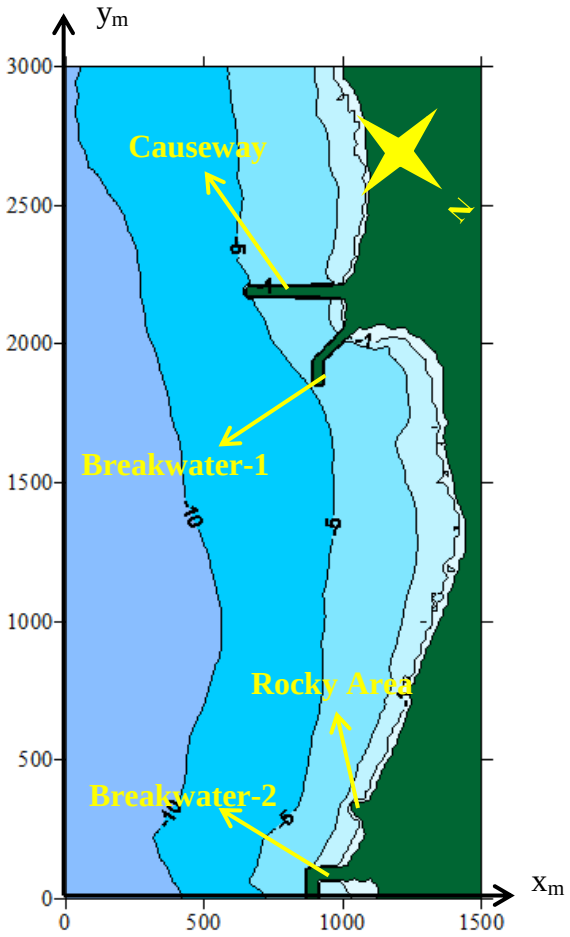

Figure 4.10: Digitized view of the study area in model coordinates in 2006

Using XBeach in model coordinates or world coordinates does not cause any difference i.e. either of solution will give the same result. The only difference between model coordinates and world coordinates is the way by which their grids are specified (Bieman, 2013). Depending on this explanation made by Bieman (2013), model coordinates are used in XBeach because of simplicity of tracking.

4.3.4. Model Wave Data

In order to run XBeach in long term, as a first step, representative waves as input must be determined. In this part of the thesis, studies made for determining the representative waves are described.

As it is said in Introduction, the main purpose of this thesis is to understand the general behaviour of sediment transport process in Yumurtalık region. Since the

available measurements are taken for 2 to 3 year-time periods yearly based wave data is assumed to represent actual wave condition. For this purpose, the representative waves are calculated by using Eq. 4.3 given below.

$$H_0 = \frac{\sum (P_i * H_i)}{\sum P_i} \quad [4.3]$$

where H_i and P_i represent wave height and occurrence probability of waves with height of H_i (Güler, 1997; Güler et al., 1998; Şafak, 2006; Baykal, 2006; Baykal, 2012).

Occurrence probability (P_i) of wave height (H_i) given in Eq. 4.3 is calculated as follows:

$$P_i = Q(H_i - k) + Q(H_i + k) \quad [4.4]$$

Here,

Q: Exceedence probability

k: Assigned range to compute occurrence probability

As model wave data, two wave data sets are prepared for the calibration and verification studies using Eq.4.3 and wave steepness calculated as 0.039 before.

First data set used in the calibration study of XBeach model includes the period between the years December, 2006 – December, 2009. The second data set includes the period between the years January, 2010 – December, 2011. In the calculation of average wave data for the given periods of times, wave data obtained from W61 mathematical model for the related time periods are used.

The probability distributions of these two data sets are shown in Fig.4.11 and Fig.4.12

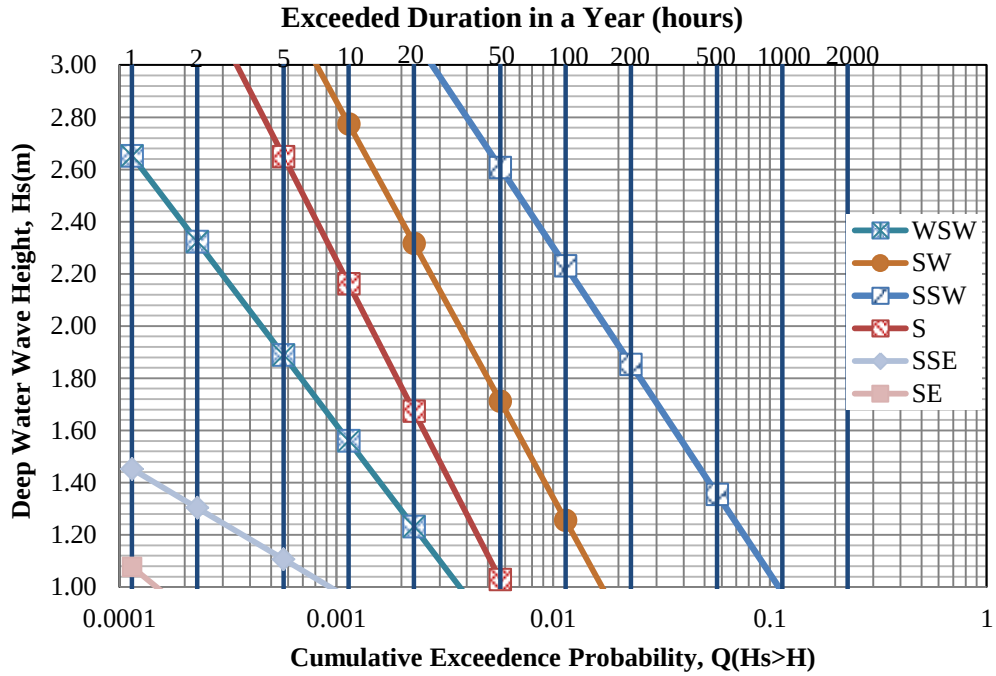

Figure 4.11: The probability distribution of first data set used in calibration study (December 2006 – December 2009)

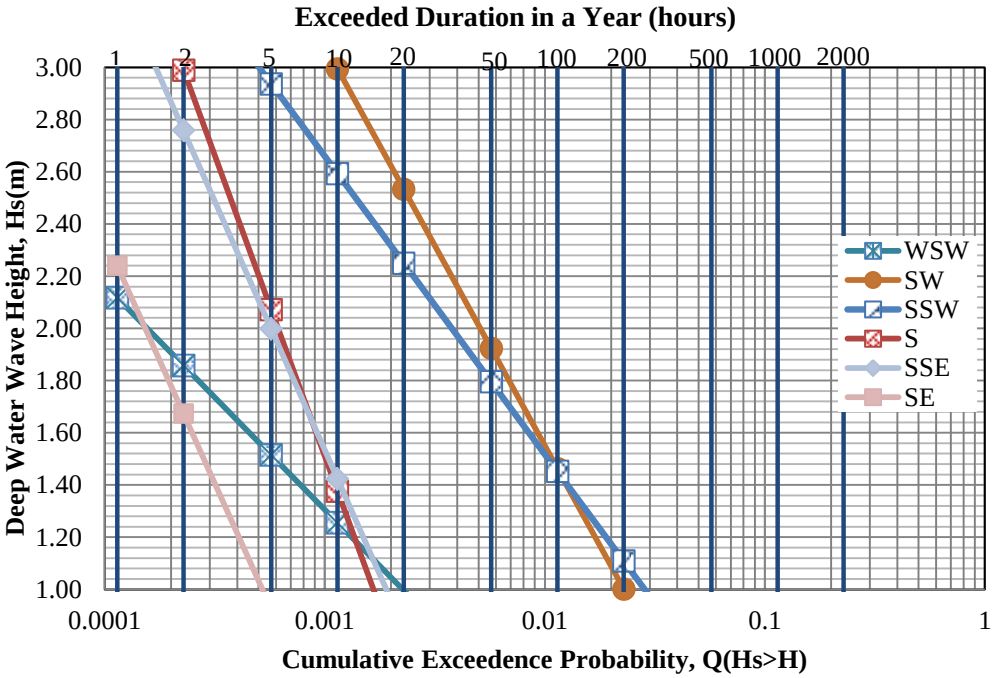

Figure 4.12: The probability distribution of second data set used in verification study (January 2010 - December 2011)

The log-linear probability distribution equations of the two data sets are shown in Table 4.3 and Table 4.4.

Table 4.3: Representative wave characteristics used in calibration study (December 2006 – December 2009)

Direction	Log-linear probability distribution equation
SE	Hs = -0.294748 * ln[Q(>Hs)] + (-1.513683)
SSE	Hs = -0.214915 * ln[Q(>Hs)] + (-0.436798)
S	Hs = -0.703759 * ln[Q(>Hs)] + (-2.404137)
SSW	Hs = -0.543488 * ln[Q(>Hs)] + (-0.044075)
SW	Hs = -0.659612 * ln[Q(>Hs)] + (-1.505030)
WSW	Hs = -0.474475 * ln[Q(>Hs)] + (-1.518607)

Table 4.4: Representative wave characteristics used in verification study (January 2010 - December 2011)

Direction	Log-linear probability distribution equation
SE	H_s = -0.817080 * ln[Q(>H_s)] + (-5.177926)
SSE	H_s = -0.829335 * ln[Q(>H_s)] + (-4.195836)
S	H_s = -1.002115 * ln[Q(>H_s)] + (-5.413073)
SSW	H_s = -0.495519 * ln[Q(>H_s)] + (-0.764047)
SW	H_s = -0.665155 * ln[Q(>H_s)] + (-1.512579)
WSW	H_s = -0.374163 * ln[Q(>H_s)] + (-1.279761)

Representative wave characteristics used in both calibration and verification analysis which are obtained from the log-linear probability distribution equations summarized in Table 4.3 and Table 4.4 are given in Table 4.5 and Table 4.6.

Table 4.5: Representative wave characteristics used in calibration study (December 2006 – December 2009)

Direction	H_s (m)	T_s (sec)	f (hours)
SE	1.35	4.72	0.52
SSE	1.30	4.63	2.68
S	1.73	5.34	24.53
SSW	1.58	5.10	440.28
SW	1.69	5.27	68.95
WSW	1.52	4.99	14.60

Table 4.6: Representative wave characteristics used in verification analysis (January 2010 - December 2011)

Direction	H_s (m)	T_s (sec)	f (hours)
SE	1.34	4.69	3.02
SSE	1.35	4.72	10.89
S	1.52	5.00	8.67
SSW	1.04	4.13	231.30
SW	1.20	4.34	149.29
WSW	0.93	3.91	23.99

After determination of representative waves in order to define offshore wave boundary conditions, spreading parameter (s) is also needed to be determined in XBeach. For the determination of best value of spreading parameter another run series is completed for different values of spreading parameter changing from 1 to 1000 which are the minimum and maximum values of this parameter defined in XBeach. Best value of spreading parameter is selected by considering the value

which covers at least 90% of wave energy confined in the related directional bin of 22.5 degrees in this study.

For determination of spreading parameter value, one-hour test case is simulated by selecting values of spreading parameter (s) given in Table 4.7.

Table 4.7: Values of spreading parameter (s) used in one-hour test case

Test Case No	**Value of Spreading Parameter (s)**
Test Case-1	1.0
Test Case-2	10.0
Test Case-3	25.0
Test Case-4	50.0
Test Case-5	100.0
Test Case-6	200.0
Test Case-7	500.0

In order to determine the correct value of spreading parameter all test cases given in Table 4.7 are simulated for one-hour. For one direction in model coordinates, simulation results for different values of spreading parameter are given in Appendix A in Fig. A.1 to Fig. A.8 as an example.

According to the result of these simulations, it is observed that when spreading parameter is selected as 1000, it covers the 90% of wave energy confined in the related directional bin 22.5 degrees. Thus, both in calibration and verification studies, 1000 is used as the value of spreading parameter.

4.3.5. Model Calibration Study

Having measurements as much as possible is important for a good modelling of sediment transport processes to understand morphological change of a beach. This is because the model is calibrated first for various values of the variables defined in

model and comparing the model results with the field data. Unfortunately, obtaining much data for model applications is not always possible and the amount of the data to be used in this study is rather limited.

In Yumurtalık region, at the study area, there is an on-going survey to monitor morphological changes for beaches between the two piers shown in Fig. 4.7. This monitoring process is carried out by an environmental engineering company called DOKAY and the data used in this study is obtained from this company.

For this monitoring process, initially, thirty sections are determined for the study area and for given the years listed in Table 4.8 field measurement have been performed.

Table 4.8: Date of Field Measurements in Yumurtalık Region

Number of Measurement	**Date of Measurement**
First Measurement	December, 2006
Second Measurement	January, 2010
Third Measurement	December, 2011
Fourth Measurement	December, 2013

As can be seen from Table 4.8, the time interval between subsequent field measurements is minimum 2 years. In addition, there are four to five elevation measurements on the profiles rather than continuous measurements along profiles. The differences between times of measurements and lack of elevation, shoreline and sediment size measurements are the main shortcomings of this monitoring process. In addition to these, profiles shown in Fig. 4.13 are not perpendicular to shoreline, which is not suitable to evaluate longshore sediment transport process, is the other shortcoming of this monitoring process. Despite these shortcomings, since field measurements are available for Yumurtalık region in order to understand the general behaviour of sediment transport process, this region is used in XBeach model. In Fig. 4.13, the profiles on which measurements were taken are shown.

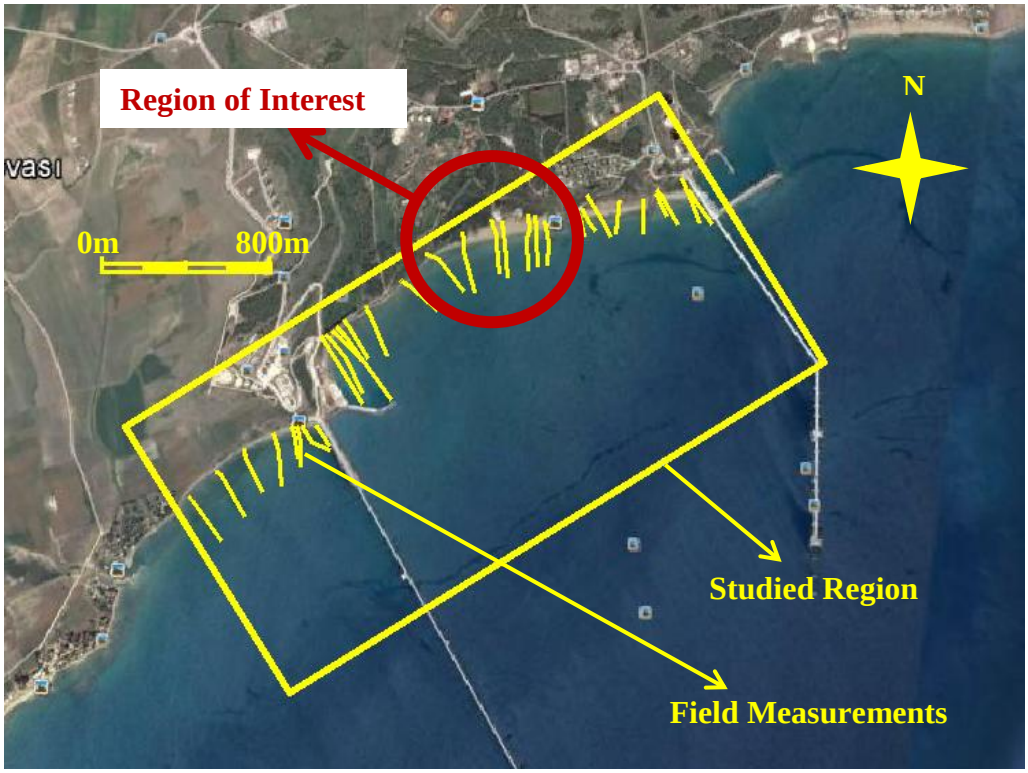

Figure 4.13: Field measurements (Google Earth, 2014).

The yellow lines shown in Fig.4.13 are the profiles on which monitoring surveys were done for the given years in Table 4.8 and the region marked with yellow rectangle represents the area on which model study is carried out. However, the focus on the comparison of the model results with the field measurements is given to the red circle in Fig. 4.13. The reason of confining the region of interest to the given measurements in the circular region is to understand the effect of marine structures nearby this region on sediment transport the morphology of the beach in front of the hotel located here. Therefore, only the profile measurements taken in this circular region are considered in both calibration and verification of the model.

Since detailed bathymetric surveys were not carried out during field measurements, the bathymetric map of the field measurement-years are obtained by combining the elevation measurements on profiles with linear interpolation.

As a first step, since there is no shoreline measurements were available, in order to understand the change of shoreline in long term, Google Earth satellite images are

evaluated. The shoreline changes between the years 2006 to 2009 and 2009 to 2013 are shown in Fig. 4.14.

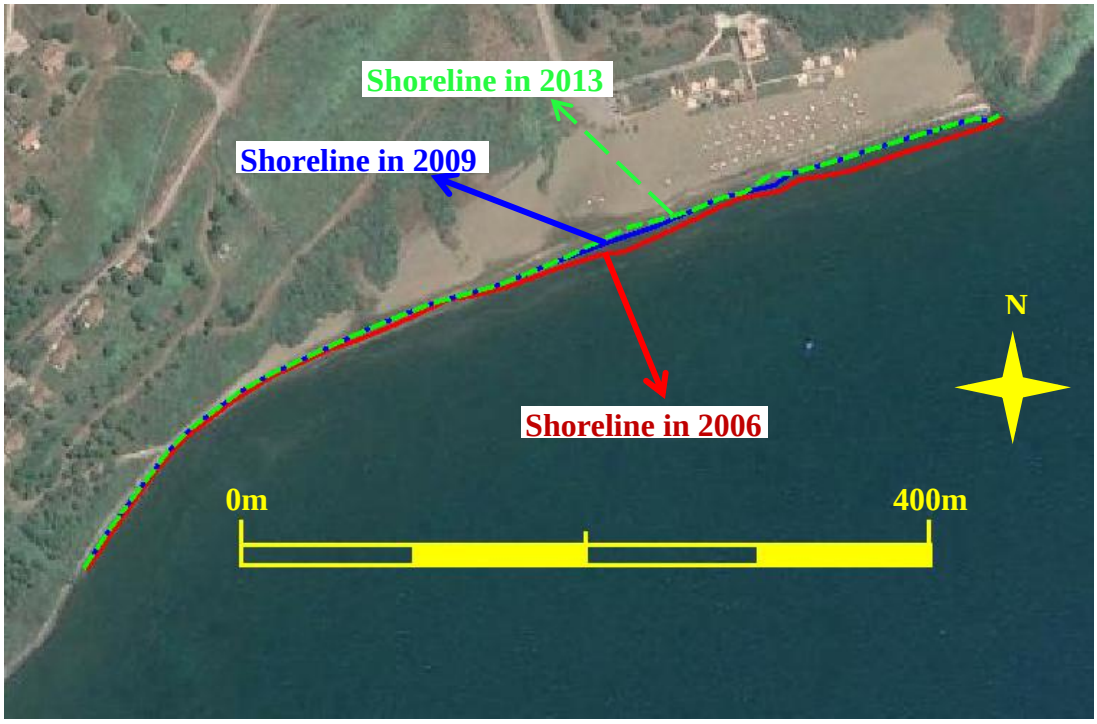

Figure 4.14: Shoreline change between the years 2006 to 2009 and 2009 to 2013 (Google Earth, 2014).

In Fig. 4.14, Google Earth satellite image is shown with the shorelines in 2006 (red line), 2009 (blue line) and 2013 (green line). It can be seen that significant erosion is observed between the years 2006 to 2009; on the other hand, for the years between the years 2009 to 2013, no significant change is observed. The reason of the significant erosion observed between the years 2006 to 2009 is not clearly understood since there is no significant change observed in the following years.

In order to calibrate XBeach model, the parameters that have significant effect on model are searched from various studies. In the study of Vousdoukas et.al.(2011), XBeach model is found to be sensitive to the parameters named *facua, wetslp* and *lws*. Using the conclusion of this study, extensive testing took place by considering the combinations of different values of these parameters. In Table 4.9, values of these important XBeach parameters with their descriptions used in test cases are

given. The combinations of these parameters used in each run series are given in Table 4.11.

Table 4.9: Values of important XBeach parameters used in calibration study

Parameter	**Description**	**Used Values For Calibration**
facua	Asymmetry transport	0, 0.5, 1
wetslp	Critical avalanching slope under water	0.1, 0.3, 1
lws	Long wave stirring	0, 1

- *facua* parameter is used to define wave asymmetry (In Eq. 3.31, when wave asymmetry defined, cross-shore and longshore depth averaged Eulerian velocities are replaced with sediment advection velocities due to skewness). For example, if the value of facua is selected zero, this means that there is no wave asymmetry; on the other hand, for the values different than zero, some asymmetry in waves is defined.
- *lws* parameter is used to include or exclude the effect of long waves (swell) (Eq. 3.33). For example if the value of *lws* is selected as zero, the effect of long waves is not considered.
- *wetslp* parameter used to describe critical avalanching slope towards offshore (Eq. 3.36). For larger values of this parameter, slope towards offshore decreases on the other hand, for small values, it increases.

For the given values of the parameters in Table 4.9, a total number of 18 runs obtained from different combination of the given parameters were performed for one year period. In calibration study, these 18-numbers of runs are repeated by 3 times for the years 2007-2009 in order test the model sensitivity to these input parameters.

Making long term runs in 2-DH XBeach model is very time consuming if a parameter called *morfac* in XBeach is not used. By definition, *morfac* is the morphological acceleration factor that speeds up the morphological time scale relative to the hydrodynamic timescale (Roelvink, et al.,2010). If an example is

given, for a 60 minutes of simulation, when a *morfac* of 6 is applied, model works just for 10 minutes and bottom change is multiplied by a factor 6 by which total computational time is saved with a factor of 6 (Roelvink, et al.,2010). Depending on this definition and example, in order to save time in simulation morfac is applied in model with a value of 20 in calibration study.

Grids used in XBeach model are defined as structured grid and grid size is selected as 20 m. In this study, the model sensitivity to grid size is not considered.

The computation time of the computer having Intel Core I7, 3.40 GHz processor and 8 GB Ram is approximately 2 hours for an approximately 200 hour-simulation with the value of *morfac* as 20.

In order to find the best combination of the parameters used in calibration study (Table 4.11), as an initial step areal comparisons of each run-series are performed by considering percentage errors. For this purpose, erosion and deposition values observed in three-years monitoring study area calculated and compared with the calculated values by XBeach. The study area used in calibration study is shown in Fig. 4.15 in terms of 2006 bathymetry.

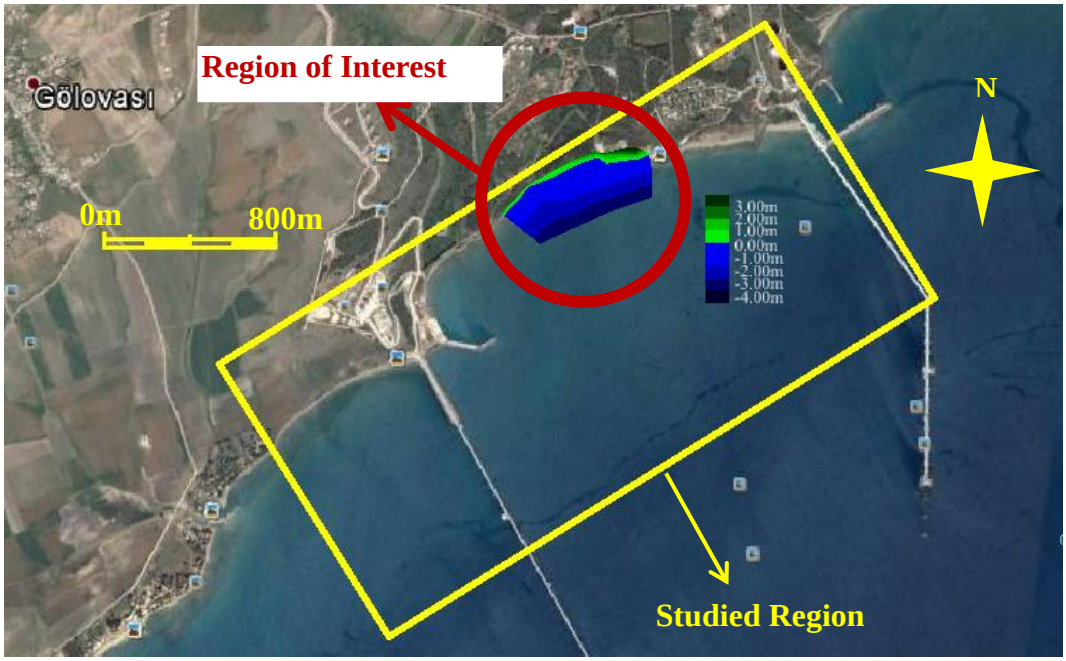

Figure 4.15: Study area used in calibration study (Google Earth, 2014).

The area shown in Fig. 4.15 is divided into four main regions by taking the areas between initial contour lines as control areas. The four-area used are shown in Fig. 4.16.

The four are shown in Fig. 4.16 covers the areas as follows:

- A1 covers the water depths between -4 m to -3 m
- A2 covers the water depths between -3 m to -2 m
- A3 covers the water depths between -2 m to -1 m
- A4 covers the water depths between -1 m to -0 m

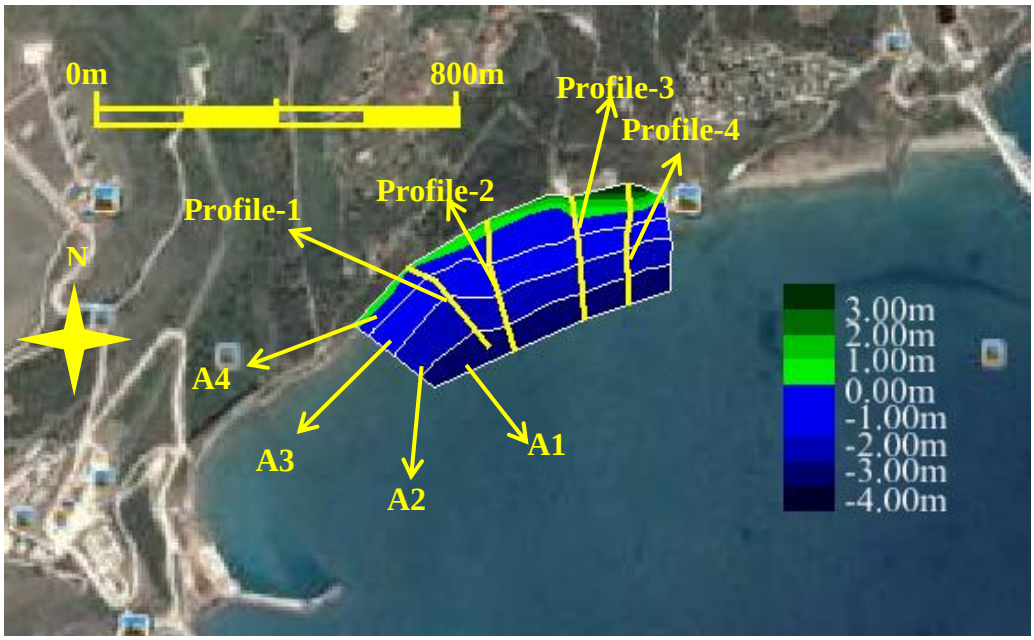

Figure 4.16: Areas used in calibration study (Google Earth, 2014).

The erosion and deposition volumes for each area shown in Fig. 4.16 are calculated for the period between the years 2006 and 2009. The ratio of net sediment transport in terms of erosion or deposition to the related area is calculated to understand the general trend of sediment transport and to make simple error calculation. The total erosion, deposition and net sediment transport ratios of each area are summarized in Table 4.10.

Table 4.10: Erosion and deposition volumes between the years 2006 to 2009

Area No	**d (m)**	**A (m^2)**	**Erosion (m^3)**	**Deposition (m^3)**	**Net Sediment Transport (m^3)**	**Type of Sediment Transport**	**Sediment Transport per m^2 (m^3/m^2)**
A1	-4 to -3	35376	0	5605	5605	Deposition	0.16
A2	-3 to -2	46178	69.5	5437	5367	Deposition	0.12
A3	-2 to -1	44217	887.6	4251	3363	Deposition	0.08
A4	-1 to 0	31640	479.4	11759	11280	Deposition	0.36

From Table 4.10, it is observed that sand deposition in the area is observed. According to shoreline evaluation performed with Google satellite images; however, some erosion is expected in the area named as A4. The main reason of this difference may depend on the fact that since elevation measurements on profiles are used to obtain bathymetric map of the area with linear interpolation for the year 2009, results obtained from these two studies are different. The errors observed in this area mainly depend on the insufficient field measurements taken in area A4 which is the most active zone in sediment transport processes. Thus, the results obtained in this area do not reveal the real world.

According to the results of calibration runs, it is observed that when model gets closer to the shoreline percentage of errors gets larger, as expected. In this part of the study the highest errors are not taken into account since the results that give bigger errors are not realistic. The error values calculated in areas A1 and A2 are used to find best run which gives the minimum total average error. After selection of the best fit run, in order to decrease the errors another calibration study is performed. The total average errors of each run in areal base are summarized in Table 4.11

Table 4.11: Percentage of errors of each run obtained from areal comparison

Run No	Value of Parameter			Σ Average Error (%)	Σ Average Error of Sum of A1 and A2 (%)
	facua	wetslp	lws		
Run-1	0	0.1	0	125.4	51.3
Run-2	0	0.1	1	131.2	50.0
Run-3	0	0.3	0	111.2	57.8
Run-4	0	0.3	1	139.1	51.0
Run-5	0	1	0	111.8	**48.7**
Run-6	0	1	1	121.5	51.6
Run-7	0.5	0.1	0	155.7	222.7
Run-8	0.5	0.1	1	130.3	175.3
Run-9	0.5	0.3	0	145.3	202.6
Run-10	0.5	0.3	1	134.9	182.6
Run-11	0.5	1	0	183.5	276.8
Run-12	0.5	1	1	1346	182.4
Run-13	1	0.1	0	872.3	1630.1
Run-14	1	0.1	1	302.8	444.6
Run-15	1	0.3	0	159.0	193.2
Run-16	1	0.3	1	295.0	433.4
Run-17	1	1	0	290.1	446.8
Run-18	1	1	1	271.8	426.2

From Table 4.11, it is observed that Run-5 gives the best result with total average error as 48.7% for the summation of areas A1 and A2; therefore, it is selected as the best fit run from areal comparison. However, when the profiles shown in Fig.4.16

which lie within the study (shown in Fig. 4.15) are evaluated; it is observed that the different values of *facua*, the parameter related to the wave asymmetry, cause very different computational results. For example, the only difference between Run-5 and Run-11 is the value of the *facua* parameter and the total average error values changes from 48.7% to 276.8% (Table 4.11). Depending on realization of the effect of *facua* parameter on computational results, profile based comparisons of these two runs (Run-5 and Run-11) is performed. According to the results of profile based comparisons, it is observed that when the value of *facua* parameter increases, deposition of sand in the shoreline increases and vice versa is also true. This observation mainly depends on the effect of wave asymmetry defined by the value of *facua* parameter.

The effect of wave asymmetry on sediment transport can be defined in simple words as follows. The wave asymmetry is the nonlinearity and asymmetry of waves relative to horizontal axis. As the asymmetry of the waves increases, the onshore velocity at crest becomes much higher than the offshore velocity at through. Since the sediment transport is directly related with these cross-shore velocities, cross shore velocity at crest causes movement of sediment towards onshore.

Profiles that show the computational results of Run-5 and Run-11 are given in Fig. 4.17 to Fig.4.20. In each profile, d refers sea bottom elevation and subscript of d refers to related run name or year. For example, d_{2006} refers to sea bottom elevation in 2006.

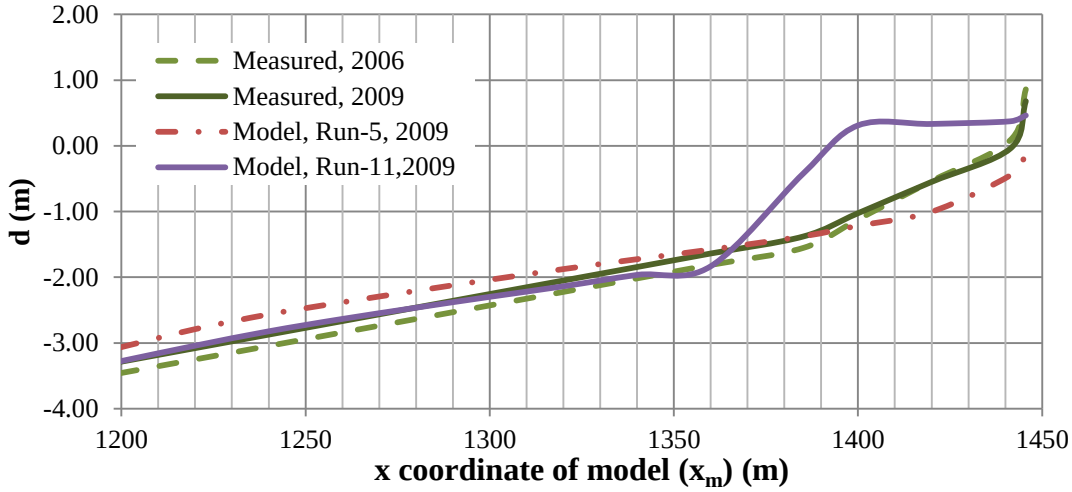

Figure 4.17: Comparison of Run-5 and Run-11 in Profile-1

The average percentage error and depth of each point (d) on Profile-1 is summarized in Table 4.12.

Table 4.12: The average percentage error and depth of each point on Profile-1

Point No	**x_m (m)**	**d_{2006} (m)**	**d_{2009} (m)**	**d_{Run-5} (m)**	**Error(%)**	**d_{Run-11} (m)**	**Error(%)**
1	1199.53	-3.46	-3.29	-3.07	6.68	-3.28	0.26
2	1220.00	-3.25	-3.08	-2.79	9.39	-3.04	1.21
3	1240.00	-3.05	-2.87	-2.57	10.72	-2.82	1.75
4	1260.00	-2.84	-2.67	-2.38	10.73	-2.63	1.23
5	1280.00	-2.63	-2.46	-2.21	10.32	-2.46	0.09
6	1300.00	-2.43	-2.26	-2.04	9.64	-2.30	1.88
7	1320.00	-2.22	-2.05	-1.88	8.48	-2.14	4.28
8	1340.00	-2.02	-1.84	-1.73	6.45	-1.96	6.53
9	1360.00	-1.81	-1.64	-1.58	3.66	-1.83	11.92
10	1385.14	-1.55	-1.38	-1.38	0.22	-0.42	69.48
11	1400.00	-1.12	-1.03	-1.22	18.70	0.31	130.32
12	1420.00	-0.54	-0.55	-1.00	82.96	0.33	160.82
13	1441.40	0.09	-0.04	-0.45	1018.75	0.37	1035.00
14	1445.58	0.86	0.68	-0.14	120.31	0.46	31.94
				ΣAve. Error(%)=	94.07	ΣAve. Error(%)=	104.05

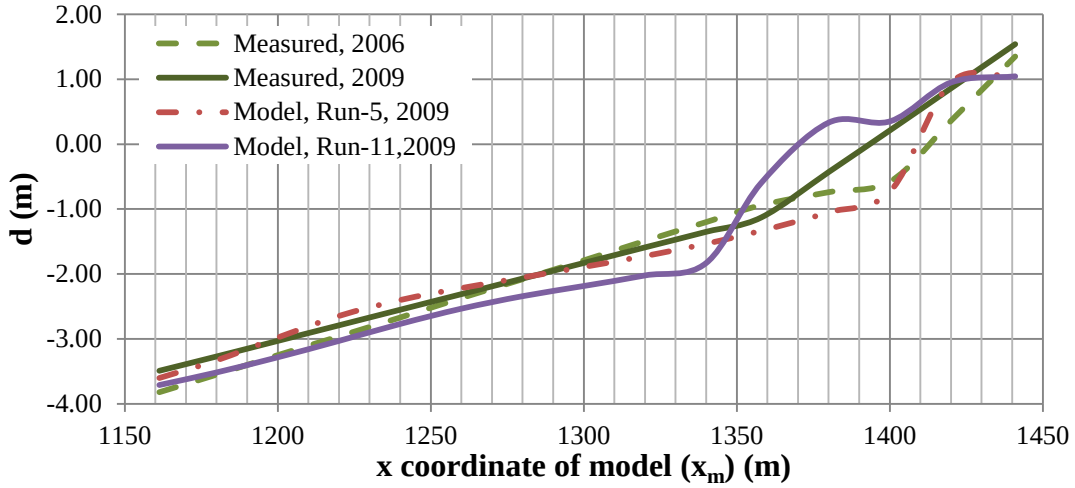

Figure 4.18: Comparison of Run-5 and Run-11 in Profile-2

The average percentage error and depth of each point (d) on Profile-2 are given in Table 4.13

Table 4.13: The average percentage error and depth of each point on Profile-2

Point No	x_m (m)	d_{2006} (m)	d_{2009} (m)	d_{Run-5} (m)	Error(%)	d_{Run-11} (m)	Error(%)
1	1161.30	-3.82	-3.49	-3.60	3.20	-3.71	6.29
2	1180.00	-3.55	-3.27	-3.33	1.83	-3.52	7.52
3	1200.00	-3.25	-3.03	-2.98	1.71	-3.28	8.33
4	1220.00	-2.96	-2.79	-2.65	5.17	-3.03	8.61
5	1240.00	-2.67	-2.55	-2.40	5.85	-2.77	8.57
6	1260.00	-2.37	-2.31	-2.22	4.03	-2.53	9.68
7	1280.00	-2.08	-2.07	-2.05	0.77	-2.34	13.10
8	1300.00	-1.79	-1.83	-1.89	3.34	-2.18	19.38
9	1320.00	-1.49	-1.59	-1.72	8.36	-2.02	27.18
10	1340.00	-1.20	-1.35	-1.53	13.61	-1.83	35.57
11	1357.94	-0.94	-1.13	-1.33	18.05	-0.60	47.00
12	1380.00	-0.74	-0.43	-1.05	144.30	0.33	177.02
13	1400.27	-0.57	0.22	-0.72	426.73	0.35	61.00
14	1420.00	0.36	0.86	0.95	10.47	0.95	10.47
15	1440.98	1.35	1.54	1.04	32.18	1.04	32.18
				Ave. Error(%)=	45.31	Ave. Error(%)=	31.46

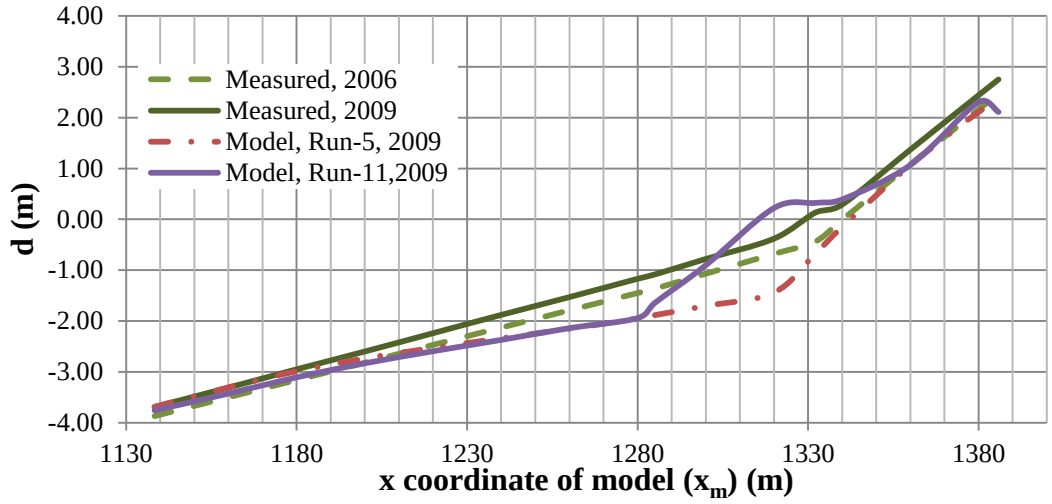

Figure 4.19: Comparison of Run-5 and Run-11 in Profile-3

The average percentage error and depth of each point (d) on Profile-3 are given in Table 4.14

Table 4.14: The average percentage error and depth of each point on Profile-3

Point No	x_m (m)	d_{2006} (m)	d_{2009} (m)	d_{Run-5} (m)	Error(%)	d_{Run-11} (m)	Error(%)
1	1138.35	-3.87	-3.69	-3.69	0.04	-3.76	1.84
2	1160.00	-3.50	-3.31	-3.31	0.13	-3.43	3.56
3	1180.00	-3.16	-2.95	-2.99	1.31	-3.11	5.35
4	1200.00	-2.82	-2.60	-2.74	5.26	-2.83	8.92
5	1220.00	-2.47	-2.24	-2.53	12.92	-2.59	15.84
6	1240.00	-2.13	-1.88	-2.34	24.46	-2.37	26.14
7	1260.00	-1.79	-1.53	-2.15	40.73	-2.14	39.88
8	1280.00	-1.45	-1.17	-1.95	66.53	-1.94	66.03
9	1285.31	-1.36	-1.08	-1.88	74.19	-1.63	51.01
10	1300.00	-1.07	-0.78	-1.70	118.32	-0.90	15.82
11	1320.00	-0.68	-0.38	-1.44	279.32	0.22	158.29
12	1332.09	-0.44	0.13	-0.68	621.00	0.32	148.46
13	1340.00	-0.01	0.29	-0.15	151.55	0.39	35.10
14	1360.00	1.08	1.37	1.07	22.08	1.07	22.08
15	1380.00	2.16	2.44	2.11	13.51	2.31	5.45
16	1385.84	2.48	2.75	2.31	16.11	2.11	23.26
				Ave. Error(%)=	96.49	Ave. Error(%)=	41.68

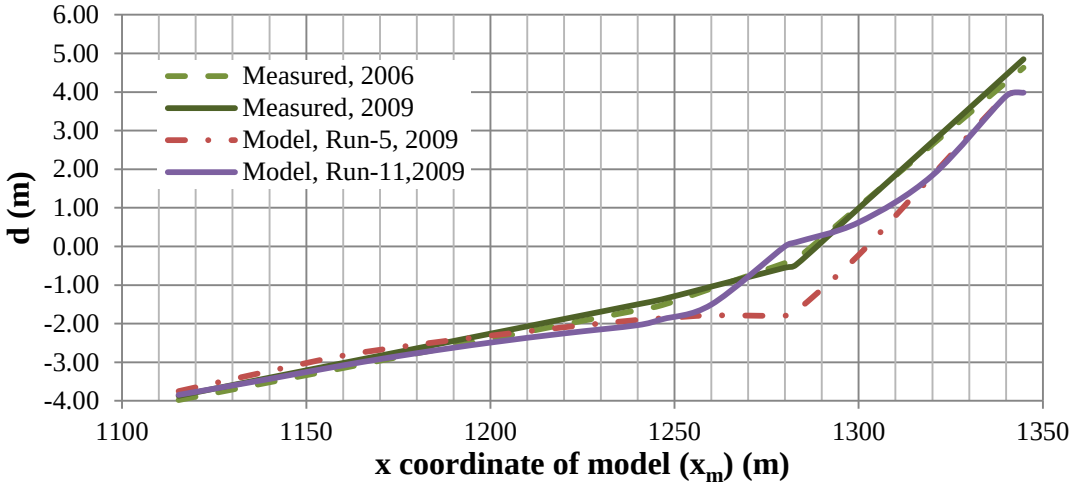

Figure 4.20: Comparison of Run-5 and Run-11 in Profile-4

The average percentage error and depth of each point (d) on Profile-4 are given in Table 4.15

Table 4.15: The average percentage error and depth of each point on Profile-4

Point No	x_m (m)	d_{2006} (m)	d_{2009} (m)	d_{Run-5} (m)	Error(%)	d_{Run-11} (m)	Error(%)
1	1115.33	-3.98	-3.87	-3.75	3.13	-3.85	0.63
2	1140.00	-3.52	-3.40	-3.23	5.05	-3.43	0.96
3	1160.00	-3.15	-3.02	-2.83	6.35	-3.08	1.99
4	1180.00	-2.77	-2.64	-2.54	3.60	-2.77	4.76
5	1200.00	-2.40	-2.26	-2.31	2.31	-2.49	10.20
6	1220.00	-2.02	-1.88	-2.09	11.40	-2.25	19.85
7	1240.00	-1.65	-1.50	-1.90	26.88	-2.04	35.93
8	1246.64	-1.52	-1.37	-1.86	35.96	-1.89	37.71
9	1260.00	-1.09	-1.04	-1.79	71.77	-1.51	44.76
10	1280.00	-0.43	-0.55	-1.79	226.02	0.00	100.69
11	1283.06	-0.33	-0.47	-1.67	255.70	0.11	123.57
12	1300.00	1.03	0.99	-0.22	122.37	0.62	37.08
13	1320.00	2.64	2.71	1.84	32.11	1.84	32.11
14	1340.00	4.25	4.44	3.89	12.31	3.89	12.31
15	1344.76	4.63	4.85	3.98	17.87	3.98	17.87
				Ave. Error(%)=	55.52	Ave. Error(%)=	32.03

From comparisons performed for areal and profile based, XBeach model is found to be sensitive to the *facua* parameter which is related to the wave asymmetry. Depending on this result, effect of wave asymmetry in sediment transport is searched in literature. Trouw et.al. (2012) say that wave asymmetry can be important in cross shore sediment transport and it should not be neglected. Depending on this suggestion and the results obtained in the first calibration study, it is understood that wave asymmetry plays an important role in Yumurtalık region; therefore, its effect must be included i.e. value of *facua* cannot be zero as it is taken in Run-5.

In addition, from these run series, it is observed that the value of *facua* parameter should be between 0 and 0.5, but should be closer to zero. In order to determine the value of *facua* parameter another run series are performed by using the parameter values of Run-5 except *facua*.

In order to determine the value of *facua* parameter, sample run series are performed by using the value of *facua* as 0.2 and 0.3. As a result of run series performed by using these values, similar results are obtained as in the case of Run-5 and Run-11. It is observed that the smaller the value of *facua* parameter the better the results. Therefore, the value of *facua* is selected as 0.2 for this study.

In addition, it also is observed that when the value of *facua* parameter gets smaller, foreshore slope gets affected from this change also. That is why the value of *wetslp* parameter, which is the parameter related to the slope underwater, also needed to be changed. The effect of this change in the value of *facua* parameter on foreshore slope can be summarized with a small example as follows. For example, when the value of *facua* parameter decreases, foreshore slope is also decreases. If the value parameter related to foreshore slope which is *wetslp* in XBeach is not changed, some erosion is observed in the areas named as A1 and A2 (Fig. 4.16). Depending on this reason, by only decreasing the value of *facua* parameter, it is not possible to obtain reliable results from model. Thus, in order to find an optimum relationship between the parameters *facua* and *wetslp*, another two run series are performed for the different values these parameters. In Table 4.16, the combinations used in these run series and areal percentage errors of each run are given.

Table 4.16: Combinations of parameters used in each run series and percent of errors of each run

Run No	Value of Parameter		Σ Average Error (%)	Σ Average Error of Sum of A1 and A2 (%)
	facua	wetslp		
1	0.2	0.1	109.9	33.2
2	0.2	0.3	115.2	37.1

As it can be seen from Table 4.15, using *facua* as 0.2 and *wetslp* as 0.1 decreased the total average error. However, error values near to shoreline cannot be lowered by changing the values of these parameters. Profiles that show the computational results of Run-1 and Run-2 are given in Fig. 4.21 to Fig.4.24 and error values are given in Table 4.17 to Table 20.

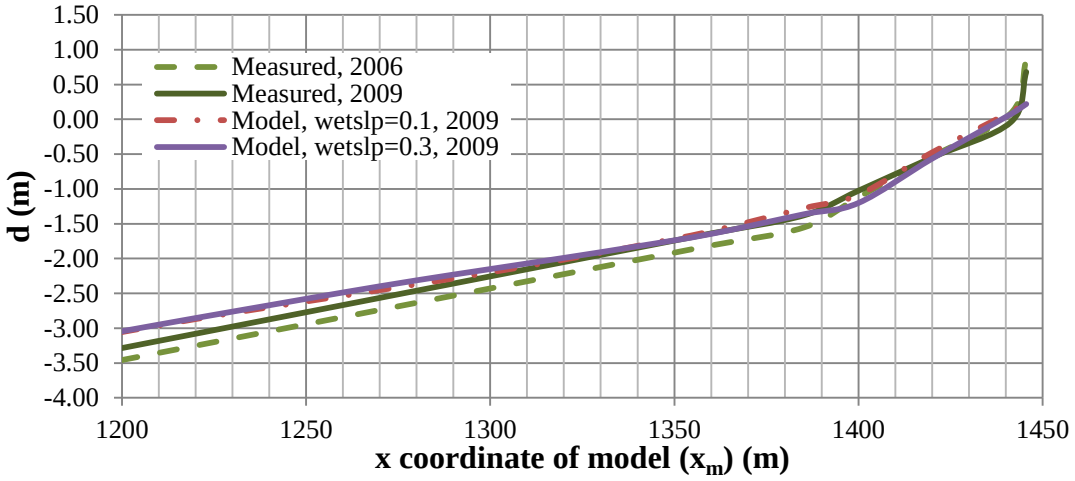

Figure 4.21: Comparison of results of wetslp=0.1and wetslp=0.3 in Profile-1

The average percentage error and depth of each point (d) on Profile-1 are given in Table 4.17.

Table 4.17: The average percentage error and depth of each point on Profile-1

Point No	x_m (m)	d_{2006} (m)	d_{2009} (m)	$d_{wetslp=0.1}$ (m)	Error(%)	$d_{wetslp=0.3}$ (m)	Error(%)
1	1200	-3.46	-3.29	-3.06	7.00	-3.05	7.35
2	1220	-3.25	-3.08	-2.87	6.85	-2.85	7.30
3	1240	-3.05	-2.87	-2.70	6.09	-2.67	7.06
4	1260	-2.84	-2.67	-2.54	4.97	-2.49	6.77
5	1280	-2.63	-2.46	-2.37	3.72	-2.31	6.06
6	1300	-2.43	-2.26	-2.20	2.52	-2.15	4.69
7	1320	-2.22	-2.05	-2.02	1.71	-1.99	2.92
8	1340	-2.02	-1.84	-1.82	1.45	-1.82	1.12
9	1360	-1.81	-1.64	-1.61	1.95	-1.65	0.43
10	1385	-1.55	-1.38	-1.28	7.43	-1.36	1.17
11	1400	-1.12	-1.03	-1.08	5.79	-1.20	17.15
12	1420	-0.54	-0.55	-0.48	13.19	-0.56	2.99
13	1441	0.09	-0.04	0.11	369.75	0.07	286.75
14	1446	0.86	0.68	0.25	63.16	0.22	67.72
				ΣAve. Error(%)=	35.40	ΣAve. Error(%)=	29.96

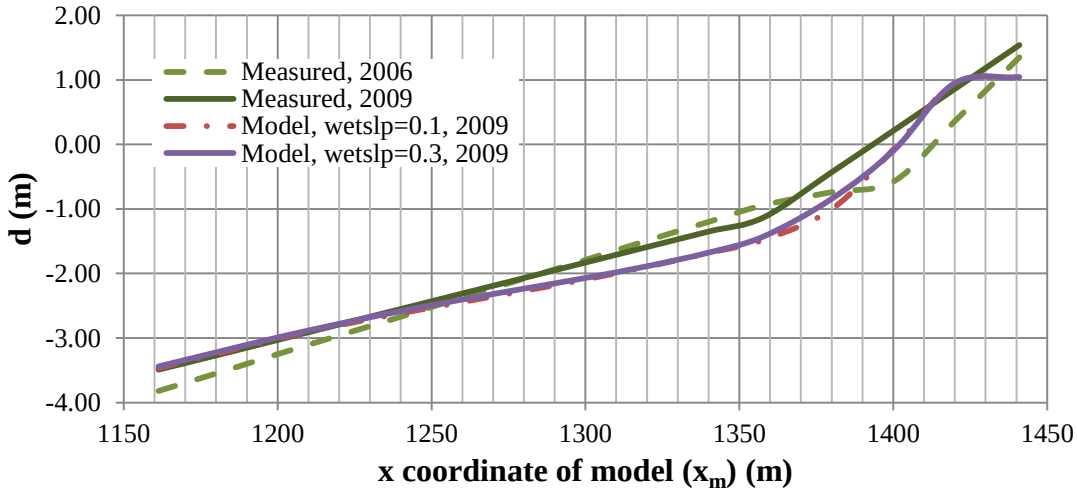

Figure 4.22: Comparison of results of wetslp=0.1and wetslp=0.3 in Profile-2

The average percentage error and depth of each point (d) on Profile-2 are given in Table 4.18.

Table 4.18: The average percentage error and depth of each point on Profile-2

Point No	x_m (m)	d_{2006} (m)	d_{2009} (m)	$d_{wetslp=0.1}$ (m)	Error(%)	$d_{wetslp=0.3}$ (m)	Error(%)
1	1161	-3.82	-3.49	-3.47	0.70	-3.44	1.42
2	1180	-3.55	-3.27	-3.25	0.75	-3.22	1.47
3	1200	-3.25	-3.03	-3.01	0.63	-2.99	1.27
4	1220	-2.96	-2.79	-2.80	0.43	-2.78	0.39
5	1240	-2.67	-2.55	-2.62	2.60	-2.58	1.29
6	1260	-2.37	-2.31	-2.44	5.69	-2.40	4.04
7	1280	-2.08	-2.07	-2.27	9.63	-2.24	7.99
8	1300	-1.79	-1.83	-2.09	14.32	-2.07	13.05
9	1320	-1.49	-1.59	-1.89	19.16	-1.89	18.70
10	1340	-1.20	-1.35	-1.68	24.57	-1.68	24.17
11	1358	-0.94	-1.13	-1.48	30.65	-1.42	26.09
12	1380	-0.74	-0.43	-1.00	133.07	-0.84	95.88
13	1400	-0.57	0.22	-0.07	130.00	-0.09	139.59
14	1420	0.36	0.86	0.95	10.47	0.95	10.47
15	1441	1.35	1.54	1.04	32.18	1.04	32.18
				ΣAve. Error(%)=	27.66	ΣAve. Error(%)=	25.20

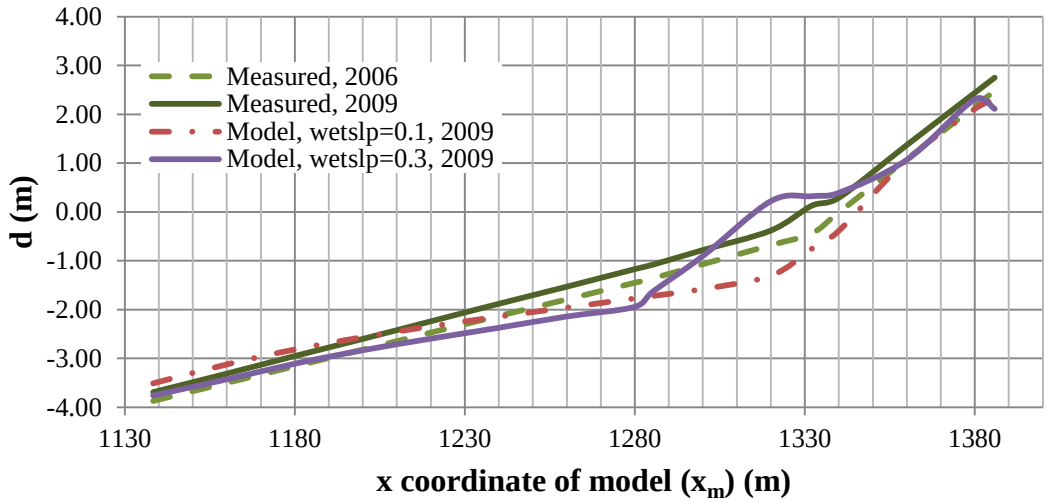

Figure 4.23: Comparison of results of wetslp=0.1and wetslp=0.3 in Profile-3

The average percentage error and depth of each point (d) on Profile-3 are given in Table 4.19.

Table 4.19: The average percentage error and depth of each point on Profile-3

Point No	x_m (m)	d_{2006} (m)	d_{2009} (m)	$d_{wetslp=0.1}$ (m)	Error(%)	$d_{wetslp=0.3}$ (m)	Error(%)
1	1138	-3.87	-3.69	-3.51	4.87	-3.76	1.84
2	1160	-3.50	-3.31	-3.12	5.68	-3.43	3.56
3	1180	-3.16	-2.95	-2.82	4.53	-3.11	5.35
4	1200	-2.82	-2.60	-2.56	1.40	-2.83	8.92
5	1220	-2.47	-2.24	-2.34	4.60	-2.59	15.84
6	1240	-2.13	-1.88	-2.14	14.04	-2.37	26.14
7	1260	-1.79	-1.53	-1.96	27.98	-2.14	39.88
8	1280	-1.45	-1.17	-1.77	51.32	-1.94	66.03
9	1285	-1.36	-1.08	-1.72	59.23	-1.63	51.01
10	1300	-1.07	-0.78	-1.58	102.42	-0.90	15.82
11	1320	-0.68	-0.38	-1.31	243.58	0.22	158.29
12	1332	-0.44	0.13	-0.75	678.69	0.32	148.46
13	1340	-0.01	0.29	-0.39	233.34	0.39	35.10
14	1360	1.08	1.37	1.07	22.08	1.07	22.08
15	1380	2.16	2.44	2.11	13.51	2.31	5.45
16	1386	2.48	2.75	2.31	16.11	2.11	23.26
				ΣAve. Error(%)=	98.57	ΣAve. Error(%)=	41.68

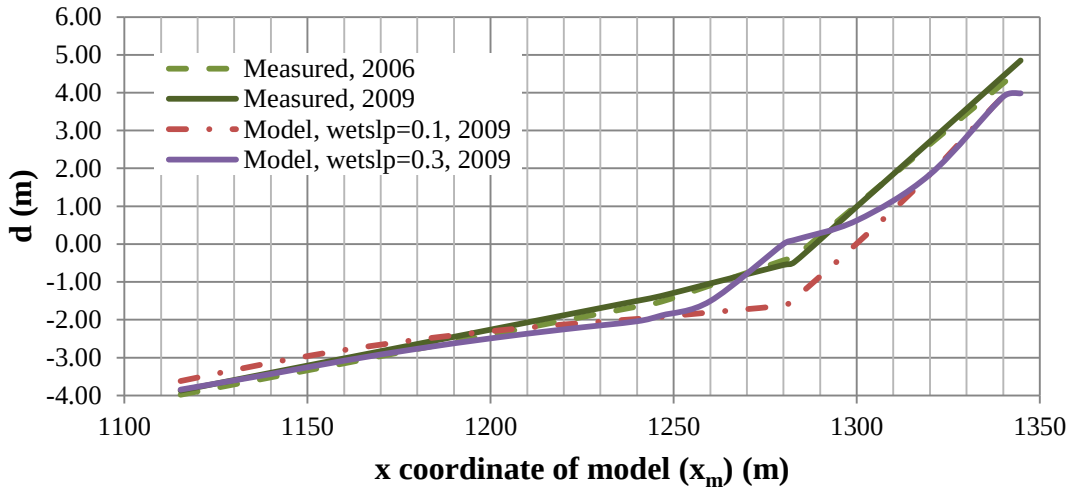

Figure 4.24: Comparison of results of wetslp=0.1and wetslp=0.3 in Profile-4

The average percentage error and depth of each point (d) on Profile-4 are given in Table 4.20.

Table 4.20: The average percentage error and depth of each point on Profile-4

Point No	**x_m (m)**	**d_{2006} (m)**	**d_{2009} (m)**	**$d_{wetslp=0.1}$ (m)**	**Error(%)**	**$d_{wetslp=0.3}$ (m)**	**Error(%)**
1	1115	-3.98	-3.87	-3.62	6.50	-3.85	0.63
2	1140	-3.52	-3.40	-3.13	7.82	-3.43	0.96
3	1160	-3.15	-3.02	-2.80	7.33	-3.08	1.99
4	1180	-2.77	-2.64	-2.53	4.30	-2.77	4.76
5	1200	-2.40	-2.26	-2.30	1.87	-2.49	10.20
6	1220	-2.02	-1.88	-2.12	12.97	-2.25	19.85
7	1240	-1.65	-1.50	-1.98	31.87	-2.04	35.93
8	1247	-1.52	-1.37	-1.92	40.40	-1.89	37.71
9	1260	-1.09	-1.04	-1.80	73.37	-1.51	44.76
10	1280	-0.43	-0.55	-1.62	193.91	0.00	100.69
11	1283	-0.33	-0.47	-1.44	205.53	0.11	123.57
12	1300	1.03	0.99	0.01	98.74	0.62	37.08
13	1320	2.64	2.71	1.84	32.11	1.84	32.11
14	1340	4.25	4.44	3.89	12.31	3.89	12.31
15	1345	4.63	4.85	3.98	17.87	3.98	17.87
				ΣAve. Error(%)=	49.79	ΣAve. Error(%)=	32.03

Although average percentage errors of the model with wetslp=0.3 is lower than the average percentage errors of the model with wetslp=0.1, depending on the shape of the profiles given in Fig.4.23 and Fig. 4.24, the value of *wetslp* is selected as 0.1. In other words, the model with wetslp=0.3 does not show similar behaviour with the field measurements; therefore the value of *wetslp* parameter is selected as 0.1 in this study.

In addition, when the percentage errors given in Table 4.17 to Table 4.20 are evaluated, it is observed that error values near to shoreline are still large. If the error values given in these tables are evaluated, it can be seen that model generally works fairly good and such errors near to shoreline may be the result of lack of field measurements described before.

In order to make the model more accurate, other parameters to which XBeach may be sensitive in this area are searched and it is observed that *dryslp*, critical

avalanching slope above water (Eq. 3.36), and *facsl*, bed slope factor (Eq. 3.33), play an important role. More detailed descriptions about these parameters are as follows:

- *dryslp*, parameter used to describe critical avalanching slope above water in XBeach, is mainly responsible for the erosion rate observed above water. For example, if large value is defined for dryslp, much erosion observed above water and vice versa is true.
- *facsl*, parameter used to define the effect of bed slope, is responsible for equilibrium sediment concentration. For higher values of this parameter, equilibrium sediment concentration decreases, on the other hand, for smaller values it increases.

By using different values of *dryslp*, it is observed that for large values of *dryslp* erosion above water increases on the other hand for low values of it, erosion decreases. Thus, the value of *dryslp* selected as 0.1. In order to understand the effect of *facsl* parameters to the model, another run series are performed by using the given values parameters in Table 4.21.

Table 4.21: Values of important XBeach parameters used in third calibration study

Parameter	**Description**	**Used Values For Calibration**
facua	Asymmetry transport	0.2
wetslp	Critical avalanching slope under water	0.1
dryslp	Critical avalanching slope above water	0.1
facsl	Bed slope factor	0.5,1.6

In this study, it is observed that when the value of *facsl* gets smaller, equilibrium sediment concentration gets higher; on the other hand, when the value of *facsl* gets larger equilibrium sediment concentration gets smaller. Another two run series are performed for the different values of *facls* (Table 4.20).

In Table 4.22, the combinations used in these run series and areal percentage errors of each run are given.

Table 4.22: Combinations of parameters used in each run series and percent of errors of each run

Run No	Value of Parameter facsl	Σ Average Error (%)	Σ Average Error of Sum of A1 and A2 (%)
1	0.5	129.1	45.5
2	1.6	194.0	213.7

From Table 4.22, it is observed that the model with facsl=0.5 gives much better results. Profiles that show the computational results of facs=0.5 and facsl=1.6 are given in Fig. 4.25 to Fig.4.28 and error values are given in Table 4.23 to Table 26.

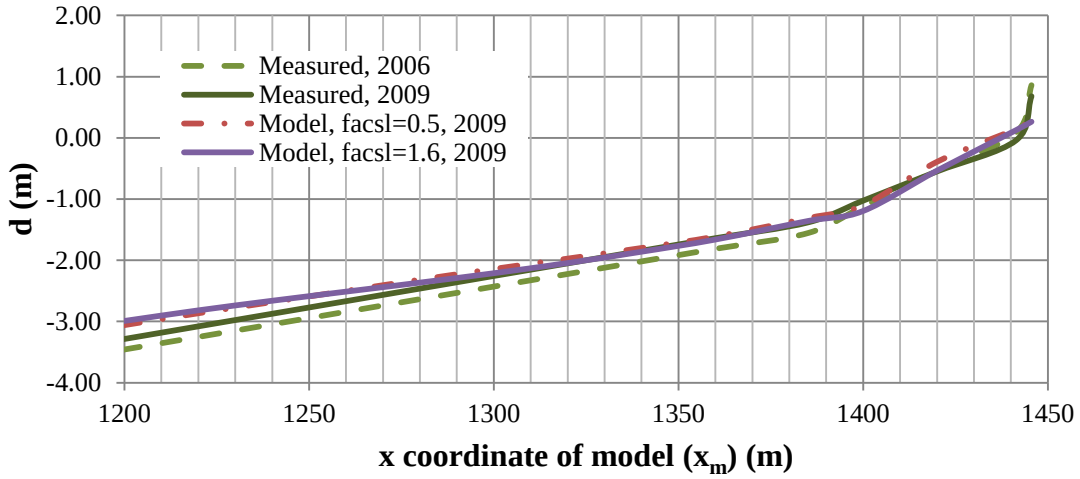

Figure 4.25: Comparison of results of facsl=0.5 and facsl=1.6 in Profile-1

The average percentage error and depth of each point (d) on Profile-1 are given in Table 4.23.

Table 4.23: The average percentage error and depth of each point on Profile-1

Point No	x_m (m)	d_{2006} (m)	d_{2009} (m)	$d_{facsl=0.5}$ (m)	Error(%)	$d_{facsl=1.6}$ (m)	Error(%)
1	1200	-3.46	-3.29	-3.06	6.89	-2.99	8.98
2	1220	-3.25	-3.08	-2.87	6.95	-2.82	8.49
3	1240	-3.05	-2.87	-2.68	6.65	-2.66	7.40
4	1260	-2.84	-2.67	-2.50	6.32	-2.51	5.84
5	1280	-2.63	-2.46	-2.32	5.91	-2.36	3.95
6	1300	-2.43	-2.26	-2.14	5.09	-2.21	2.00
7	1320	-2.22	-2.05	-1.97	3.81	-2.04	0.31
8	1340	-2.02	-1.84	-1.80	2.48	-1.86	0.83
9	1360	-1.81	-1.64	-1.61	1.63	-1.66	1.36
10	1385	-1.55	-1.38	-1.31	5.06	-1.36	1.69
11	1400	-1.12	-1.03	-1.10	7.55	-1.19	16.48
12	1420	-0.54	-0.55	-0.39	28.64	-0.53	2.43
13	1441	0.09	-0.04	0.14	457.25	0.13	414.75
14	1446	0.86	0.68	0.28	59.31	0.26	61.24
				ΣAve. Error(%)=	43.11	ΣAve. Error(%)=	38.27

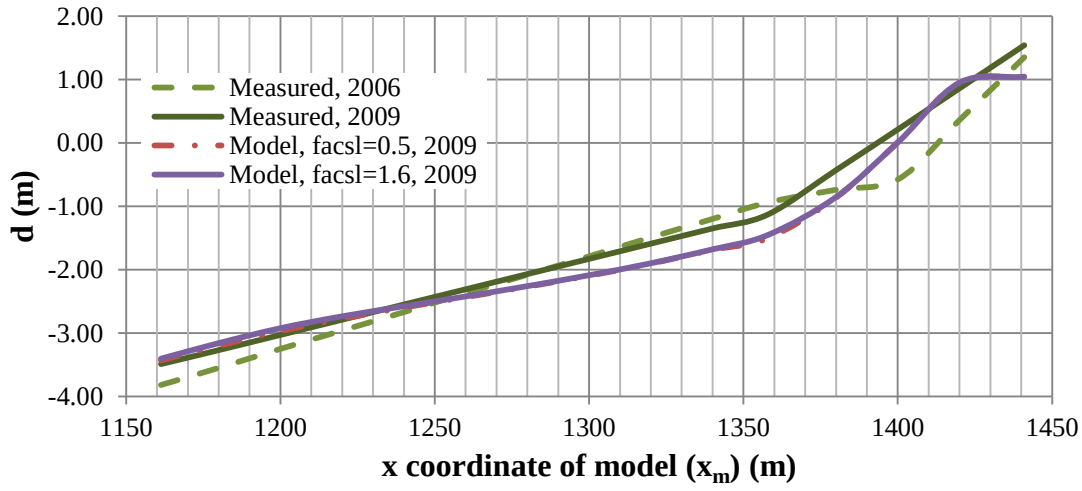

Figure 4.26: Comparison of results of facsl=0.5 and facsl=1.6 in Profile-2

The average percentage error and depth of each point (d) on Profile-2 are given in Table 4.24.

Table 4.24: The average percentage error and depth of each point on Profile-2

Point No	x_m (m)	d_{2006} (m)	d_{2009} (m)	$d_{facsl=0.5}$ (m)	Error(%)	$d_{facsl=1.6}$ (m)	Error(%)
1	1161	-3.82	-3.49	-3.43	1.66	-3.40	2.45
2	1180	-3.55	-3.27	-3.20	2.11	-3.16	3.40
3	1200	-3.25	-3.03	-2.97	1.95	-2.92	3.52
4	1220	-2.96	-2.79	-2.77	0.56	-2.74	1.92
5	1240	-2.67	-2.55	-2.60	1.89	-2.58	1.09
6	1260	-2.37	-2.31	-2.43	5.35	-2.42	4.87
7	1280	-2.08	-2.07	-2.27	9.64	-2.26	9.18
8	1300	-1.79	-1.83	-2.10	14.54	-2.09	14.09
9	1320	-1.49	-1.59	-1.91	19.85	-1.90	19.45
10	1340	-1.20	-1.35	-1.69	24.99	-1.68	24.41
11	1358	-0.94	-1.13	-1.51	33.22	-1.45	28.60
12	1380	-0.74	-0.43	-0.86	100.88	-0.85	98.70
13	1400	-0.57	0.22	0.02	90.23	0.02	90.91
14	1420	0.36	0.86	0.95	10.47	0.95	10.47
15	1441	1.35	1.54	1.04	32.18	1.04	32.18
				ΣAve. Error(%)=	23.30	ΣAve. Error(%)=	23.01

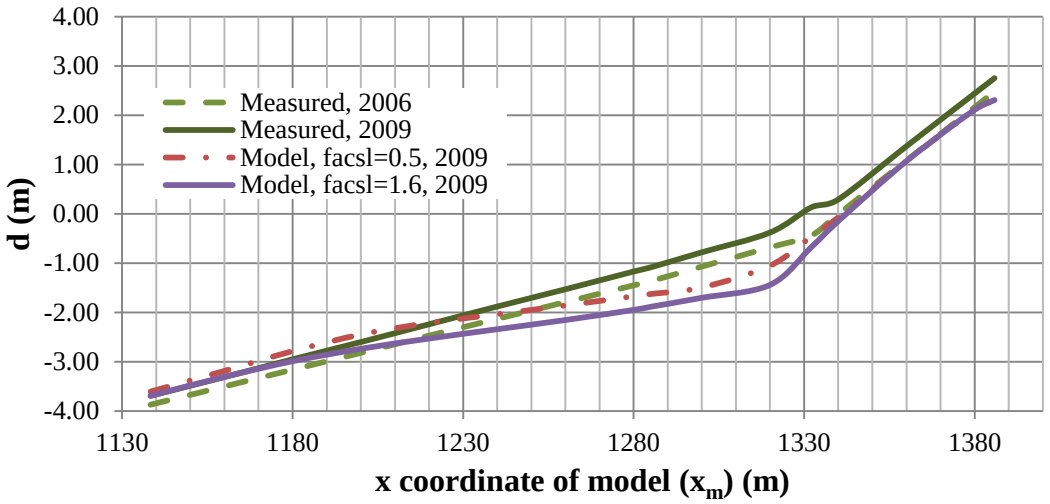

Figure 4.27: Comparison of results of facsl=0.5 and facsl=1.6 in Profile-3

The average percentage error and depth of each point (d) on Profile-3 are given in Table 4.25.

Table 4.25: The average percentage error and depth of each point on Profile-3

Point No	x_m (m)	d_{2006} (m)	d_{2009} (m)	$d_{facsl=0.5}$ (m)	Error(%)	$d_{facsl=1.6}$ (m)	Error(%)
1	1138	-3.87	-3.69	-3.60	2.33	-3.69	0.04
2	1160	-3.50	-3.31	-3.19	3.77	-3.31	0.13
3	1180	-3.16	-2.95	-2.78	5.62	-2.99	1.31
4	1200	-2.82	-2.60	-2.45	5.87	-2.74	5.26
5	1220	-2.47	-2.24	-2.21	1.25	-2.53	12.92
6	1240	-2.13	-1.88	-2.04	8.34	-2.34	24.46
7	1260	-1.79	-1.53	-1.86	21.49	-2.15	40.73
8	1280	-1.45	-1.17	-1.67	42.89	-1.95	66.53
9	1285	-1.36	-1.08	-1.62	50.31	-1.88	74.19
10	1300	-1.07	-0.78	-1.49	91.64	-1.70	118.32
11	1320	-0.68	-0.38	-1.05	176.71	-1.44	279.32
12	1332	-0.44	0.13	-0.46	455.00	-0.68	621.00
13	1340	-0.01	0.29	-0.07	125.48	-0.15	151.55
14	1360	1.08	1.37	1.07	22.08	1.07	22.08
15	1380	2.16	2.44	2.11	13.51	2.11	13.51
16	1386	2.48	2.75	2.31	16.11	2.31	16.11
				ΣAve. Error(%)=	69.34	ΣAve. Error(%)=	96.49

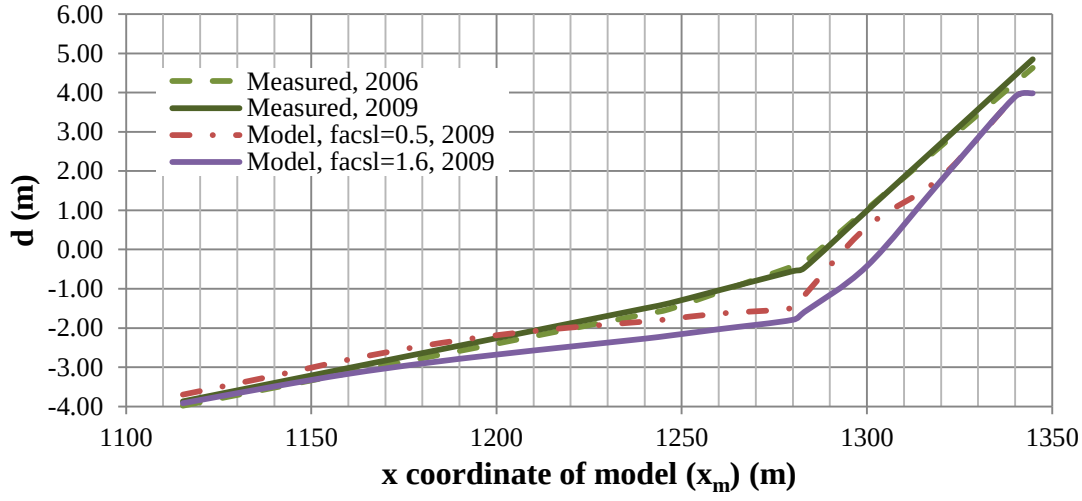

Figure 4.28: Comparison of results of facsl=0.5 and facsl=1.6 in Profile-4

The average percentage error and depth of each point (d) on Profile-4 are given in Table 4.26.

Table 4.26: The average percentage error and depth of each point on Profile-4

Point No	x_m (m)	d_{2006} (m)	d_{2009} (m)	$d_{facsl=0.5}$ (m)	Error(%)	$d_{facsl=1.6}$ (m)	Error(%)
1	1115	-3.98	-3.87	-3.70	4.44	-3.92	1.22
2	1140	-3.52	-3.40	-3.22	5.39	-3.49	2.67
3	1160	-3.15	-3.02	-2.81	7.03	-3.17	4.91
4	1180	-2.77	-2.64	-2.46	6.91	-2.90	9.98
5	1200	-2.40	-2.26	-2.18	3.35	-2.68	18.49
6	1220	-2.02	-1.88	-1.99	5.74	-2.47	31.52
7	1240	-1.65	-1.50	-1.84	22.39	-2.27	51.42
8	1247	-1.52	-1.37	-1.77	29.34	-2.19	60.20
9	1260	-1.09	-1.04	-1.63	56.96	-2.03	95.35
10	1280	-0.43	-0.55	-1.49	170.71	-1.79	225.53
11	1283	-0.33	-0.47	-1.17	149.89	-1.60	239.36
12	1300	1.03	0.99	0.58	41.64	-0.42	142.76
13	1320	2.64	2.71	1.84	32.11	1.76	35.18
14	1340	4.25	4.44	3.89	12.31	3.89	12.31
15	1345	4.63	4.85	3.98	17.87	3.98	17.87
				ΣAve. Error(%)=	37.74	ΣAve. Error(%)=	63.25

When total average errors are evaluated, it is observed that, for *facsl*=0.5 more accurate results are obtained in general. Thus, this combination is selected as best fit combination in this study.

In addition, it is observed that XBeach model fits better for Profile-1, Profile -2 and Profile-4; however, Profile-3 has large error due to the erosion and deposition difference observed in near shore. The reason of such error may be the result of insufficient, improper or wrong field measurements available for this region since when the other points are evaluated; it is observed that model works fairly well.

4.4. XBeach Model Calibration Results

In Chapter 4.3.5, extensive calibration study done in order to determine the parameters that give best fit for Yumurtalık region is presented. During this study;

- *facua*, parameter used to describe wave asymmetry effect in cross shore sediment transport, is found to be effective in this study. The effect of this parameter, as recommended by Trouw (2012) is included by using the value of it as 0.2

- *lws*, parameter used to describe long wave stirring, is found not to be effective. The model results that include and do not include the effect of long wave stirring are found to be similar. In this study, model is found to give a little bit better results when the effect of long wave is not included. Although, swell waves as long waves are expected to be effective in Mediterranean Sea, depending on the selection of spreading parameter in defining offshore boundary conditions and the insufficient field measurements, effects cannot be truly observed. Thus, according to the error comparisons, the value of *lws* is selected as 0.

- *wetslp*, parameter used to describe critical avalanching slope under water, is found to be effective in this study. The model results are highly affected from the values defined. For example, if large value is defined for *wetslp*, sediment deposition observed underwater decreases. That is why, one should be careful in the selection of this parameter while using XBeach. In this study, as a result of different runs, value of *wetslp* is selected as 0.1

- *dryslp*, parameter used to describe critical avalanching slope above water, is also found to be effective in this study. The model results obtained in nearshore affected from the values defined. For example, if large value is defined for *dryslp*, much erosion observed above water. For this area, erosion observed above water is small; therefore, the value of *dryslp* is selected as 0.1 according to this observation.

- *facsl*, parameter used to describe bed slope factor, is responsible for equilibrium sediment concentration. For higher values, equilibrium sediment concentration decreases, on the other hand, for smaller values it increases. That is why an optimum value of this parameter should be determined. In this study, as a result of different runs, 0.5 is found to be suitable value for this model.

In Table 4.27, the parameters that give the best fit for this region is summarized.

Table 4.27: Best XBeach parameters obtained as a result of calibration study

Parameter	Description	Used Values For Calibration
lws	Long wave stirring	0
facua	Asymmetry transport	0.2
wetslp	Critical avalanching slope under water	0.1
dryslp	Critical avalanching slope above water	0.1
facsl	Bed slope factor	0.5

Although some errors observed in nearshore, the model can be used to understand general behaviour of sediment transport in Yumurtalık region by using the parameters given in Table 4.27.

4.5. XBeach Model Verification

In this chapter, by using the best fit parameters summarized in Table 4.26, model verification study is performed. In the verification study of XBeach model, representative waves given in Table 4.6 (in Chapter 4.3.4) and the bathymetric map obtained by linear interpolation of elevation measurements of 2011 are used.

In Table 4.28, the combinations used in these run series and areal percentage errors of each run are given.

Table 4.28: Percent of errors of in verification run

	Σ Average Error (%)	Σ Average Error of Sum of A1 and A2 (%)
Verification Run	145.1	208.1

According to the results of areal comparisons, it is observed that calibrated model with the parameters given in Table 4.27 does not work good enough to represent change of sediment in areal based. In order to understand the results of model more clearly, profile evaluation is also performed.

Profiles that show the computational results of verification study are given in Fig. 4.29 to Fig.4.32 and error values are given in Table 4.29 to Table 32.

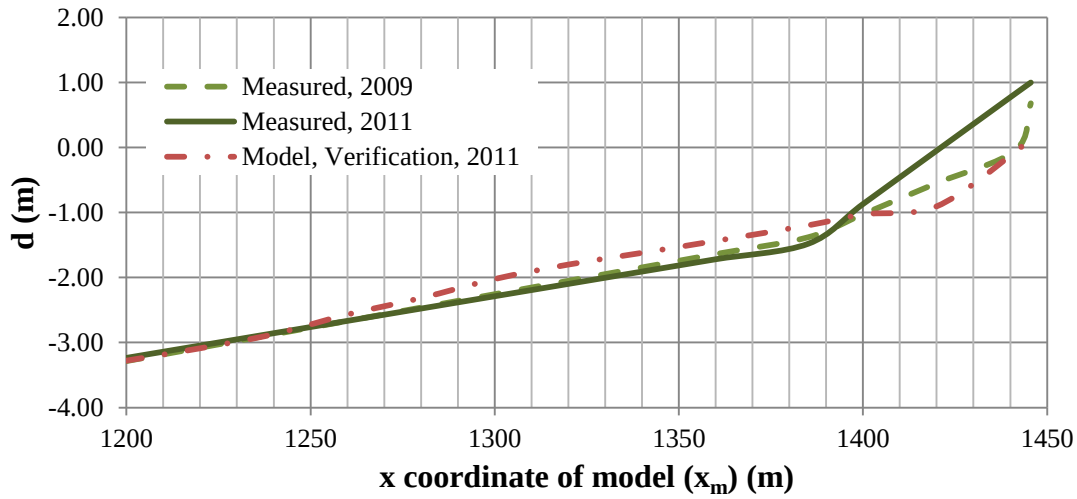

Figure 4.29: Computational results of verification study in Profile-1

The average percentage error and depth of each point (d) on Profile-1 are given in Table 4.29.

Table 4.29: The average percentage error and depth of each point on Profile-1

Point No	**x_m (m)**	**d_{2009} (m)**	**d_{2011} (m)**	**$d_{verification}$ (m)**	**Error(%)**
1	1199.53	-3.29	-3.24	-3.28	1.31
2	1220.00	-3.08	-3.05	-3.09	1.38
3	1240.00	-2.87	-2.86	-2.87	0.53
4	1260.00	-2.67	-2.67	-2.57	3.67
5	1280.00	-2.46	-2.48	-2.32	6.53
6	1300.00	-2.26	-2.29	-2.02	11.57
7	1320.00	-2.05	-2.10	-1.80	14.18
8	1340.00	-1.84	-1.91	-1.62	15.09
9	1360.00	-1.64	-1.72	-1.44	16.43
10	1385.14	-1.38	-1.48	-1.20	19.16
11	1400.00	-1.03	-0.87	-1.03	18.29
12	1420.00	-0.55	-0.05	-0.90	1797.06
13	1441.40	-0.04	0.83	-0.06	107.79
14	1445.58	0.68	1.00	0.16	84.42
				ΣAve. Error(%)=	149.81

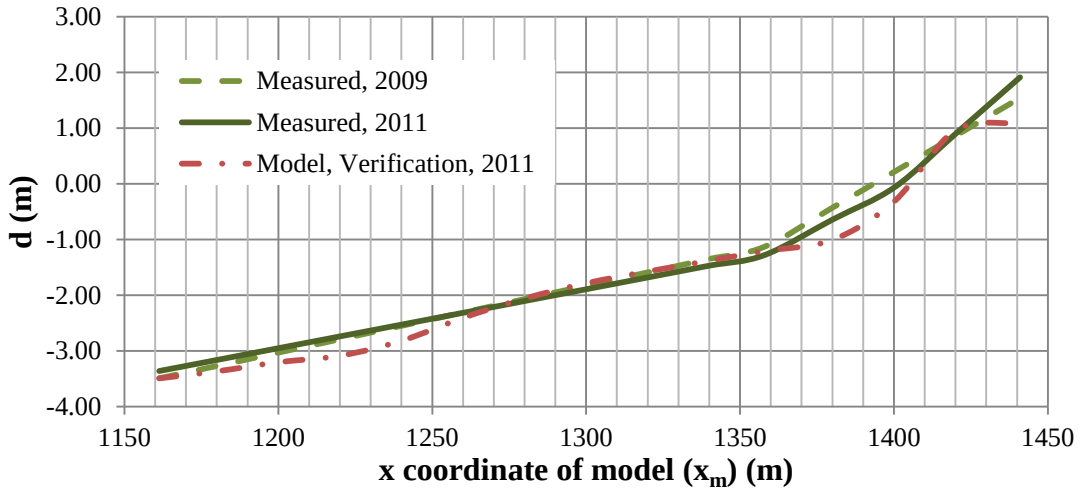

Figure 4.30: Computational results of verification study in Profile-2

The average percentage error and depth of each point (d) on Profile-2 are given in Table 4.30.

Table 4.30: The average percentage error and depth of each point on Profile-2

Point No	x_m (m)	d_{2009} (m)	d_{2011} (m)	$d_{verification}$ (m)	Error(%)
1	1161.30	-3.49	-3.36	-3.49	3.91
2	1180.00	-3.27	-3.16	-3.37	6.45
3	1200.00	-3.03	-2.95	-3.20	8.53
4	1220.00	-2.79	-2.74	-3.09	12.67
5	1240.00	-2.55	-2.53	-2.82	11.49
6	1260.00	-2.31	-2.32	-2.41	3.88
7	1280.00	-2.07	-2.10	-2.06	2.14
8	1300.00	-1.83	-1.89	-1.79	5.68
9	1320.00	-1.59	-1.68	-1.57	6.42
10	1340.00	-1.35	-1.47	-1.38	6.02
11	1357.94	-1.13	-1.28	-1.21	5.72
12	1380.00	-0.43	-0.64	-1.01	56.21
13	1400.27	0.22	-0.06	-0.31	413.33
14	1420.00	0.86	0.89	0.96	7.29
15	1440.98	1.54	1.91	1.09	42.68
				Ave. Error(%)=	39.49

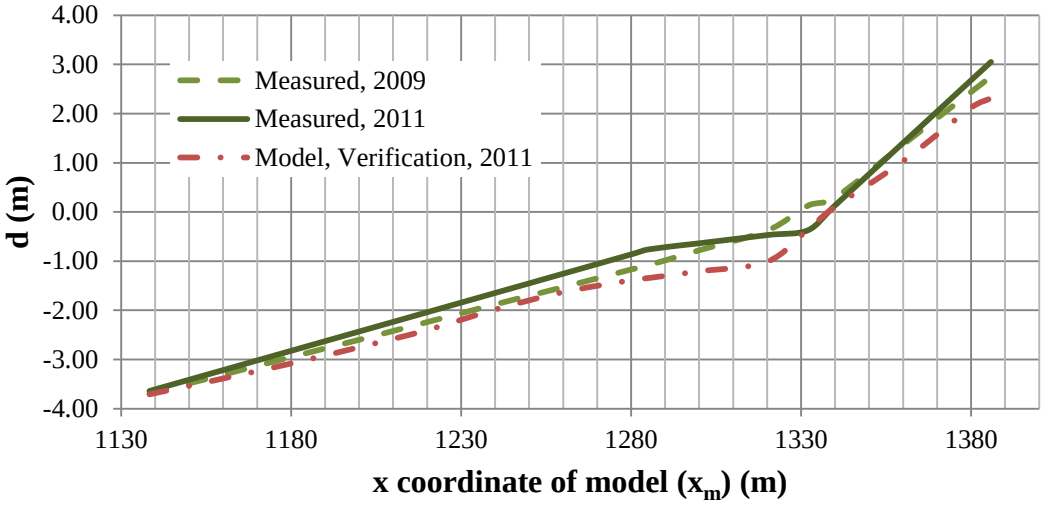

Figure 4.31: Computational results of verification study in Profile-3

The average percentage error and depth of each point (d) on Profile-3 are given in Table 4.31.

Table 4.31: The average percentage error and depth of each point on Profile-3

Point No	x_m (m)	d_{2009} (m)	d_{2011} (m)	$d_{verification}$ (m)	Error(%)
1	1138.35	-3.69	-3.64	-3.71	1.89
2	1160.00	-3.31	-3.22	-3.39	5.34
3	1180.00	-2.95	-2.82	-3.08	9.13
4	1200.00	-2.60	-2.43	-2.75	13.15
5	1220.00	-2.24	-2.04	-2.40	17.79
6	1240.00	-1.88	-1.65	-1.98	20.41
7	1260.00	-1.53	-1.26	-1.63	29.82
8	1280.00	-1.17	-0.86	-1.39	60.76
9	1285.31	-1.08	-0.76	-1.34	76.63
10	1300.00	-0.78	-0.64	-1.21	89.44
11	1320.00	-0.38	-0.47	-1.01	114.95
12	1332.09	0.13	-0.37	-0.35	6.00
13	1340.00	0.29	0.13	0.11	21.23
14	1360.00	1.37	1.41	1.03	26.42
15	1380.00	2.44	2.68	2.12	20.83
16	1385.84	2.75	3.05	2.31	24.24
				Ave. Error(%)=	35.74

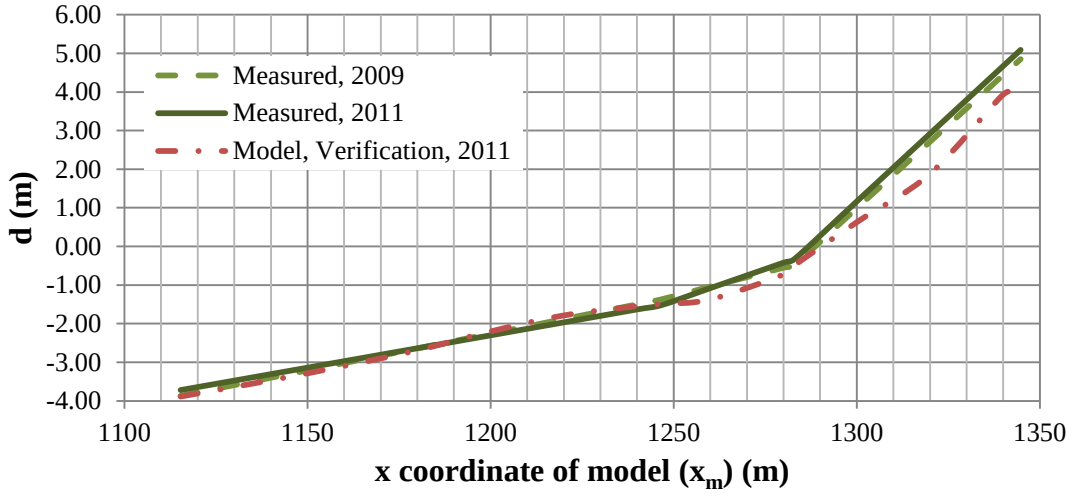

Figure 4.32: Computational results of verification study in Profile-4

The average percentage error and depth of each point (d) on Profile-4 are given in Table 4.32.

Table 4.32: The average percentage error and depth of each point on Profile-4

Point No	**x_m (m)**	**d_{2009} (m)**	**d_{2011} (m)**	**$d_{verification}$ (m)**	**Error(%)**
1	1115.33	-3.87	-3.72	-3.89	4.49
2	1140.00	-3.40	-3.31	-3.46	4.78
3	1160.00	-3.02	-2.97	-3.10	4.16
4	1180.00	-2.64	-2.64	-2.69	2.01
5	1200.00	-2.26	-2.30	-2.20	4.37
6	1220.00	-1.88	-1.97	-1.79	9.14
7	1240.00	-1.50	-1.63	-1.55	5.19
8	1246.64	-1.37	-1.52	-1.49	1.97
9	1260.00	-1.04	-1.08	-1.37	27.15
10	1280.00	-0.55	-0.42	-0.73	72.21
11	1283.06	-0.47	-0.32	-0.48	50.28
12	1300.00	0.99	1.17	0.63	46.21
13	1320.00	2.71	2.92	1.88	35.61
14	1340.00	4.44	4.67	3.93	15.84
15	1344.76	4.85	5.09	4.04	20.54
				Ave. Error(%)=	20.26

When profiles given in Fig.32 to Fig.35 are evaluated, model looks like not give good results. However, if the values obtained from model given Table 4.29 to Table 4.32 are evaluated; it is observed that measured and calculated values are close to each other. In addition error values obtained are fairly good since they are generally not very large except near shore as observed in other runs. The main reason of these errors observed in Fig.32 to Fig.35 is the improper field measurements. This is because there are not enough measurements available; therefore, actual bathymetry of the related year cannot be defined as it in in real.

Despite the errors, it can be said that the model generally works well enough to model long term sediment transport for the given profiles studied in Yumurtalık region. The model can be used with the given parameters in Table 4.27 (Chapter 4.4) to determine general behaviour of sediment transport process in the region and rate of sediment transport can be calculated.

4.6. Depth of Closure

For the wave data calculated in Section 4.3.4, depth of closure of the study area is calculated by using Eq. 2.14 suggested by Hallermeier (1978) for the dominant wave direction which is SSW.

Significant wave height exceeded 12 hours per year ($H_{s,12}$) and significant wave period exceeded 12 hours per year ($T_{s,12}$) are determined as 3.54 m and 7.63 sec for calibration, 2.50 m and 6.41 sec of verification studies. Using these values, depths of closure of the study area are determined as 6.6 m and 4.6m in these studies.

When the model results are evaluated in terms of depth of closure, it is observed that morphological changes start at approximately 5 m (Fig. 4.34 and Fig. 4.35) both field measurements and model which is compatible with the calculated depth of closure values (6.6m and 4.6m). The location of the sample profile taken perpendicular to the shoreline, on which depth of closure is shown, is given in Fig. 4.33.

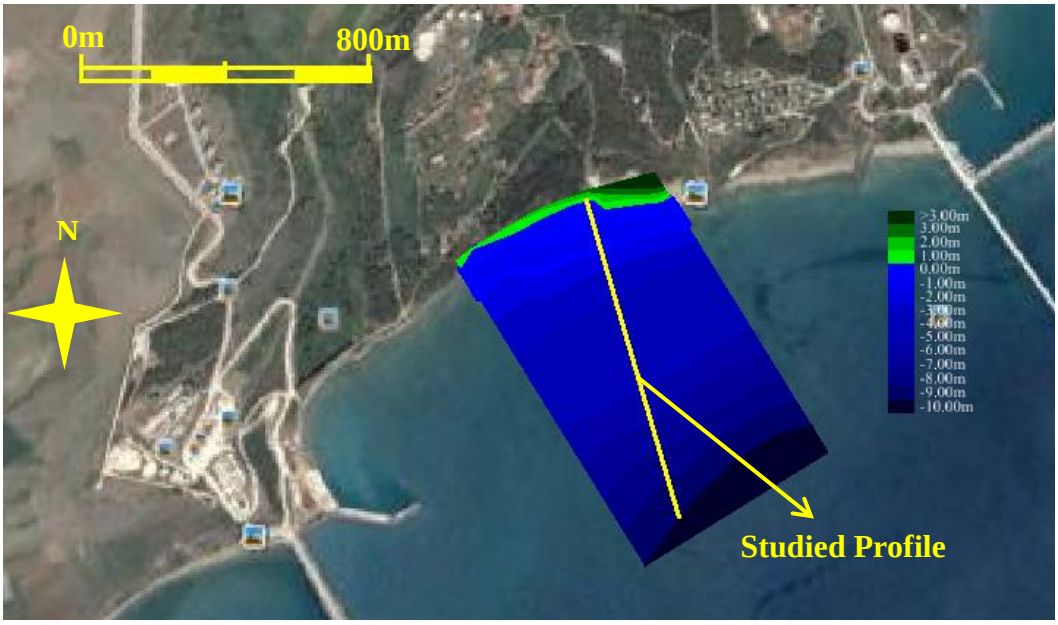

Figure 4.33: Location of the sample profile (Google Earth, 2014)

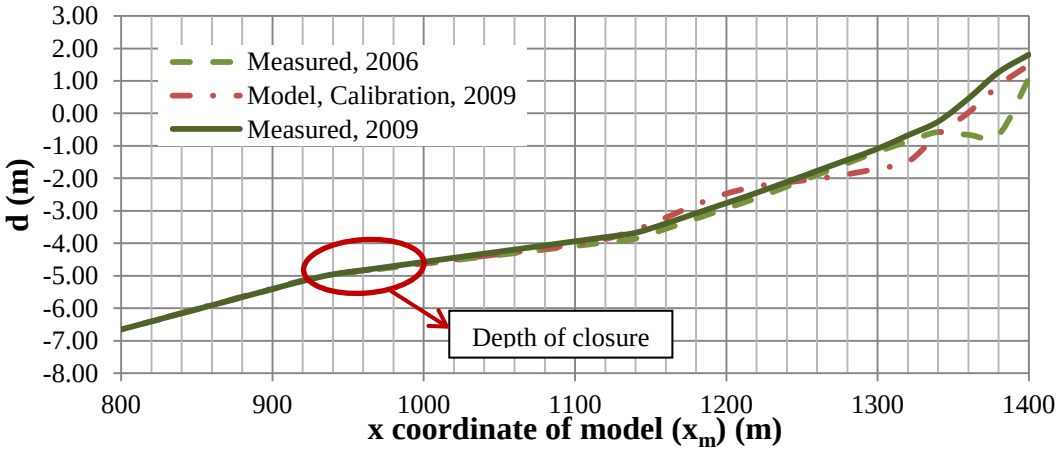

Figure 4.34: Depth of closure in calibration study

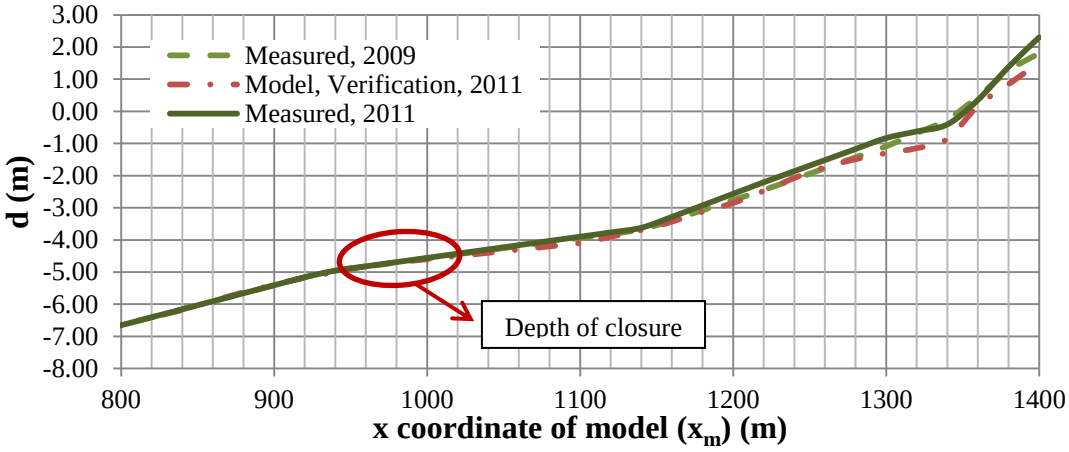

Figure 4.35: Depth of closure in verification study

CHAPTER 5

CONCLUSION

In this study, the numerical model called XBeach which is mainly developed to understand the nearshore responses under storm and hurricane conditions is used to determine the long term behaviour of sediment transport process observed in Yumurtalık region in Adana, Turkey. Since both alongshore and cross-shore sediment transport processes could be model in XBeach, it is preferred to be used in this study.

Since XBeach is mainly developed for storm and hurricane conditions, it has a limitation in time of simulation. In order to make a long-term study, this limitation is to be overcome. For this purpose, consecutive runs are made by using the bathymetry of the previous run.

The bathymetries of the field measurement years used in this study are obtained by linear interpolation of the elevation measurements available since there are no other detailed bathymetric surveys except the available elevation measurements. Using the bathymetries obtained by this way resulted in high errors and unrealistic results near the shoreline. In addition, there is no information available about the sediment size in Yumurtalık region. Therefore, the average sediment grain size is assumed as 2 mm in this study.

There are 12 options to define offshore wave boundary conditions in XBeach. In this study, as offshore wave boundary condition, the 12^{th} option given in Section 3.4, which is the sequence of various sea states, is used. With this option, user is able to define series of various sea states in one simulation. For example, if the way that reads SWAN spectrum is selected, for each wave direction SWAN spectrums are

needed to be obtained and used as source term for XBeach simulation which significantly increases the number of simulations. Thus, in order both to decrease number of simulations and create randomness during simulations 12th option given in Section 3.4 is used. The sequence of sea states that is used as the offshore wave boundary condition in the simulation is obtained as given in Section 4.3.4 by using the representative wave approach suggested by Güler (1997) and Güler et al. (1998). During the calibration and verification studies, the representative waves given in Table 4.5 and Table 4.6, which are used as offshore wave boundary conditions, are used in the model in the order of SE to WSW. The effect of using wave data in another order such as from WSW to SE is not considered in this study. In further studies, use of wave data in different orders can be tried and the effect of this phenomena can be evaluated.

In the definition of sea states, spreading parameter (s) is also needed to be given in XBeach. For the determination of the best value of spreading parameter compatible with the methodology used in the determination of sequence of sea states (Section 4.2.3 to Section 4.2.5), a run series is carried out for different values of spreading parameter changing from 1 to 1000 which are the minimum and maximum values of this parameter defined in XBeach. Best value of spreading parameter is selected by considering the value which covers at least 90% of wave energy confined in the related directional bin of 22.5 degrees in this study. 1000 is found as the most suitable value for the spreading parameter since, for this value, 90% of wave energy is confined in each directional bin which 22.5 degrees selected.

As a first step, since there are no available shoreline measurements, in order to understand the change of shoreline in long term, Google Earth satellite images are evaluated. From the evaluation of these satellite images, significant erosion is observed between the years 2006 and 2009; however, there is no significant change of shoreline observed for the years 2009 and 2013. The reason of the significant erosion observed between the years 2006 and 2009 could not be clearly understood since this erosion is not observed to continue in the following years.

By using different values of the selected parameters defined in XBeach both calibration and verification studies are performed. The results of the model are compared with the field measurements to determine the model efficiency and to determine general behaviour of sediment transport process.

The results obtained from this study can be summarized as follows;

The important parameters to which XBeach model is sensitive are determined as:

- *facua* which is the parameter used to define the ratio of wave asymmetry. For example, if the value of facua is selected zero, this means that there is no wave asymmetry; on the other hand, for the values different than zero, some asymmetry in waves is defined. This parameter is found to be effective in this study. The effect of this parameter is important when cross-shore sediment transport process is important for a region as recommended by Trouw (2012). Thus, in this study, as a first step, calibration study is performed different values of *facua* and as a result the most suitable value is found as 0.2.

- *lws* which is the parameter used to describe long wave stirring. For example if the value of *lws* is selected as zero, the effect of long waves (swell waves) is not considered. This parameter is found not to be effective. In this study, model is found to give a little bit better results when the effect of long wave is not included. The main reason of selecting the value of *lws* as zero depends on the following reason. The wave data used to determine offshore wave boundary conditions does not include swell wave parameters; therefore, the effect of swell waves found not to be effective in sediment transport as a result of the model.

- *wetslp* which is used to define critical avalanching slope under water. If a sample about the effect of this parameter in model is given; for larger values of this parameter the slope towards is found to be decreasing towards offshore; on the other hand, for small values, it increases. In other words, this parameter affects the sediment transport concentration towards offshore. As a result of this study, *wetslp* parameter is found to be effective as also found in other studies in literature. The model results get highly affected for the values defined for the

values of *wetslp*. Therefore, an optimum value of this parameter is searched by performing different runs. As a result of these runs, the optimum value of *wetslp* parameter is selected as 0.1

- *dryslp*, parameter used to describe critical avalanching slope above water, is also found to be effective in this study. This parameter in XBeach is mainly responsible for the erosion rate observed above water. For example, if the value of *dryslp* increases, erosion observed above water also increases and vice versa is true. In Yumurtalık region, erosion observed above water is small; that is why, 0.1, minimum value of *dryslp* in XBeach, is selected as the value of *dryslp* for this study.

- *facsl*, which is the parameter used to define the effect of bed slope, is responsible for equilibrium sediment concentration. For higher values of this parameter, equilibrium sediment concentration decreases, on the other hand, for smaller values it increases. That is why an optimum value of this parameter should be determined. Two runs are performed for the different values of *facsl* and 0.5 is found to be suitable value for this model.

By following the steps defined in Chapter 4 and using the values of the parameters given above, a long-term modelling study in Yumurtalık region to define the dominant sediment transport process has been carried out in this study.

Although field measurements are not accurate enough for a long-term study, from the profiles given in study area, a bar formation is observed. Similarly, from the numerical modelling studies performed by using XBeach, a bar formation is again observed in the study area.

Furthermore, when the sediment transport rates are evaluated, it is observed that in addition to the cross-shore sediment transport, there is also alongshore sediment transport in this region since waves reach to shoreline with an angle. Although both of the sediment transport processes are observed in Yumurtalık region, during this study it is observed that the effect of longshore sediment transport process is not as

much as cross shore sediment transport. Thus, it can be said that cross shore sediment transport is dominant in Yumurtalık region.

In addition, when both field measurements and model results are evaluated, it is observed that depth of closure of the area is approximately 5 m which is compatible with the calculated values 6.6 m and 4.6 m by using Eq. 2.14 for calibration and verification studies according to dominant wave direction which is SSW.

In this study, structured grids with 20 m grid sizes are used. The sensitivity of the model to the grid sizes is not evaluated. For future works, by using smaller structured grid sizes or unstructured grids (smaller grid sizes near the shoreline), model sensitivity can be checked.

In conclusion, The numerical model results are found to be generally in good agreement with small differences changing from 5cm to 20cm except near the shoreline. The high error values obtained near the shoreline may be the result of the inaccurate and not very detailed field measurements. In order to understand the model efficiency in this region, more detailed field measurements should be taken and the results of the model should be compared with these measurements. With the available measurements used in this study, proper modelling of XBeach that shows good results in the region near the shoreline is not possible. If more detailed field measurements are taken, more accurate results can be obtained for this region.

REFERENCES

Andrews, D. G., McIntyre, M., (1978). "*An Exact Theory Of Nonlinear Waves on a Lagrangian-Mean Flow*." Journal of Fluid Mech. Vol.89, No. 4, pp. 609–646

Bailard, J.A. (1981)."*An Energetics Total Load Sediment Transport Model for a Plane Sloping Beach.*" Journal of Geophysical Research 86, Cl 1, pp. 938-954.

Bailard, J. A. (1984). "*A Simplified Model for Longshore Sediment Transport*." Proceedings of the 19th International Conference on Coastal Engineering, ASCE, 1454-1470.

Baykal, C., (2006), "*Numerıcal Modelling of Wave Diffraction in One-dimensıonal Shoreline Change Model*", M.S. Thesis, METU, Ankara

Baykal, C., (2012), "*Two Dimensional Depth Averaged Beach Evolution Modelling*", Ph.D. Thesis, METU, Ankara

Bodge, K. R., (1992). "*Representing Equilibrium Beach Profiles with an Exponential Expression*", Journal of Coastal Research, Vol.8, No. 1, pp. 47-55

Bruun, P., (1954),"*Coast Erosion and the Development of Beach Profiles*", Beach Erosion Board Technical Memorandum No.44, U.S. Army Engineer Waterways Experiment Station, Vicksburg, MS.

Capobianco, M., Hanson, H., Larson, M., Steetzel, H., Stive, M.J.F., Chatelus, Y., Aarninkhof, S., Karambas, T., (2002), "*Nourishment design and evaluation: applicability of model concepts*", Coastal Engineering, Vol.47, pp.113-135

Coastal Engineering Manual, "CEM" (2003), U.S. Army Corps of Engineers, Coastal Engineering Research Center, U.S.Government Printing Office

Dabees, M.A., (2000), "*Efficient Modelling of Beach Evolution*", Ph.D. Thesis, Queen's University, Kingston, Ontario, Canada

Dally, W.R., and Dean, R.G., (1984), "*Suspended Sediment Transport and Beach Profile Evolution*", Journal of Waterways, Harbors and Coastal Engineering Division, ASCE, Vol.110, No.1, pp.15-33

De Vriend, H.J., (1991a). "*Mathematical Modelling and Large-Scale Coastal Behaviour. Part 1: Physical Processes*", Journal of Hydraulic Research, Vol. 29, No. 6, pp. 727–740.

Dean, R. G., (1977), "*Equilibrium Beach Profiles: U.S. Atlantic and Gulf Coasts*", Department of Civil Engineering, Ocean Engineering Report No.12, University of Delaware, Newark, DE.

Dean, R. G., (1987b), "*Coastal Sediment Processes: Toward Engineering Solutions*", Coastal Sediments'87, American Society of Civil Engineers, New Orleans, LA, Vol.1, pp.1-24

Dean, R. G., (1991), "*Equilibrium Beach Profiles: Characteristics and Applications*", Journal of Coastal Research, Vol.7, No.1 pp.53-84

del Valle, R., Medina, R., and Losada, M. A. (1993). "*Dependence of Coefficient K on Grain Size*" Technical Note No. 3062, Journal of Waterway, Port, Coastal, and Ocean Engineering Vol.119, No. 5, pp. 568-574.

Den Beimen, J. (2013)," *XBeach Grid Tutorial*"

Dong, P., (2008), "*Long-term Equilibrium Beach Profile Based on Maximum Information Entropy Concept*", Journal of Waterway, Port, Coastal, and Ocean Engineering, Vol. 134, No. 3, May 1, 2008

Ergin, A. (2009) *"Coastal Engineering"*, METU Press, Ankara, Turkey

Ergin, A., and Özhan, E., (1986), "*15 Deniz Yöresi için Dalga Tahminleri ve Tasarım Dalgası Özelliklerinin Belirlenmesi*" (in Turkish), Middle East Technical University, Ocean Engineering Research Center

Fowler, J. E., Rosati, J. D., Hamilton, D. G., and Smith, J. M. (1995). "*Development of a Large-Scale Laboratory Facility For Longshore Sediment Transport Research*," The CERCular, CERC-95-2, U.S. Army Engineer Waterways Experiment Station, Vicksburg, MS.

Fredsoe, J., Deigaard, R (1992), "*Mechanics of Coastal Sediment Transport*", World Scientific

Galappatti, R., Vreugdenhil, C. B., (1985). "*A Depth Integrated Model For Suspended Transport*." Journal of Hydraulic Research Vol. 23, No. 4, pp. 359–377

Goda, Y., (1985), "*Random Seas and Design of Maritime Structures*", University of Tokyo Press

Güler, I., (1997), "*Investigation on Protection of Manavgat River Mouth*", Yüksel Proje International Co. Inc., Research Project Report

Güler, I., Ergin, A., and Yalçıner, A.C., (1998), "*The Effect of the Use of Wave Data for the Numerical Solution of Shoreline Evolution*", Journal of Coastal Research, Special Issue No.26, pg. 195-200

Hallermeier, R.J., (1978), "*Uses for a Calculated Limit Depth to Beach Erosion*", Proc. 16th Int. Conf. on Coastal Engrg., ASCE, New York, pg.1493-1512

Hanson, H., (1987), "*GENESIS: A Generalized Shoreline Change Numerical Model for Engineering Use*", Ph.D. Thesis, University of Lund, Lund, Sweden

Hanson, H., Aarninkhof, S., Capobianco, M., Jimenez, J. A., Larson, M., Nicholls, R. J., Plant. N. G., Southgate H. N., Steetzel, H. J:, Stive, M. J. F. and de Vried H. J., (2003), "*Modelling of Coastal Evolution on Yearly to Decadal Time Scales*", Journal of Coastal Research, Vol. 19, No. 4, pp. 790-811

Hayden, B., Felder, W., Fisher, J., Resio, D., Vincent, L., and Dolan, R., (1975),"*Systematic Variations in Inshore Bathymetry*." Department of Environmental Sciences, Technical Report No.10, University of Virginia, Charlottesville, VA.

Hsu, S.A., (1980), "*On the correction of Land-Based Wind Measurements for Oceanographic Applications*", Proc. Of 17th Conf. on Coastal Engineering, Sydney, Vol.1, pp.709-721

Kamphuis, J.W., (2000), "*Introduction to Coastal Engineering and Management*", World Scientific

Kamphuis, J. W. (2002). "*Alongshore Transport of Sand*." Proceedings of the 28th International Conference on Coastal Engineering. ASCE, pp. 2478-2490.

Kamphuis, J.W., (2010), "*Introduction to Coastal Engineering and Management*", World Scientific, 2nd edition

Kriebel, D.L. and Dean, R.G., (1984), "*Beach and Dune Response to Severe Storms*", Proc. 19th Int. Conf on Coastal Engrg., ASCE, pp.1584-1599

Kriebel, D.L., Kraus, N. C. and Larson, M., (1991), "*Engineering Methods for Predicting Beach Profile Response*", Proceedings of Conference on Coastal Sediments'91, American Society of Civil Engineers, pp. 557-571

Larson, M., (1988), "*Quantification of Beach Profile Change*", Report No.1008, Department of Water Resources and Engineering, University of Lund, Lund, Sweden

Larson, M and Kraus, N. C., (1989), "*SBEACH: Numerical Model for Simulating Storm-induced Beach Change; Report 1: Empirical Foundation and Model Development*", Technical Report CERC-89-9, U.S. Army Engineer Waterway Experiment Station, Vicksburg, MS.

Larson, M. and Kraus, N.C., (1995). "*Prediction of Cross-shore Sediment Transport at Different Spatial and Temporal Scales*", Marine Geology, Vol. 126, pp. 111–127.

Larson, M., Kraus, N. C., Wise, R. A., (1998), "*Equilibrium beach profiles under breaking and non-breaking waves*", Coastal Engineering, Vol.36, pp.59-85

Miller, H. C. (1998). "*Comparison of Storm Longshore Transport Rates to Predictions*." Proceedings of the 26th Conference on Coastal Engineering. ASCE, pp. 2954-2967.

Miller, J.K. and Dean R.G., (2004), "*A Simple New Shoreline Change Model*", Coastal Engineering, Vol.51, pp.531-556

Moore, B. D., (1982), "*Beach Profile Evolution in Response to Changes to Water Level and Wave Height*", M.S. Thesis, Department of Civil Engineering, University of Delaware, Newark

Özkan-Haller, H. T., Brundidge, S., (2007), "*Equilibrium Beach Profile Concept for Delaware Beaches*", Journal of Waterway, Port, Coastal, and Ocean Engineering, Vol. 133, No. 2, March 1, 2007

Pelnard-Considère, R. (1956). "*Essai de theorie de 1'Evolution des Formes de Rivage en Plages de Sable et de Galets*." 4th Journees de 1' Hydraulique, Les Energies de la Mar, Question Ill, Rapport No.1, pp 289-298.

Perlin, M., and Dean, R.G. (1978), "*Prediction of Beach Planforms with Littoral Controls*" Proc. 16"' lnt. Coastal Engrg. Confi, ASCE, pp. 18 18- 1838.

Reniers, A. J. H. M., Roelvink, J. A., Thornton, E. B., (2004a). "*Morphodynamic Modelling of Anembayed Beach Under Wave Group Forcing*." Journal of Geophysical Research Vol.109, C01, 030, doi:10.1029/2002JC001586.

Roelvink, J.A., (1993a). "*Dissipation in Random Wave Groups Incident on a Beach*". Coastal Engineering No.19, pp. 127–150.

Roelvink, D., Reniers, A., Van Dongeren, A., de Vries, J. T., Lescinski, J., McCall, R., (2010), "*XBeach Model Description and Manual*"

Roelvink, J. A., Meijer, Th. J., Houwman K., Bakker R., and Spanhoff, R., (1995). "*Field Validation and Application of a Coastal Profile Model*" Proceedings, Coastal Dynamics'95. ASCE, pp 818-828

Schoonees, J. S., and Theron, A. K. (1993). "*Review of The Field Data Base For Longshore Sediment Transport*" Coastal Engineering, No.19, pp. 1-25.

Smith E. R., Ebersole B. A., Wang P., (2004) " *Dependence of Total Longshore Sediment Transport Rates on Incident Wave Parameters and Breaker Type"* .S. Army Corps of Engineers, Coastal Engineering Research Center

Soulsby, R., (1997), "*Dynamics of Marine Sands: a Manual for Practical Applications*", Thomas Telford Publications

Stive, M.J.F. and Battjes, J.A., (1984), "*A Model for Offshore Sediment Transport*", Proc. 19th Int. Conf. On Coastal Engrg., ASCE, pp.1420-1436
Swart, D.H. (1974),"*Offshore Sediment Transport and Equilibrium Beach Profiles*", Publ. No.131, Deft Hydraulics Lab, Delft, The Netherlands.

Şafak, I., (2006), "*Numerical Modeling of Wind Wave Induced Longshore Sediment Transport*", M.S. Thesis, METU, Ankara

Trouw, K., Zimmermann, N., Mathys, M., Delgado, R. and Roelvink, D. (2012), "*Numerical Modelling of Hydrodynamics and Sediment Transport in the Surfzone: A Sensitivity Study with Different Types of Numerical Models*", Coastal Engineering

Van Dongeren, A.R. and Svendsen, I. A., (1997), "*An Absorbing-Generating Boundary Condition for Shallow Water Models*", Journal of Waterways, Ports, Coastal and Ocean Engineering, Vol. 123, No. 6, pp. 303-313.

Vellinga, P. (1983), "*Predictive Computational Model for Beach and Dune Erosion During Storm Surges*", Proceedings, American Society of Civil Engineers Specialty Conference on Coastal Structures'83, pp. 806-819

Verboom, G.K., Stelling, G.S. and Officier M.J. (1981), "*Boundary Conditions for the Shallow Water Equations*", In: Abbott, M.B. and J.A. Cung, eds, Engineering Applications of Computational Hydraulics, Vol. 1, pp. 230-262.

Vousdoukas, M. I., Almeida, L. P., Ferreira, O., (2011), "*Modelling Storm-induced Beach Morphological Change in a Meso-tidal, Reflective Beach Using XBeach*", Journal of Coastal Research, Vol.64, pp. 1916-1920

Wang, P., Kraus, N. C., (2005),"*Beach Profile Equilibrium and Patterns of Wave Decay and Energy Dissipation across the Surf Zone Elucidated in a Large-Scale Laboratory Experiment*", Journal of Coastal Research, Vol.21, No.3, pp. 522-534.

Wang, P., Kraus, N. C., and Davis, R. A., Jr. (1998). "*Total Rate of Longshore Sediment Transport In The Surf Zone: Field Measurements and Empirical Predictions*," Journal of Coastal Research Vol. 14, No 1, pp. 269-283.

Wang, P., and Kraus, N. C. (1999). "Longshore sediment transport rate measured by short-term impoundment," Journal of Waterway, Port, Coastal and Ocean Engineering ASCE, Vol.125, pp. 118-126.

APPENDIX A

DETERMINATION OF SPREADING PARAMETER

In Fig. A.1 to Fig. A.8, the vertical axis shows the percent of energy confined in directional bin and the horizontal axis show the each directional bin which corresponds to 22.5^0.

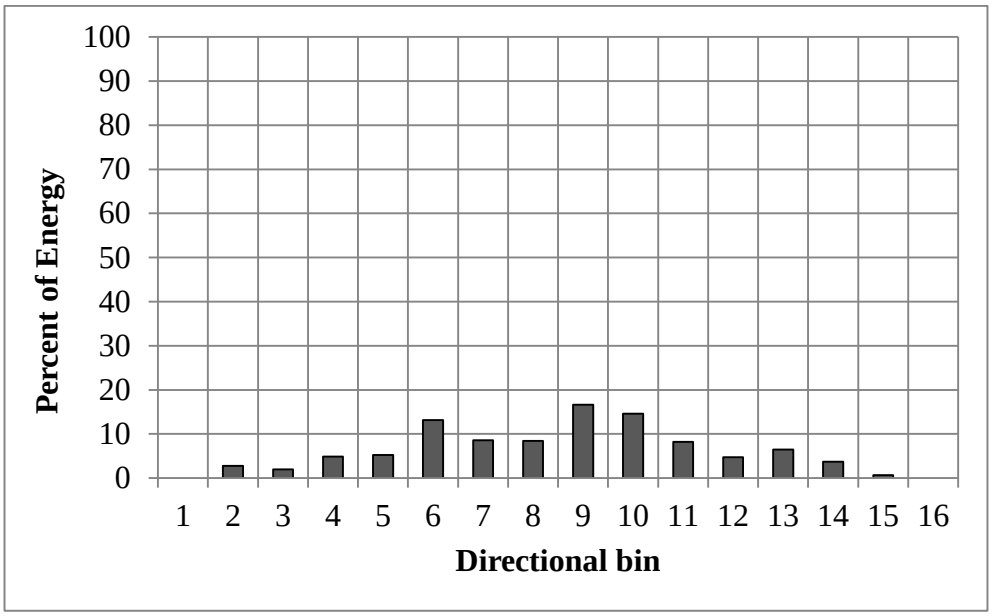

Figure A.1: Test Case-1, Value of spreading parameter, s=1

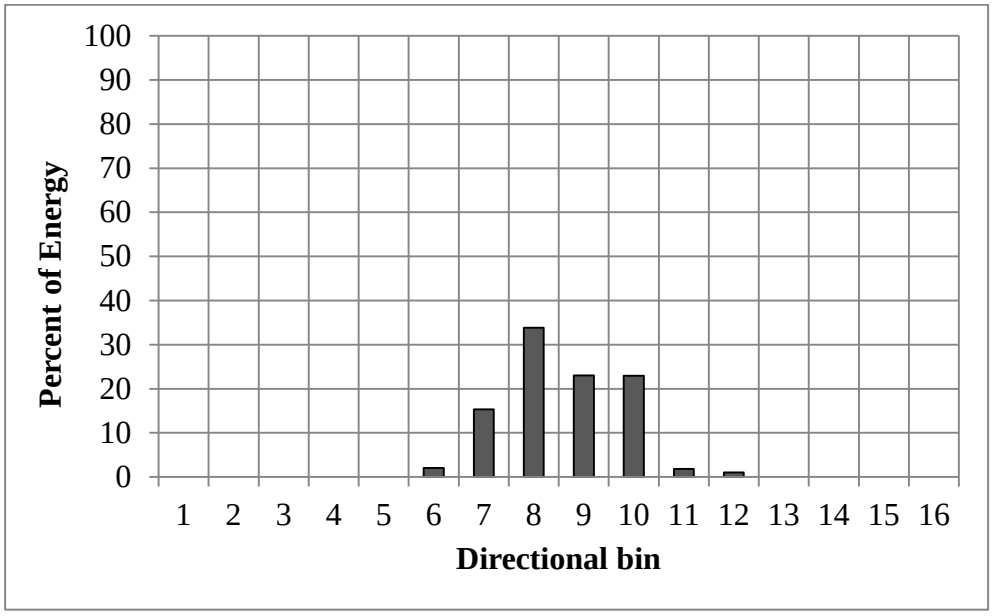

Figure A.2: Test Case-2, Value of spreading parameter, s=10

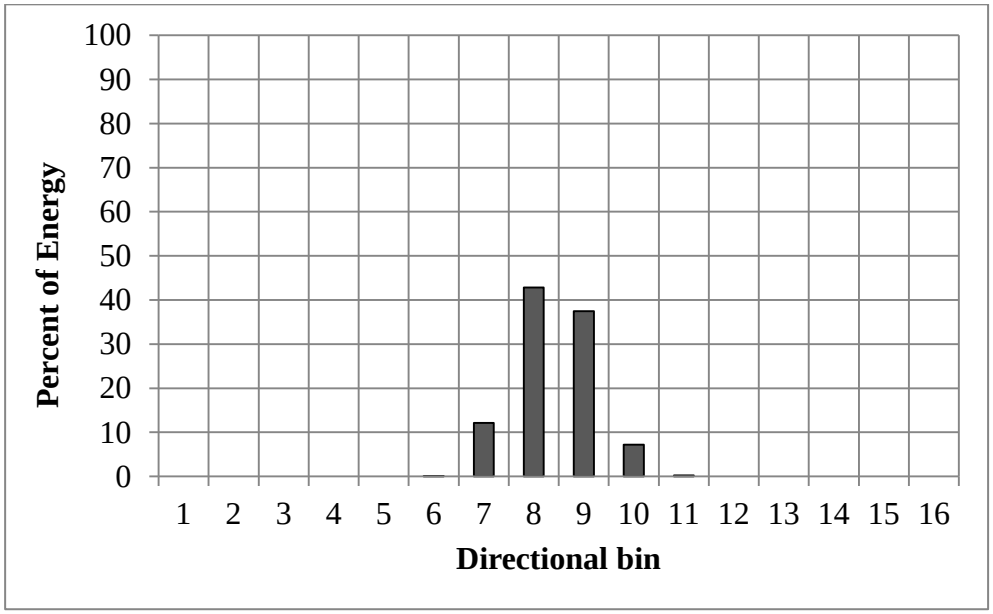

Figure A.3: Test Case-3, Value of spreading parameter, s=25

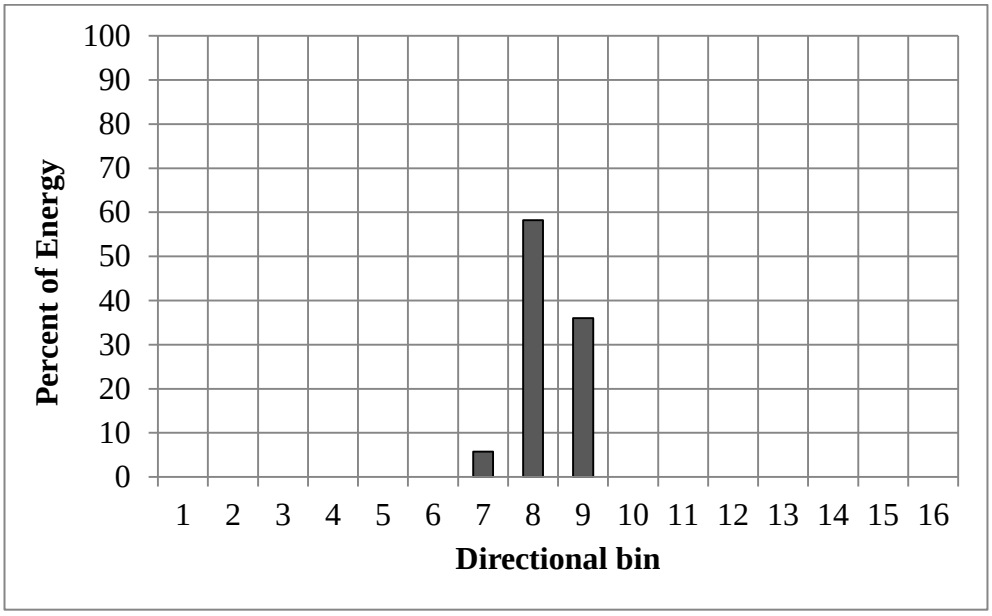

Figure A.4: Test Case-4, Value of spreading parameter, s=50

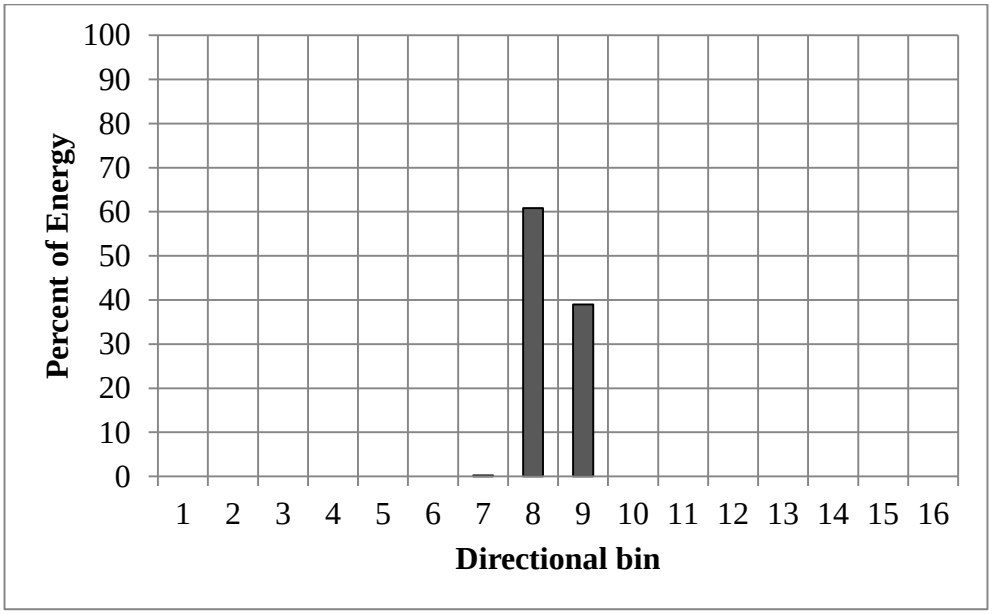

Figure A.5: Test Case-5, Value of spreading parameter, s=100

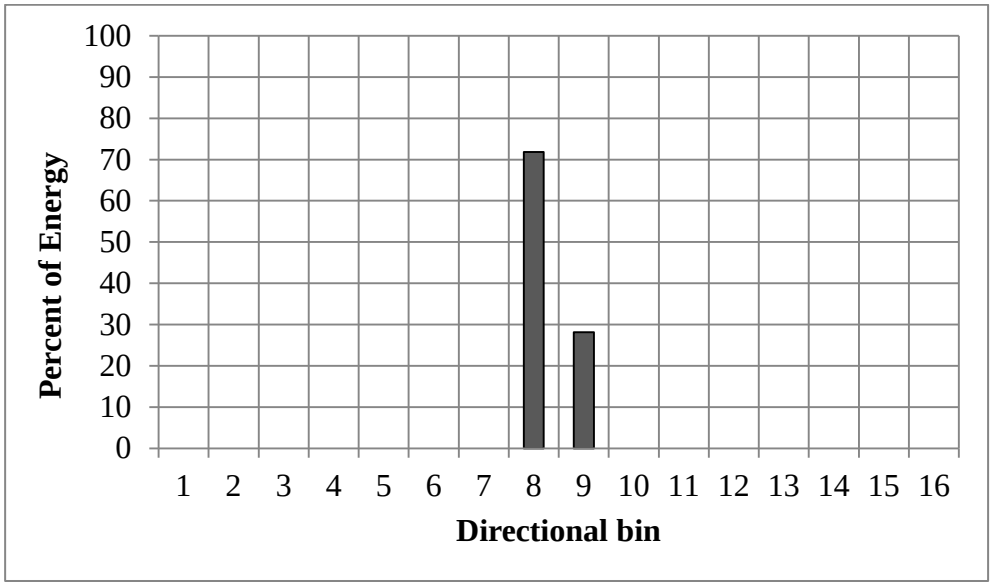

Figure A.6: Test Case-6, Value of spreading parameter, s=200

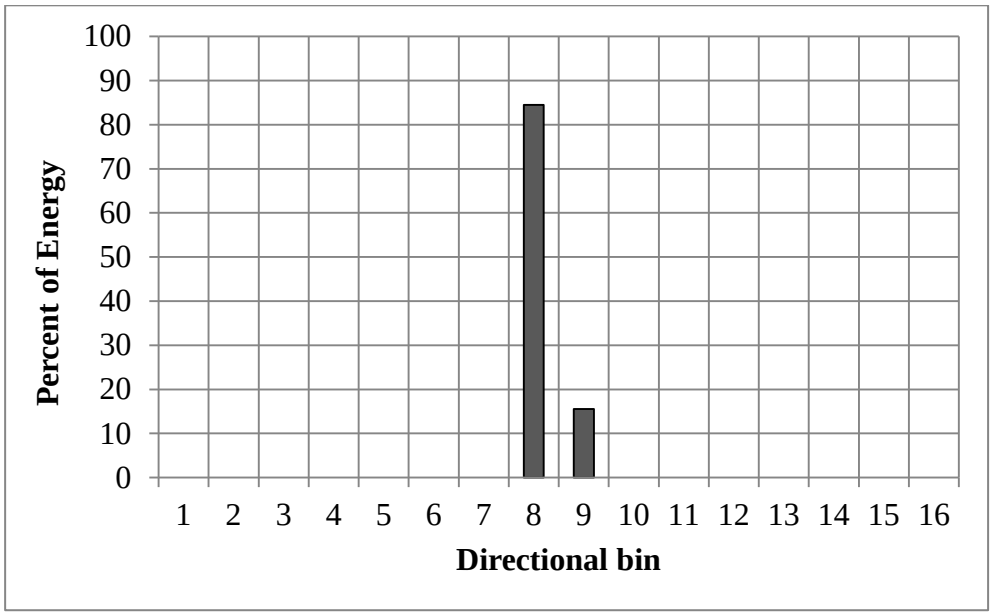

Figure A.7: Test Case-7, Value of spreading parameter, s=500

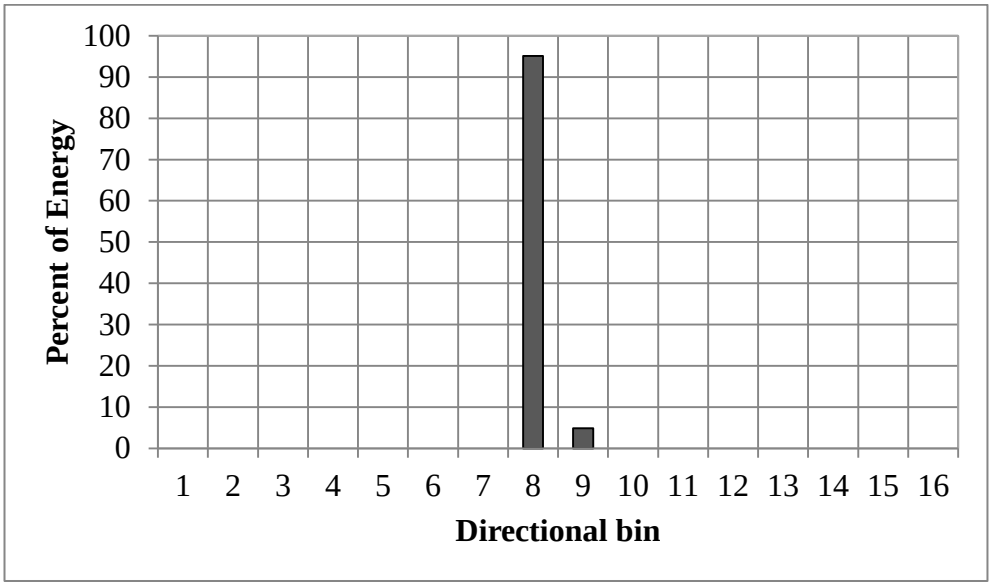

Figure A.8: Test Case-8, Value of spreading parameter, s=1000